AN ANALYTICAL INVESTIGATION OF AN OSCILLATING WEDGE IN A SUPERSONIC PERFECT GAS FLOW

by

ROBERT MERRILL BENNETT

A thesis submitted to the Graduate Faculty of
North Carolina State University at Raleigh
in partial fulfillment of the
requirements for the Degree of
Doctor of Philosophy

DEPARTMENT OF MECHANICAL AND AEROSPACE ENGINEERING

RALEIGH

1971

ABSTRACT

BENNETT, ROBERT MERRILL. An Analytical Investigation of an Oscillating Wedge in a Supersonic Perfect Gas Flow. (Under the direction of ROBERT W. TRUITT).

Several aspects of the oscillating wedge are investigated to evaluate both the resulting trends for the wedge and methods of analyzing unsteady flows.

The existing hypersonic small disturbance theory for the oscillating wedge is considered. Algebraic expressions are obtained for the low reduced frequency aerodynamic forces. Series expansions of the resulting forces in powers of $1/M\theta_w$ reveal weak similarity parameters for the pitching rate derivatives that indicate that a simple scaling of flutter with ratio of specific heats is not apparent. The importance of the reflections of the waves generated by the surface from the shock is reemphasized. Aerodynamic damping terms are found to have significant influence on flutter even for large values of the mass ratio parameter. The corresponding effects of angle of attack are shown to be small for the thin wedge.

The equations are developed for linearized perturbations about the known steady flow conditions that can be applied for any wedge angle or Mach number for which the local flow is supersonic. The method of integral relations is applied to the resulting equations in a one-strip approximation. Algebraic expressions for low reduced-frequency aerodynamics are obtained and a set of ordinary differential equations are obtained for general oscillatory motion. The method gives accurate

results for low reduced-frequency. However, for cases in which the aerodynamic forces vary rapidly with frequency the results are qualitatively correct but of limited accuracy. Calculations indicate that for a range of inclination angles near shock detachment such that the flow in the shock layer is transonic, the aerodynamic forces vary rapidly both with inclination angle and with reduced frequency indicating potentially serious flutter problems near detachment.

The governing nonlinear flow equations are formulated in a body-fixed axis system. The first order numerical finite-difference method of Lax is applied and discussed with simplified treatments of the boundaries. Although the formulation is suitable for numerical treatment, and may have merit for unsteady blunt body investigations, the need is indicated for further refinement of the treatment of the boundary conditions and for use of a second order difference scheme. A brief quasi-static analysis of oscillating wedge flows indicated that significant nonlinear effects may exist near detachment and for large amplitude motions of a thin wedge at high Mach numbers.

AN ANALYTICAL INVESTIGATION OF AN OSCILLATING WEDGE IN A SUPERSONIC PERFECT GAS FLOW

by

ROBERT MERRILL BENNETT

A thesis submitted to the Graduate Faculty of
North Carolina State University at Raleigh
in partial fulfillment of the
requirements for the Degree of
Doctor of Philosophy

DEAPRTMENT OF MECHANICAL AND AEROSPACE ENGINEERING

RALEIGH

1971

APPROVED BY:

L. Carson Yates, Jr. — Carl F. Zorowski

James C. Williams III — Robert C. Bullock

Robert N. Smith

Chairman of Advisory Committee

BIOGRAPHY

The author was born [redacted] He received his elementary and secondary education in Buncombe County, North Carolina, graduating from Weaverville High School in 1953.

He received the Bachelor of Mechanical Engineering, Aeronautical Option in 1957, from North Carolina State University at Raleigh. From 1957 to 1959, he was a graduate student and research assistant in the flight mechanics group of the Aeronautical Engineering Department of Princeton University, receiving a Master of Science in Engineering in 1960.

Since 1959, the author has been engaged in research in the field of aeroelasticity in the Aeroelasticity Branch of the Loads Division of the National Aeronautics and Space Administration's Langley Research Center at Hampton, Virginia. During the period of 1959-1962, he was on active duty as a U. S. Air Force officer and subsequently has been employed by the NASA.

The author was married in 1962 to the former Miss Winifred Irene Reeves of Erwin, Tennessee. They have three children, David aged five, Alan aged four, and Frances aged one.

ACKNOWLEDGMENTS

The author wishes to express his sincere appreciation to all persons who have contributed to this study. The research was supported by his employer, the National Aeronautics and Space Administration. Appreciation is extended to the author's supervisors in the Aeroelasticity Branch and Loads Division for their support and to the Training Office for their general assistance.

The helpful advice and guidance of the Advisory Committee and, in particular, that of Dr. Robert W. Truitt, Chairman of the Committee, and of Dr. E. Carson Yates, Jr., of NASA Langley is gratefully acknowledged. The assistance of the author's coworker, Mr. R. N. Desmarais, in the area of computer programming has also been helpful.

The author wishes to thank Mary Hachey and Ruth Stanfield for their typing of the manuscript version of this thesis, and to thank Alice Guilford and Queenella Perrin for their typing of the draft version.

Finally, the author expresses his thanks to his wife Winifred, and his children for their patience and sacrifice during a rather extended period of graduate study.

TABLE OF CONTENTS

LIST OF FIGURES

1. INTRODUCTION

Aeroelastic problems such as flutter have been a design consideration for aerospace vehicles for many years, and as such, have been the subject of considerable research. The need still exists for further refined analytical techniques as the potential economic savings of careful design of advanced vehicles can be significant. Recent developments in computer technology have led to several highly-developed aerodynamic methods for the analysis and computation of steady flow fields. The corresponding unsteady aerodynamics for analyzing flutter, loads, and stability have not been as well developed. In this thesis some of the techniques that have been applied to the calculation of steady flow fields are applied to a simplified configuration – an oscillating two-dimensional wedge in a supersonic or hypersonic flow of a perfect gas.

The steady supersonic flow over a sharp two-dimensional wedge is one of the few exact solutions of the nonlinear governing equations of inviscid flow. No such corresponding solution for unsteady flow is available. However, the uniform steady wedge flow permits significant simplification of perturbation methods. This fact has been used to advantage in several phenomenological investigations, perturbation analyses, and approximating techniques in order to evaluate such processes as unsteady wave reflections. Herein the oscillating wedge is treated both to gain insight into the application of several methods of analysis and computation, and to examine the resulting trends for the wedge airfoil.

First, after discussion of the problem and literature, an existing hypersonic small distrubance theory for an oscillating thin wedge is

extended and applied. A perturbation method involving linearization about the known steady flow is then derived and discussed. Subsequently, a finite difference technique for calculating the complete unsteady flow field of the wedge in motion is presented and discussed in conjunction with some calculated quasi-static nonlinear trends. Emphasis herein is given to the high supersonic and hypersonic Mach number range and to the effects of the ratio of specific heats.

2. DISCUSSION OF PROBLEM AND RELATED LITERATURE

The literature of the general area of aeroelasticity is extensive and has been recently reviewed, for example, by Ashley (1970). Various aspects of aeroelasticity have also been discussed by Bisplinghoff and Ashley (1962) and Garrick (1969). Supersonic-hypersonic unsteady problems have also been reviewed by Wood (1966) and Ashley and Zartarian (1961). Thus, the discussion here will be principally concerned with several aspects of the specific problem treated in this thesis.

2.1 The Oscillating Wedge

The effect of airfoil thickness on flutter at supersonic-to-hypersonic speeds can be large and destabilizing (for example, see Ashley and Zartarian, 1956; Morgan, et al., 1958; and Runyan and Morgan, 1962). This effect generally results primarily from a forward chordwise shift of the aerodynamic center with increasing thickness. Other factors such as lift-curve-slope and pitch damping are also involved, however. In order to assess the role of thickness before the destabilizing effect of thickness was well known, the wedge airfoil was attractive for further treatment since the exact steady flow field was known. In more recent years, it has also been a basic check case for evaluating simplified theories and for phenomenological studies. Although the wedge airfoil is often studied for research purposes only, such airfoils are infrequently used such as on the vertical tail of the X-15 airplane.

Carrier (1949b) presented a perturbation analysis of the oscillating wedge in supersonic flow as based on his earlier study of the

stability of the strong and weak shock solutions for steady wedge flow (Carrier, 1949a). The analysis was further developed and applied by Van Dyke (1953), who gave some brief results. It had been shown (e.g., Garrick and Rubinow, 1946) from linearized supersonic flow theory, that unstable values of damping-in-pitch of a flat plate exist for forward locations of the pitch axis and for Mach numbers less than $\sqrt{2}$. Van Dyke (1953) demonstrated that the range of Mach numbers and of pitch axes for unstable pitch-damping was enlarged for a thin wedge.

The results of the above-mentioned analysis were used by Van Dyke (1954a) to verify the low-frequency results obtained from second order theory. Van Dyke (1954a) also presented a solution obtained from second-order theory for a thin wedge oscillating at arbitrary frequency. A sample comparison with linear theory indicated that the effects of thickness on the damping-in-pitch (for $k \to 0$) are alleviated at higher values of k.

With the development of the relatively simple piston theory, which is applicable to thin surfaces and high Mach numbers, Hayes (1947), Lighthill (1953), and Ashley and Zartarian (1956), the wedge airfoil was again treated (e.g., Chawla, 1958). Piston theory is limited to values of $M\theta_w < 1$ and it has also been noted that stable values of the damping-in-pitch are inherent in the piston approximation.

McIntosh (1965a , 1965b) presented a perturbation solution for the oscillating wedge as based on hypersonic small disturbance theory (Van Dyke, 1954b), that is essentially a generalization of piston theory to include the effects of the shock wave on the local external flow properties and the effects of reflections of surface motion-generated

waves from the shock wave. McIntosh's analysis indicated that inclusion of the wave reflection process was essential; otherwise the perturbation in pressure approaches infinity as $\gamma \to 1$. Such was observed by Miles (1960) in a local flow perturbation analysis. The wave reflection process had been earlier studied by Chu (1952). An analysis similar to McIntosh's was presented by Appleton (1964) and discussed by Orlik-Rückemann (1966b, 1969). The results of McIntosh (1965a) have been applied to pitch-plunge flutter of wedge airfoils by Bailie and McFeely (1966) and to panels mounted on wedges by Bailie and McFeely (1968). The hypersonic small disturbance theory for the oscillating wedge of McIntosh (1965a) is again applied and discussed in this thesis in Chapter 3.

Hui (1969a) developed an exact perturbation theory for pitching motions of a symmetrical wedge for angles up to detachment and has also applied the method to the caret wing. Unstable values of damping-in-pitch for the wedge were shown to exist at any Mach number if the wedge angle was sufficiently large. For the caret wing, this result was eliminated by three-dimensional effects. With an approximate perturbation solution, Hui (1969b) also indicated that waves generated by the moving shock wave can be significant for large wedge angles. A perturbation method is developed here in Chapter 4 that is quite similar to that of Hui; however, the method of solution is quite different and the analysis is done in more general terms such that any rigid-body motion of an inclined-flat compression surface can be described.

Kuiken (1969) has presented a higher-order perturbation solution based on hypersonic small disturbance theory. The quasi-static wedge

flow, that is based on the effective wedge angle at the vertex including motion, was perturbed to give an effective phase shift of the quasi-static solution. The surface pressure was calculated for constant-amplitude harmonic motion. As the quasi-static solution is nonlinear, the resulting pressure waves are unsymmetrical, indicating the presence of higher harmonics, and a shift in mean pressure level was noted.

Curve fits to Kuiken's results have been given by Orlik-Rückemann (1969). The quasi-static solution will be subsequently discussed in Chapter 5. In a similar analysis, Kacprzynski (1968) has treated the full equations of motion in an approximate solution giving similar results. Hui (1970) has subsequently given an exact solution with no further numerical results.

Several other simplified theoretical developments have been given that could be applied to the wedge airfoil such as Newtonian flow theory (i.e., Zartarian and Sauerwein, 1952). Some have been examined by applying them to a diamond airfoil by Yates and Bennett (1971).

An important aspect of hypersonic flow, at least, is the interaction of the boundary layer with the steady flow field. Some research into unsteady effects of a laminar boundary layer on wedges in the weak interaction regime is given by King (1966), Orlik-Rückemann (1966a, 1970), and Hui and East (1971). The general trend is to shift the moment center forward and to reduce the damping-in-pitch for forward locations of pitch axis.

Several investigators have also given experimental data relating to the overall aerodynamic forces for the pitching wedge. Pugh and Woodgate (1963) give the results of two-dimensional tests at supersonic

speeds in air. East (1962) has presented some results of measurements in air at M = 10, but with some tip effects. Orlik-Rückemann (1970) has also given some hypersonic results measured in helium. Martuccelli (1958) has also presented some measured results at low supersonic speeds. Unfortunately, the author is unaware of corresponding two-dimensional flutter data as available data are generally for swept-tapered wings (i.e., Hanson, 1961).

2.2 Flow Field Calculations

Several numerical methods have recently been developed which permit computation of highly-complex, steady flow fields over various types of bodies using the governing nonlinear flow equations and a modern digital computer. The proceedings of a recent symposium (NASA publ., 1970) gives a broad survey of several of the available techniques. An annotated bibliography has also been given by Harlow (1969) and a survey volume given by Chu (1968). These methods generally consist of (1) direct solution by constructing finite difference approximations to the partial differential equations and then solving the resulting system of equations numerically, or (2) reducing the governing partial differential equations in some approximate manner and then integrating the ordinary differential equations.

Methods of the first type as based on a characteristics approach have been given, for example, by Sauerwine (1964, 1965, 1966) and also by Rakich (1969). Various other finite-difference approaches have been developed and applied, for example, by Barnwell (1971), MacCormack (1969), Moretti and Abbett (1966), Lax and Wendroff (1964), and Lax (1954).

Many of these methods involve determining the steady flow field by the time evolution from an assumed approximate initial solution.

Examples of methods of the second type are the method of integral relations (see for example, South, 1968, and Belotserkovskiy and Chushkin, 1962) and the method of lines (Klunker, et al., 1971, for example). These methods usually treat the boundary or initial value problem directly or iteratively in contrast to the time-asymtotic approach.

Very little work has been done in relation to applying any of these methods to unsteady flows except for some simplified one-dimensional problems such as given by Bohachevsky and Rubin (1966), although they have been occasionally discussed (i.e., Ashley and Zartarian, 1961).

In this thesis two of the above methods are applied to the unsteady aerodynamics of the oscillating wedge, the method of integral relations is applied to the perturbation equations (Chapter 4) and a first-order difference method of Lax (1954) is applied to the full nonlinear unsteady flow equations written in a body-axis system (Chapter 5).

2.3 Comments on Nonlinear Aeroelastic Analysis

Aeroelastic problems have generally been treated with linearized analyses that essentially consider initial tendencies for infinitesimal amplitudes. For example, flutter is conventionally posed as a linear eigenvalue problem based on linear representations of both struture and aerodynamics. The resulting eigenvalues are then independent of initial conditions or initial disturbance by the assumption of linearity. A nonlinear problem requires considerably more effort to determine the overall characteristics as the stability characteristics are dependent

on the level of input, etc. Furthermore, the nonlinear characteristics are not generally as well known as the level of effort of testing or analysis is considerably increased. However, some aeroelastic analyses have been performed that consider nonlinearities. Some simplified structural nonlinearities have been considered by Woolston, et al. (1955) both experimentally and by analog computation. Nonlinear structural representations of panels in the problem of panel flutter have recently been considered by Dowell (1970) and Morino, et al. (1969).

The corresponding aerodynamic nonlinear considerations are also sparse. However, Landa and Gtrelkov (1963) have given some results of an analog computation using Newtonian aerodynamics at high angle of attack and including the second harmonic resulting from the derivative of $C_p = 2 \sin^2 \delta$. A second dip in the flutter speed was demonstrated as $\omega_h/\omega_\alpha \to 2$ in addition to the usual dip for $\omega_h/\omega_\alpha \to 1$. The implications of such a trend are potentially serious in a multimodal situation if such nonlinear effects in the aerodynamics generate large second or higher harmonics. Zartarian and Sauerwine (1962) have indicated the presence of second harmonics for large amplitude oscillations of a biconvex airfoil as calculated from third order piston theory and from a local shock-expansion theory, but no application was made. As previously discussed the analyses of Kuiken (1968), Kacprzynski (1968), and of Hui (1970) give nonlinear aerodynamic forces on a wedge executing simple harmonic motion of low frequency. The quasi-static solution is briefly analyzed in Chapter 5 in order to determine where nonlinear effects might need consideration for the oscillating wedge. The analysis of the quasi-static results is discussed with the results of

the finite-difference calculation which has the potential for calculating nonlinear forces. It might also be noted that for second order piston theory (small $M\theta_w$), the second harmonic cancels (Lighthill, 1953). Such would not be the case for a flat plate at high angle of attack, for example, where only one surface would be effective.

It might also be noted that Muhlstein (1971) has measured large second harmonics in the pressure distribution over a wavy wall in the transonic range.

3. A STUDY OF HYPERSONIC SMALL DISTURBANCE THEORY FOR AN OSCILLATING WEDGE

3.1 Aerodynamic Forces for Pitching and Plunging Oscillations

A thin, two-dimensional wedge undergoing small oscillations in a perfect gas flow has been treated by McIntosh (1965a, 1965b) from the standpoint of the hypersonic small disturbance theory given by Van Dyke (1954b). McIntosh's solution differs from piston theory, which is also based on hypersonic small disturbance theory, in that it considers the change in the local external flow field resulting from the bow shock wave; considers the effects of reflection of acoustic waves generated by the surface motion from the bow shock onto the surface; and is not limited to $M\theta_w \ll 1$. The resulting surface pressure coefficient for linearized oscillatory motion about the nonlinear steady flow field (in somewhat different notation) is:

$$C_p(x,t) = \frac{2FK_\tau}{M} \left\{ f_w'(x) + 2ik\, f_w(x) + 2\sum_{n=1}^{\infty} (-\lambda)^n\, e^{2ik(\Gamma^n - 1)} \left[f_w'(\Gamma^n x) + 2ik\, f_w(\Gamma^n x) \right] \right\} \zeta\, e^{2ikt} \qquad 3.1$$

where $f_w(x)$ and $f_w'(x)$ are the normalized wedge deformation mode shape amplitude $(\bar{f}_w/\bar{c})$, and slope; ζ is modal amplitude, h or θ here; k is reduced frequency, $\bar{c}\bar{\omega}/2\bar{V}_\infty$; $K_\tau = M\tau$ where M is Mach number and τ is steady shock wave slope; $F = \left[\dfrac{2\gamma K_\tau^2 - (\gamma - 1)}{2 + (\gamma - 1) K_\tau^2} \right]^{1/2}$; λ is the attenuation factor for disturbances reflected from the shock; and Γ is

a reflection length coefficient. The physical interpretation of (3.1) is that the pressure at point x is proportional to the effective local slope at x, $(f'_w + 2ik\, f_w)$, multiplied by the linearized slope-pressure relation $\frac{2}{M}$ and the factor that gives the local flow correction, FK_T; plus the additional portion given by the sum which results from acoustic reflection effects, made up of the reflection attenuation $(-\lambda)^n$, a phase factor $e^{2ik(\Gamma^n - 1)}$, and the effective slope at point $(\Gamma^n x)$. Thus the point x is affected by points upstream Γx, Γx^2, ..., (as $\Gamma \leq 1$).

The surface pressure, coefficient is integrated over the chord of airfoil. The resulting aerodynamic forces are expressed as coefficients in the form given by Garrick and Rubinow (1946) and subsequently discussed and defined herein in section 4.3.3. The resulting expressions for the coefficients for pitching about the leading edge and for plunging motions are (multiplied by factors of M and k, and with moments taken about the vertex):

$$ML_1 = 4FK_T \sum_{n=1}^{\infty} (-\lambda)^n (1 - \Gamma^n) \frac{(1 - \cos \beta_n)}{\beta_n^2}$$

$$kML_2 = FK_T \left[1 + 2 \sum_{n=1}^{\infty} (-\lambda)^n \frac{\sin \beta_n}{\beta_n} \right]$$

$$MM'_1 = 8FK_T \sum_{n=1}^{\infty} (-\lambda)^n (\Gamma^n - 1) \frac{\left[\cos \beta_n - \frac{\sin \beta_n}{\beta_n} \right]}{\beta_n^2}$$

$$kMM'_2 = 2kML_2 - FK_T \left[1 + 4 \sum_{n=1}^{\infty} (-\lambda)^n \frac{(1 - \cos \beta_n)}{\beta_n^2} \right]$$

$$k^2 ML_3' = kML_2 + 8k^2 FK_T \sum_{n=1}^{\infty} (-\lambda)^n (\Gamma^n)(\Gamma^n - 1) \frac{\left[\cos \beta_n - \frac{\sin \beta_n}{\beta_n}\right]}{\beta_n^2}$$

$$kML_4' = -(ML_1) + FK_T \left[1 + 4 \sum_{n=1}^{\infty} (-\lambda)^n (\Gamma^n) \left(\frac{\cos \beta_n - 1}{\beta_n^2} + \frac{\sin \beta_n}{\beta_n}\right)\right]$$

$$k^2 MM_3' = kMM_2'$$

$$+ 16k^2 FK_T \sum_{n=1}^{\infty} (-\lambda)(\Gamma^n)(\Gamma^n - 1) \frac{\left[\cos \beta_n - \frac{2 \sin \beta_n}{\beta_n} + \frac{2(1 - \cos \beta_n)}{\beta_n^2}\right]}{\beta_n^2}$$

$$kMM_4' = -(MM_1')$$

$$+ 4 FK_T \left\{\frac{1}{3} + 2 \sum_{n=1}^{\infty} (-\lambda)^n (\Gamma^n) \left[\frac{\sin \beta_n}{\beta_n} + \frac{2}{\beta_n^2} \left(\cos \beta_n - \frac{\sin \beta_n}{\beta_n}\right)\right]\right\} \tag{3.2}$$

The transfer of the moment coefficients to axes other than the leading edge is discussed in section 8.3.

As $\beta_n = 2k(\Gamma^n - 1)$, and λ and Γ are functions of $M\theta_w$ and γ only, the coefficients written in the form of equations (3.2) are functions of γ, $M\theta_w$, and k, and are valid for $M \gg 1$, $\theta_w \ll 1$, $0 \leq M\theta_w \leq \infty$, and $k < 1$ (for the restriction on k see Hayes and Probstein (1966, pp. 113-116)). These coefficients have also been given by Bailie and McFeely (1966) and McIntosh (1965b) in somewhat different form. The form given herein is such that each term should be finite as

$k \to 0$. However, note that as $k \to 0$, $\beta_n \to 0$ and each of expressions (3.2) involve indeterminant forms and must be given special attention for the small values of k of interest in the hypersonic speed range. Computational forms for $k \ll 1$ are developed by using series expansions for the sine and cosine converting the summations of (3.2) to double summations. For example ML_1 becomes,

$$ML_1 = 4FK_T \sum_{n=1}^{\infty} (-\lambda)^n (1 - \Gamma^n) \sum_{m=1}^{\infty} (-1)^{m+1} \frac{\beta_n^{2(m-1)}}{2m!}$$

The expressions for K_T, λ, and Γ from McIntosh (1965a) are functions of $K = M\theta_w$ and γ as follows.

$$K_T = B + \sqrt{1 + B^2}$$

where,

$$B = \frac{(\gamma + 1)K}{4}$$

$$\lambda = \frac{C - D}{C + D} \tag{3.4}$$

where

$$C = \frac{2(K_T^2 + 1)}{(\gamma + 1)K_T^2}$$

$$D = \frac{4}{(\gamma + 1)F}$$

and

$$\Gamma = \frac{-1 + \frac{K}{K_T} + \frac{F}{(\gamma + 1)}\left(\gamma - 1 + \frac{2}{K_T^2}\right)}{1 - \frac{K}{K_T} + \frac{F}{(\gamma + 1)}\left(\gamma - 1 + \frac{2}{K_T^2}\right)}$$

where

$$F = \left(\frac{2\gamma K_T^2 - (\gamma - 1)}{2 + (\gamma - 1) K_T^2} \right)^{1/2}$$

Note that the expression for K_T as given above is that of thin shock theory (for example, see Truitt (1959), eqs. 2-153 and 2-156).

3.2 Low Reduced-Frequency Limiting Case

In the low frequency (k) expansions for the aerodynamic forces (3.2), each inner sum for the sine and cosine expansions is of the form of the series of (3.3) involving only even powers of $\beta_n = 2k\,(\Gamma^n - 1)$. If one neglects the terms of $0(k^2)$ and higher and retains only the constant term, the series over n sum in closed form. The following simplified expressions are then obtained.

$$ML_1 = -2FK_T \left(\frac{\lambda}{1 + \lambda} \right) \left(\frac{1 - \Gamma}{1 + \lambda\Gamma} \right)$$

$$kML_2 = FK_T \left(\frac{1 - \lambda}{1 + \lambda} \right)$$

$$kML_4' = -ML_1 + FK_T \left(\frac{1 - \lambda\Gamma}{1 + \lambda\Gamma} \right) \tag{3.5}$$

$$k^2 L_3' = k^2 M_3' = kM_2' = kL_2$$

$$M_1' = \frac{4}{3} L_1$$

$$kM_4' = \frac{4}{3} kL_4'$$

Only the three coefficients ML_1, kML_2, and kML_4' are required with (8.12) for a complete description of aerodynamic forces for small values of k. As subsequently discussed in Chapter 4, computations have

also shown that the effect of frequency is negligible for the applicable range of $k < 1$ except for a k^2 - variation in $k^2 L_3'$ and $k^2 M_3'$ for $\gamma < 1.2$. Thus, the above results can be considered the complete solution for the normal range of reduced frequencies for hypersonic flutter. Some of the above relations, in different notation, and some approximating functions have also been given by Orlik-Rückemann (1966b and 1969).

Substituting for λ, F, and K_T from equations (3.4) gives

$$kML_2 = \frac{\gamma + 1}{2} K + \frac{(\gamma + 1)^2 K^2 + 8}{2\sqrt{(\gamma + 1)^2 K^2 + 16}} \tag{3.6}$$

which gives a result that can be obtained by differentiating the well known thin shock layer result, that is, equation (2-156) of Truitt (1959). Thus, a closed form solution is obtained for the major portion of the aerodynamic forces. However, no such reduction has been obtained for ML_1 or kML_4'.

It might also be noted that the flutter derivatives used herein, and stability derivatives are related for $k \to 0$ and to first order in k as (for example, see Van Dyke (1954a)):

$$C_{l_\alpha} = 4KL_2 \qquad C_{m_\alpha} = -2kM_2$$

$$C_{l_{\dot{\alpha}}} = -4L_1 \qquad C_{m_{\dot{\alpha}}} = 2M_1$$

$$C_{l_{\dot{\alpha}}} + C_{l_q} = 4kL_4' \qquad C_{m_{\dot{\alpha}}} + C_{m_q} = -2kM_4' \tag{3.7}$$

3.3 Limiting Case for Large $M\theta_w$

For $M\theta_w \gg 1$ for which the effects of wave reflections become more significant, limiting forms of (3.5) can be obtained that reveal

the role of the shock reflection process and γ. Expanding F, K_T, λ and Γ as series in $1/K$ and substituting in (3.5) gives

$$kML_2 = (\gamma + 1)\, K + \dot{O}(1/K^3) \tag{3.8}$$

$$ML_1 = -\frac{(\gamma + 1)}{2}\frac{(2 - \gamma)}{(2\gamma - 1)} K + \frac{(3 + 14\gamma - 7\gamma^2)}{(\gamma + 1)(2\gamma - 1)^2}\frac{1}{K} + O(1/K^3)$$

$$kML_4' = \frac{(\gamma + 1)^2}{(2\gamma - 1)} K - \frac{2\,(3 + 14\gamma - 7\gamma^2)}{(\gamma + 1)(2\gamma - 1)^2}\frac{1}{K} + O(1/K^3)$$

$$ML_1' + kML_4' = \frac{3\gamma(\gamma + 1)}{2(2\gamma - 1)} - \frac{(3 + 14\gamma - 7\gamma^2)}{(\gamma + 1)(2\gamma - 1)^2}\frac{1}{K} + O(1/K^3)$$

The result for kML_2 is given by the well-known limiting case of thin shock layer theory (Truitt, 1959, eq. 2-157) for large $M\theta_w$ with $C_p = (\gamma + 1)\,\theta_w^2$. The parameter $(\gamma + 1)K$ is thus a similarity parameter for static pressure and thus for lift-curve slope. The above expressions are the consistent relations for the stability derivatives to the same level of approximation and the leading terms are identified as similarity parameters. Results from the complete expressions (3.5) are compared in figure 3.1 with the results from (3.8) retaining terms $O(K)$ and also retaining terms $O(1/K)$. The use of the leading terms of (3.8) as similarity parameters gives results comparable to the results shown in figure 3.1 for retaining only $M\theta_w$ terms. These similarity parameters are thus somewhat weak. It has been noted that the use of the leading term for ML_1 and for $(kML_4' + ML_1)$ is somewhat better than for kL_4' which implies that the similarity parameter for $\dot{\alpha}$-type terms (see

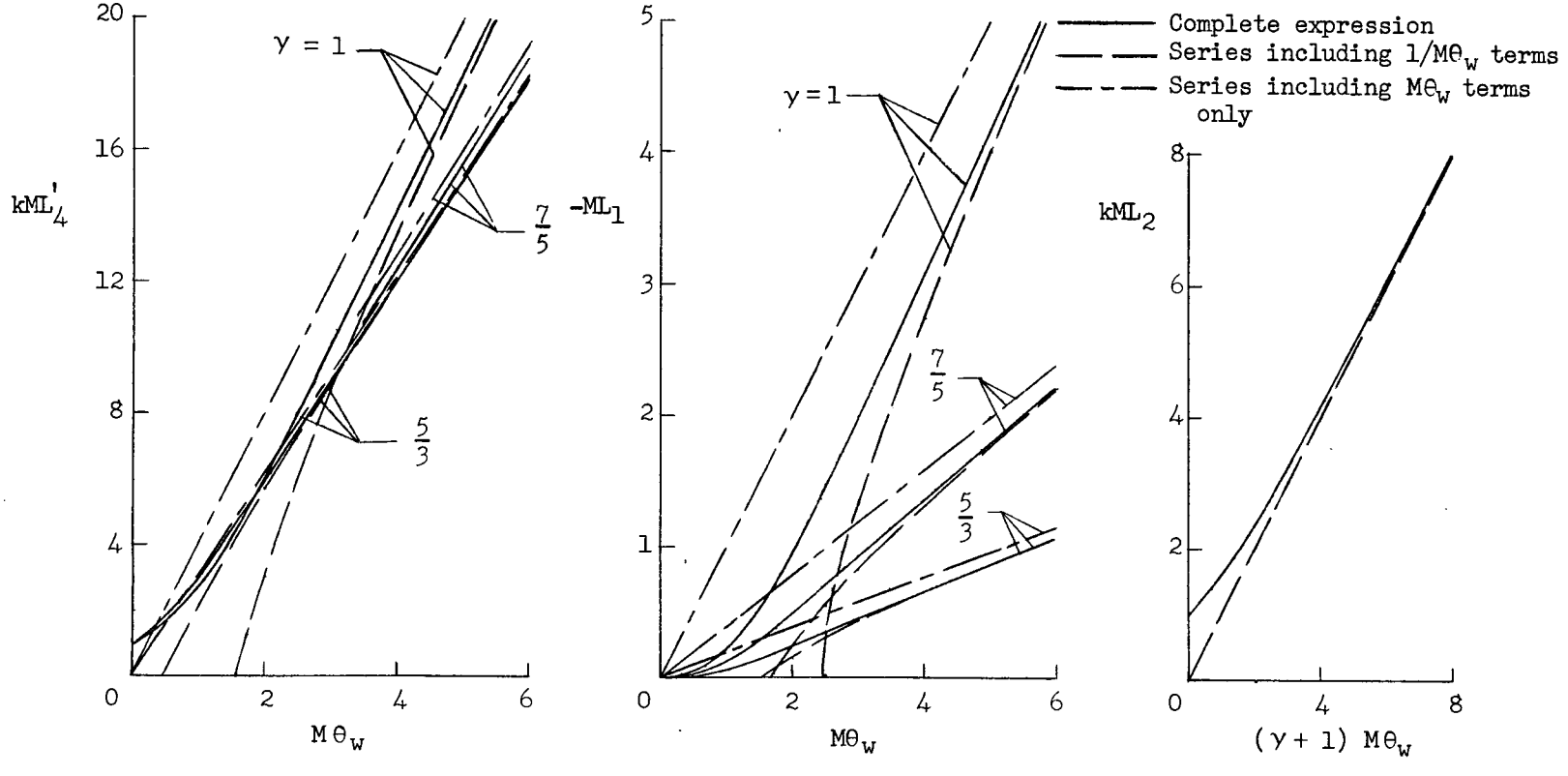

Figure 3.1.- Comparison of aerodynamic forces at $k = 0$ from complete expressions (3.5) and series expansions (3.8)

eq 3.7) is of different form than for $\dot{\theta}$-type terms.

3.3.1 Limiting Forms for λ and Γ

Series expansions for λ and Γ in $1/K$ give:

$$\lambda = \frac{1 - \sqrt{2(\gamma - 1)/\gamma}}{1 + \sqrt{2(2 - 1)/\gamma}} + O(1/K^2)$$

$$\Gamma = \frac{2 - \sqrt{2(\gamma - 1)/\gamma}}{2 + \sqrt{2(\gamma - 1)/\gamma}} + O(1/K^2)$$

These are the expressions used in deriving (3.8) and are the limiting forms for $K \gg 1$ given by Chernyi (1961, p. 189). The strong effect of γ on λ is apparent as $0.0557 \leq \lambda \leq 1$ for $5/3 \leq \gamma \leq 1$.

3.3.2 Effect of Wave Reflections on Aerodynamic Forces

For no wave reflections $\lambda = 0$ in equations (3.5) such that:

$$ML_1 = MM_1' = 0$$

$$kML_2 = kML_4' = kMM_2' = k^2ML_3 = k^2MM_3' = FK_T \qquad (3.9)$$

These are the results given by linearized piston theory (see, for example, Ashley and Zartarian, 1956) multiplied by FK_T which accounts for local external flow effects. Series expansion for FK_T for $K \gg 1$ gives,

$$FK_T = \frac{(\gamma + 1)}{\sqrt{2(\gamma - 1)/\gamma}} K + \frac{(\gamma + 1)}{\sqrt{2(\gamma - 1)/\gamma}} \left[\frac{3\gamma^2 - 6\gamma - 1}{\gamma(\gamma - 1)(\gamma + 1)^2}\right] \frac{1}{K} + O(1/K^3)$$

Thus all aerodynamic terms are singular as $\gamma \to 1$ and wave reflections are essential for the theory to yield reasonable results as $\gamma \to 1$. This singular behavior has been discussed by Miles (1960).

For $M\theta_w \to \infty$, $\lambda \to 0.14$ for $\gamma = 1.4$. The modification of the above results for kML_2 resulting from the inclusion of wave reflections is, from (3.5), a multiplying factor of $1 - 2\lambda + O(\lambda^2) = 0.72$ for $\gamma = 1.4$. Thus the correction to lift curve slope can be more than 25 percent for large values of $M\theta_w$ for $\gamma = 1.4$ and a "local flow theory" which would neglect this effect could be considerably in error for $M\theta_w > 1$.

Omitting the wave reflections also gives $ML_1 = MM_1' = 0$ which is also the case with piston theory in which the local pressure depends only on the local effective piston velocity. These terms are essentially $C_{l_{\dot\alpha}}$ and $C_{m_{\dot\alpha}}$, respectively, which result normally from downwash lags. The wave reflection process is one mechanism for generating an effect like a downwash lag, resulting in nonzero values for these coefficients when the reflections are included. A further discussion of $\dot\alpha$ effects at hypersonic speeds had been given by Ericsson (1968).

3.4 Comparison With Other Theories

Chawla (1958) has given the corresponding aerodynamic forces for third order piston theory for a wedge as:

$$L_1 = M_1' = 0$$

$$kML_2 = 1 + \frac{(\gamma + 1)}{2} K \left[1 + \frac{K}{2}\right]$$

$$kML_4' = k^2 ML_3' = kMM_2' = k^2 MM_3' = kML_2$$

$$kMM_4' = \frac{4}{3} kML_2 \qquad (3.10)$$

For $M\theta_w \ll 1$ expansion of equation (3.6) gives,

$$kML_2 = 1 + \frac{(\gamma + 1)}{2} K \left[1 + \frac{3(\gamma + 1)}{16} K \right] + O(K^3)$$

which agrees with (3.5) to $O(K)$. The coefficients of K^2 are slightly different, as they should be, as piston theory is based on the series for an expansion wave which differs slightly in the third order term from the series for a shock wave (Lighthill, 1953). For small K the effects of wave reflections become small so that L_1 and M_1' also become negligibly small. Thus, it is demonstrated that piston theory is a small K subcase of equations (3.5).

Van Dyke (1954b) has shown that the Newtonian plus centrifugal force (sometimes called Newtonian snowplow theory) is one limit of the hypersonic small disturbance theory. For Newtonian conditions, $\gamma \to 1$ and $K \gg 1$, the leading term of equations (3.8) give the results for Newtonian theory with centrifugal forces included. Letting $\gamma = 1$ and using equations (3.8) it can be shown that results agree with those of Aroesty, et al. (1966) which were obtained by an expansion about $\gamma = 1$ in a different fashion. The results for the wedge (3.8) can be regarded as a generalization of the Newtonian plus centrifugal force theory to arbitrary γ and somewhat small values of K.

The pitch rate derivatives are often computed on tangent wedge basis, or Newtonian theory omitting centrifugal force effects, by assuming that the local pressure is that of a wedge having the same slope as local effective slope of the airfoil including motion effects. The effective slope of a lower surface is given by:

$$\theta_e = \theta_w + \dot{h} + \theta + x\dot{\theta}$$

where superscript dot indicates $\frac{d}{d\bar{t}}$, and $\bar{V}_\infty$ is used as the reference external velocity consistent with small disturbance theory. Using

$$C_p = (\gamma + 1)\ \theta_e^{\ 2}$$

and performing the appropriate integrations, the relations (3.9) are obtained with $kML_2 = (\gamma + 1)\ K$. Thus the dependence upon γ and K is considerably different than that given by (3.8) for the rate derivatives. The value of a tangent wedge method for large K for the dynamic derivatives would be heuristic in view of this comparison. Piston theory, however, is one form of a tangent wedge theory which is satisfactory for $K \ll 1$.

3.5 Flutter of a Typical Section

An analytical model that has been extensively used to examine flutter trends is a rigid, two-dimensional airfoil restrained in an airstream by torsional and translation springs. The dynamical equations and an exact solution for the neutral stability boundary based on piston theory aerodynamics are well known (for example, Bisplinghoff and Ashley, 1962, chapter 6). No such exact solution can be obtained using aerodynamic forces that vary with frequency such as equations (3.2) and the flutter condition must be sought by an iterative or other technique. However, if frequency independent aerodynamic forces such as (3.5) are used, the following exact solution results:

$$\frac{\bar{V}_f}{\bar{b}\,\omega_\alpha\sqrt{\mu M}} = \left[\frac{r_\alpha^2}{kML_2}\left(\frac{\omega_f}{\omega_\alpha}\right)^2 \frac{N}{D}\right]^{1/2}$$

$$N = \left[1 - \left(\frac{\omega_\alpha}{\omega_f}\right)^2\right]\left[1 - \left(\frac{\omega_h}{\omega_\alpha}\right)^2\left(\frac{\omega_\alpha}{\omega_f}\right)^2 - \frac{ML_1}{\mu M}\right] - \left[\frac{x_\alpha}{r_\alpha^2}\right]\left[x_\alpha - \left(\frac{4}{3} - 2x_0\right)\frac{ML_1}{\mu M}\right]$$

$$D = \left[1 - 2x_0\right]\left[1 - \left(\frac{\omega_h}{\omega_\alpha}\right)^2\left(\frac{\omega_\alpha}{\omega_f}\right)^2\right] - x_\alpha + \frac{ML_1}{3\mu M} + \frac{kML_4'}{3\mu M}$$

and

$$\left(\frac{\omega_f}{\omega_\alpha}\right)^2 = \frac{\bar{N}}{\bar{D}}$$

where

$$\bar{N} = 1 - \frac{1}{r_\alpha^2}\left(\frac{\omega_h}{\omega_\alpha}\right)^2\left[2x_0\,(1 - 2x_0) - \left(\frac{4}{3} - 2x_0\right)\frac{kML_4'}{kML_2}\right]$$

$$\bar{D} = 1 - \frac{1}{r_\alpha^2}\left[2x_0\,(1 - 2x_0) - \left(\frac{4}{3} - 2x_0\right)\frac{kML_4'}{kML_2}\right]$$

$$- \frac{1}{r_\alpha^2}\left[\frac{2x_0\,ML_1}{3\mu M} + x_\alpha\left(1 - 4x_0 + \frac{MkL_4'}{MkL_2}\right)\right]$$

The above solution can be applied with aerodynamics from (3.5), (3.8), or (3.9). If piston theory (3.10) is used, then the same result as Chawla (1958) is obtained. The present solution (3.11) includes ML_1 and MM_1', which are zero in piston theory, and thus retains terms of one higher order in k. The solution (3.11) is a function of the structural parameters $\frac{\omega_h}{\omega_\alpha}$, x_α, x_0, r_α^2 and of the aerodynamic similarity parameters $K = M\theta_w$, γ, and μM only. The parameter μM

gives an equivalence between Mach number and altitude ($\mu = \bar{m}/\rho\,\bar{c}^2$) which has previously appeared in piston theory results (see Bisplinghoff and Ashley 1962, p. 253).

Some results are presented in figure 3.2 to indicate the relative importance of ML_1, or $\dot{\alpha}$ terms, and kML_4', or $q = \frac{\dot{\theta}\,\bar{c}}{2V_\infty}$ terms. The effect of ML_1 is apparent at low values of μM and as can be seen from (3.11) where it appears only in the ratio $ML_1/\mu M$. However, kML_4' has an effect even for large values of μM as it appears in (3.11) independent of μM. (Similar results have been presented for low speed flutter by Lambourne (1967).) The results are accentuated for large values of ω_h/ω_α and inclusion of kML_4' is essential for flutter prediction. A decrease in γ to 1 (not shown) also affects the result by about 10 percent. It is also of some significance that at flutter, k decreases rapidly as μM increases, and is small for large values of μM; the approximations (3.8) are thus applicable for practical cases of large μM.

One consequence of the different effects of γ on each of MkL_4', MkL_2, and ML_1 as indicated by the similarity parameters of equations 3.8 is that a combined similarity parameter for flutter is not apparent. Thus, boundaries such as given in figure 3.2 must be calculated for each value of γ and $M\theta_w$.

With an attached bow wave, the upper and lower surfaces of the wedge are independent. The preceding development can thus be applied for determining the effects of initial angle of attack for $\alpha_0 < \theta_w$ and $\alpha_0 \ll 1$ by taking half of (3.2), (3.5), or (3.8), using $\theta_c = \theta_w + \alpha_0$

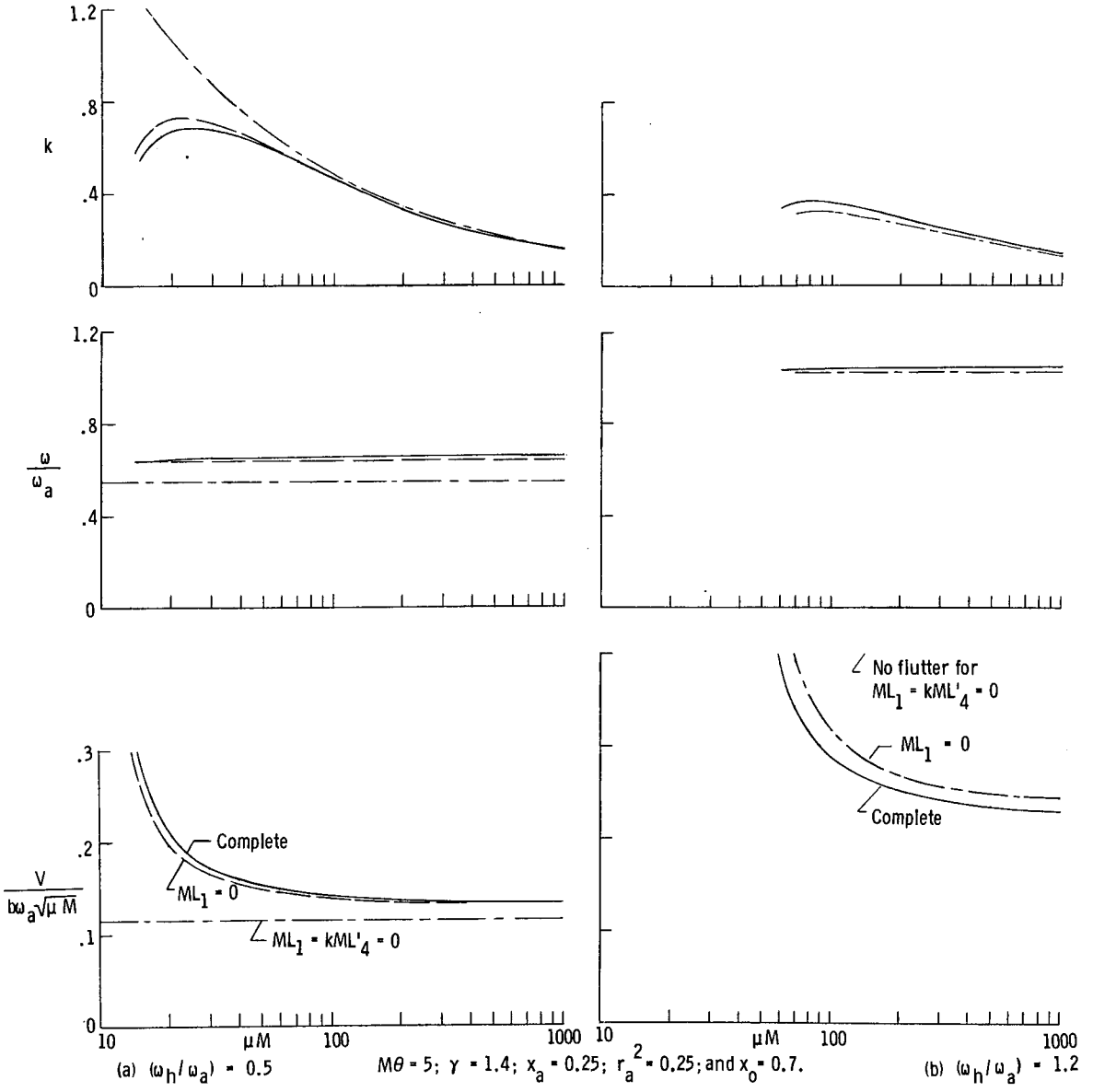

Figure 3.2.- Flutter characteristics of wedge airfoil

for the lower surface, and adding similar results based on $\theta_c = \theta_w - \alpha_0$ for the upper surface. For $K \gg 1$, the leading terms of (3.8) are proportional to K and the resulting expressions involve only the average K, which is $M\theta_w$, and there is no effect of angle of attack on any of the aerodynamic forces. The effect of the terms $O(\frac{1}{K})$ would give a very small modification of this result as $\alpha_0 \ll 1$. From piston theory for $M\theta_w \ll 1$, including initial angle of attack gives (Chawla, 1958):

$$kML_2 = 1 + \frac{(\gamma + 1)}{2}\left[K + \frac{K^2}{2} + \frac{(M\alpha_0)^2}{2}\right]$$

where $\left|K \pm M\alpha_0\right| < 1$. For $K \to 0$ and $M\alpha_0 = 0.5$, for example, the effect of $M\alpha_0$ is 15 percent for $\gamma = 1.4$. Thus the effects of a small initial angle of attack for a thin wedge airfoil varies from a modest effect for $M\theta_w < 1$ to no effect for $M\theta_w \gg 1$. The initial flutter speed gradient can, however, be sizeable if M is very large and θ_w is small.

4. LINEARIZED PERTURBATIONS ABOUT STEADY FLOW CONDITIONS

A two-dimensional flat surface with a sharp leading edge and exposed to a supersonic freestream flow of a perfect gas at a mean inclination angle of θ_w is considered while undergoing a specified time-dependent motion (figure 4.1). Three types of simple-harmonic oscillations are considered separately – pitching about the leading edge θ, translation normal to the mean position of the surface h_y, and translation parallel to the mean position of the surface h_x. The motion is considered to be an infinitesimal perturbation about the mean or steady-flow condition which leads to a linearized analysis describing the region between the moving surface and shock-wave boundaries beginning at the wedge tip and extending a preassigned distance downstream. Linearization of the governing equations permits the application of the boundary conditions at the mean position of the moving boundaries and also permits treatment of any rigid-body, time-dependent motion of the flat surface by superposition of the three motions considered. There are essentially three criteria that govern the amplitude limits for "small" oscillations: (1) fraction of $\lambda_0 = \beta_0 - \theta_w$ (2) fraction of θ_w (or for very small θ_w, fraction of p_∞), or (3) fraction of $\theta_d - \theta_w$ where θ_d is the detachment angle. It might be noted that only compression surfaces are treated; however, in a linearized analysis of an expansion surface, the linear theory of Garrick and Rubinow (1946) can be applied considering the mean surface flow to be the effective freestream. Also for application to wedges, the base pressure is assumed constant and thus does not enter into the motion-related force and moment coefficients.

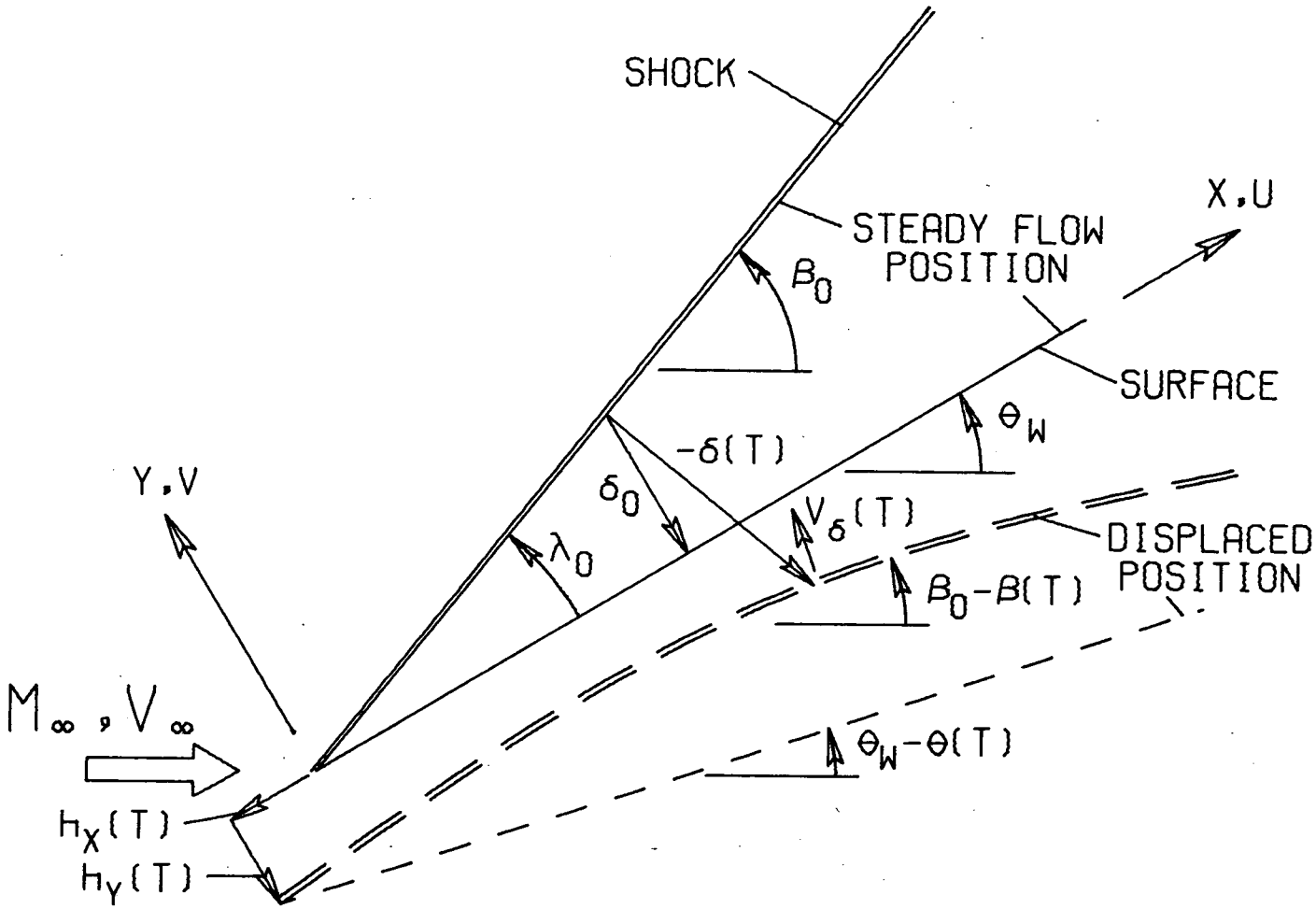

Figure 4.1.- Oscillating flat surface and coordinate system

The hypersonic small distrubance theory treated in Chapter 3 also considers perturbations about the steady flow for thin wedges and hypersonic Mach numbers. Here both supersonic and hypersonic Mach numbers are treated, both large and small inclination angles are considered, and the fore-and-aft translational motion h_x, which is not significant for hypersonic small disturbance conditions, is also analyzed.

4.1 Development of Perturbation Equations

The governing equations written in divergence form for the x-y coordinate system (e.g., Leipmann and Roshko, 1957, Chapter 7):

continuity:

$$\frac{\partial \bar{\rho}}{\partial \bar{t}} + \frac{\partial(\bar{\rho}\bar{u})}{\partial \bar{x}} + \frac{\partial(\bar{\rho}\bar{v})}{\partial \bar{y}} = 0 \qquad (4.1a)$$

x-momentum:

$$\frac{\partial(\bar{\rho}\bar{u})}{\partial \bar{t}} + \frac{\partial(\bar{p} + \bar{\rho}\bar{u}^2)}{\partial \bar{x}} + \frac{\partial(\bar{\rho}\bar{u}\bar{v})}{\partial \bar{y}} = 0 \qquad (4.1b)$$

y-momentum:

$$\frac{\partial(\bar{\rho}\bar{v})}{\partial \bar{t}} + \frac{\partial(\bar{\rho}\bar{u}\bar{v})}{\partial \bar{x}} + \frac{\partial(\bar{p} + \bar{\rho}\bar{v}^2)}{\partial \bar{y}} = 0 \qquad (4.1c)$$

energy:

$$\frac{\partial}{\partial \bar{t}}\left[\frac{\bar{p}}{\gamma} + \frac{(\gamma - 1)}{2\gamma}\,\bar{\rho}(\bar{u}^2 + \bar{v}^2)\right] + \frac{\partial}{\partial \bar{x}}\left[\bar{u}\left(\bar{p} + \frac{(\gamma - 1)}{2\gamma}\,\bar{\rho}(\bar{u}^2 + \bar{v}^2)\right)\right] + \frac{\partial}{\partial \bar{y}}\left[\bar{v}\left(\bar{p} + \frac{(\gamma - 1)}{2\gamma}\,\bar{\rho}(\bar{u}^2 + \bar{v}^2)\right)\right] = 0 \qquad (4.1d)$$

where the barred quantities are dimensional.

Small variations about the steady flow are considered by substituting in equation 4.1:

$$\bar{p} = \bar{p}_0 + \epsilon\, \bar{p}_1\, (\bar{x},\bar{y})\, e^{i\bar{\omega}\,\bar{t}}$$

$$\bar{\rho} = \bar{\rho}_0 + \epsilon\, \bar{\rho}_1\, (\bar{x},\bar{y})\, e^{i\bar{\omega}\,\bar{t}}$$

$$\bar{u} = \bar{u}_0 + \epsilon\, \bar{u}_1\, (\bar{x},\bar{y})\, e^{i\bar{\omega}\,\bar{t}}$$

$$\bar{v} = \epsilon\, \bar{v}_1\, (\bar{x},\bar{y})\, e^{i\bar{\omega}\,\bar{t}}$$

where ϵ is a small quantity; $\bar{\omega}$ is the frequency of oscillation; $\bar{p}_1$, and so forth, are complex-valued perturbations in the flow variables (subscript 1); and $\bar{p}_0$, and so forth, pertain to the steady or mean wedge flow. Neglecting terms $O(\epsilon^2)$ and higher gives, for the y-momentum equation, for example

$$\bar{\rho}_0\, \bar{u}_0\, \frac{\partial \bar{v}_1}{\partial \bar{x}} + \frac{\partial \bar{p}_1}{\partial \bar{y}} + i\bar{\omega}\, \bar{\rho}_0\, \bar{v}_1 = 0$$

The equations are simpler in form if normalized by the shock-layer variables $\bar{\rho}_0$ and $\bar{u}_0$ and if the shock-layer wavelength, $\bar{u}_0/\bar{\omega}$ is used as the characteristic length. Setting $p_1 = \bar{p}_1/(\bar{\rho}_0\, \bar{u}_0^{\,2})$, $\rho_1 = \bar{\rho}_1/\bar{\rho}_0$, $u_1 = \bar{u}_1/\bar{u}_0$, $v_1 = \bar{v}_1/\bar{u}_0$, $x = \bar{x}\bar{\omega}/\bar{u}_0$, and $y = \bar{y}\bar{\omega}/\bar{u}_0$

the resulting equations are:

y-momentum:

$$\frac{\partial v_1}{\partial x} + \frac{\partial p_1}{\partial y} + i v_1 = 0 \qquad (4.2a)$$

x-momentum:

$$\frac{\partial u_1}{\partial x} + \frac{\partial p_1}{\partial x} + i u_1 = 0 \qquad (4.2b)$$

energy:

$$\frac{\partial p_1}{\partial x} + \frac{1}{B_0^2} \frac{\partial v_1}{\partial y} + i \frac{(M_0^2 p_1 - u_1)}{B_0^2} = 0 \qquad (4.2c)$$

continuity:

$$\frac{\partial \rho_1}{\partial x} + \frac{\partial u_1}{\partial x} + \frac{\partial v_1}{\partial y} + i \rho_1 = 0 \qquad (4.2d)$$

where $B_0^2 = M_0^2 - 1$. Equation (4.2c) is obtained by subtracting (4.2b) from the complete energy equation. Note that the continuity equation (4.2d) is not needed except to calculate ρ and will be disregarded here. Thus, (4.2a-c) is a system of three simultaneous, linear partial differential equations for p_1, u_1, and v_1 as functions of x and y and with complex, constant coefficients.

4.2 Boundary Conditions

4.2.1 Boundary Conditions at the Wedge Tip

For the assumed attached leading edge shock, the shock displacement boundary condition at the wedge tip for pitching motion is

$$\delta (0) = 0 \qquad (4.3a)$$

for plunging motion normal to surface (omitting $h_y e^{i\bar{\omega} \bar{t}}$)

$$\delta (0) = - \cos \lambda_0 \qquad (4.3b)$$

and for translation parallel to surface

$$\delta (0) = \sin \lambda_0 \qquad (4.3c)$$

4.2.2 Boundary Condition at the Wedge Surface

The tangent flow condition at the wedge surface (subscript s) for infinitesimal pitching motion is (also omitting $\theta e^{i\bar{\omega} \bar{t}}$)

$$v_{1,s} = -(1 + ix) \tag{4.4a}$$

for plunging motion normal to the surface

$$v_{1,s} = -i \tag{4.4b}$$

and for translation parallel to the surface

$$v_{1,s} = 0 \tag{4.4c}$$

4.2.3 Boundary Conditions at the Shock Wave

The perturbations of the flow variables at the moving oblique shock wave are discussed in Section 8.2. At the shock boundary (subscript δ) the changes in the flow variables are given by equations (8.2 – 8.5) in the following form

$$p_{1,\delta} = P_\beta \beta + i P_v \delta \tag{4.5a}$$

$$u_{1,\delta} = U_\beta \beta + i U_v \delta \tag{4.5b}$$

$$v_{1,\delta} = V_\beta \beta + i V_v \delta \tag{4.5c}$$

where

$$\beta = \frac{d\delta}{dx} \cos \lambda_0 \tag{4.5d}$$

and $P_\beta = \partial p_{1,\delta}/\partial\beta$ and so forth, are derivatives of the shock relations evaluated at the steady or mean conditions.

4.3 Approximate Solution by the Method of Integral Relations

For the one-strip integral-relations approach used here, a linear y-variation of p, u, and v is assumed. For example

$$p_1(x,y) = p_s(x) + \left[p_\delta(x) - p_s(x)\right] y/\delta(x)_{total} \tag{4.6}$$

where subscripts s and δ refer to the surface and to the shock wave, respectively, $\delta(x)_{total} = \delta_0 + \delta(x)/\cos\lambda_0$ is the total shock layer thickness, and p_s and p_δ are perturbation variables (subscript 1 omitted). Equation (4.6) and similar relations for u and v are used in (4.2a-c) and integrated in the y-direction. Sample terms in (4.2) are:

$$\int_0^\delta p_1(x,y)\, dy = \left[p_s(x) + p_\delta(x) \right] \delta(x)/2 + O(\epsilon^2)$$

$$\int_0^\delta \frac{\partial p_1(x,y)}{\partial y}\, dy = p_\delta(x) - p_s(x) + O(\epsilon^2)$$

and using Leibnitz's rule,

$$\int_0^\delta \frac{\partial p_1(x,y)}{\partial x}\, dy = \frac{d}{dx} \int_0^\delta p_1(x,y)\, dy - \frac{d\delta}{dx} p_\delta(x)$$

$$= \left[\frac{dp_s(x)}{dx} + \frac{dp_\delta(x)}{dx} \right] \frac{\delta_0(x)}{2}$$

$$+ \frac{1}{2} \left[p_s(x) - p_\delta(x) \right] \frac{d\delta_0(x)}{dx} + O(\epsilon^2)$$

This procedure leads to:

$$\frac{d}{dx}(p_\delta + p_s + u_\delta + u_s) - \frac{1}{\delta_0}(p_\delta - p_s + u_\delta - u_s) \frac{d\delta_0}{dx} + i(u_\delta + u_s) = 0$$

$$\frac{d}{dx}(v_\delta + v_s) - \frac{1}{\delta_0}(v_\delta - v_s) \frac{d\delta_0}{dx} + \frac{2}{\delta_0}(p_\delta - p_s) + i(v_\delta + v_s) = 0$$

$$\frac{d}{dx}(p_\delta + p_s) - \frac{1}{\delta_0}(p_\delta - p_s) \frac{d\delta_0}{dx} + \frac{2}{\delta_0 B_0^2}(v_\delta - v_s)$$

$$+ \frac{i}{B_0^2} \left[M_0^2 (p_\delta + p_s) - (u_\delta + u_s) \right] = 0$$

Now

$$\delta_0(x) = x \tan \lambda_0$$

$$\frac{d\,\delta_0(x)}{dx} = \tan \lambda_0$$

Furthermore, the δ-terms are given by the boundary conditions at the shock wave (eq. 4.5). For example,

$$p_\delta(x) = P_\beta\, \beta(x) + i\, P_v\, \delta(x)$$

and thus

$$\frac{d\, p_\delta}{dx} = P_\beta \frac{d\,\beta(x)}{dx} + i\, P_v \frac{d\,\delta(x)}{dx} = P_\beta \frac{d\,\beta(x)}{dx} + i \frac{P_v}{\cos \lambda_0}\, \beta(x)$$

as $\beta = \frac{d\delta}{dx} \cos \lambda_0$. Using similar terms for u_δ and v_δ, and so forth, gives the following equations.

$$x \frac{d\beta}{dx} + \left[\frac{2\, P_\beta}{V_\beta} \cot \lambda_0 - 1 + i\, x\left(1 + \frac{V_v}{V_\beta \cos \lambda_0}\right)\right] \beta + i \left[\frac{2\, P_v}{V_\beta} \cot \lambda_0 - (1 - i\, x) \frac{V_v}{V_\beta}\right] \delta - \frac{2 \cot \lambda_0}{V_\beta}\, p_s = - \frac{x}{V_\beta} \frac{dv_s}{dx} - \frac{v_s}{V_\beta} (1 + i\, x) \qquad (4.7a)$$

$$x \frac{du_s}{dx} + (1 + i\, x)\, u_s + x \frac{dp_s}{dx} + p_s + x\, (P_\beta + U_\beta) \frac{d\beta}{dx} - \left[P_\beta + (1 - i\, x)\, U_\beta - i\, x \frac{(P_v + U_v)}{\cos \lambda_0}\right] \beta - i \left[P_v + U_v\, (1 - i\, x)\right] \delta = 0 \qquad (4.7b)$$

$$x \frac{dp_s}{dx} + \left(1 + i\, x \frac{M_0^2}{B_0^2}\right) p_s - i \frac{x}{B_0^2} u_s + x P_\beta \frac{d\beta}{dx}$$

$$+ \left[\frac{2 V_\beta}{B_0^2 \tan \lambda_0} - P_\beta \left(1 - i\, x \frac{M_0^2}{B_0^2}\right) + i\, x \left(\frac{P_v}{\cos \lambda_0} - \frac{U_\beta}{B_0^2}\right)\right] \beta$$

$$+ i \left[\frac{2 V_v}{B_0^2 \tan \lambda_0} - P_v \left(1 - i\, x \frac{M_0^2}{B_0^2}\right) - i\, x \frac{U_v}{B_0^2}\right] \delta = \frac{2 v_s}{B_0^2 \tan \lambda_0} \tag{4.7c}$$

with

$$\frac{d\delta}{dx} = \beta / \cos \lambda_0 \tag{4.7d}$$

The partial differential equations (4.2) and their boundary conditions have been transformed to four inhomogeneous, complex, variable-coefficient, ordinary differential equations, in p_s, u_s, δ and β. The known surface velocity, $v_s(x)$, appears as a forcing function, and the required initial conditions are also contained in (4.7) as will be subsequently shown.

4.3.1 Initial Values at the Wedge Tip

Taking the limit as $x \to 0$ in (4.7) gives

$$\beta(0) = \frac{v_s(0)}{V_\beta} - i \frac{V_v}{V_\beta} \delta(0) \tag{4.8a}$$

$$p_s(0) = P_\beta\, \beta(0) + i\, P_v\, \delta(0) \tag{4.8b}$$

$$u_s(0) = U_\beta\, \beta(0) + i\, U_v\, \delta(0) \tag{4.8c}$$

These conditions are the exact quasi-static linearized conditions from oblique shock theory.

4.3.2 Initial derivatives at the wedge tip

Differentiating (4.7) with respect to x, taking the limit as $x \to 0$, and applying (4.8) gives an algebraic system which can be solved for

$$d\beta/dx\Big|_{x=0},\ dp_s/dx\Big|_{x=0},\ \text{and}\ \ du_s/dx\Big|_{x=0}$$

The results are as follows:

$$\left.\frac{d\beta}{dx}\right|_{x=0} = \frac{1}{\Delta}\left\{(1 - B_0^2 \tan^2 \lambda_0) \left.\frac{dv_s}{dx}\right|_{x=0}\right.$$
$$- i \tan \lambda_0 \left[\frac{B_0^2 \tan \lambda_0}{2}\ v_s(0) + i \left(M_0^2 P_v - U_v + V_v \frac{B_0^2}{2} \tan \lambda_0\right) \delta(0)\right.$$
$$\left.\left. + \left(M_0^2 P_\beta - U_\beta + \frac{V_v}{\sin \lambda_0} + \frac{B_0^2}{2}\ V_\beta \tan \lambda_0 + \frac{P_v B_0^2}{\cos \lambda_0}\right)\ \beta(0)\right]\right\} \quad (4.9a)$$

where

$$\Delta = V_\beta + P_\beta B_0^2 \tan \lambda_0 \quad (4.9b)$$

and

$$\left.\frac{dp_s}{dx}\right|_{x=0} = P_\beta \left.\frac{d\beta}{dx}\right|_{x=0} + \tan \lambda_0 \left.\frac{dv_s}{dx}\right|_{x=0}$$
$$+ i \frac{\tan \lambda_0}{2} \left[v_s(0) + i V_v \delta(0) + \left(V_\beta + \frac{2 P_v}{\sin \lambda_0}\right) \beta(0)\right] \quad (4.9c)$$

$$\left.\frac{du_s}{dx}\right|_{x=0} = - \left.\frac{dp_s}{dx}\right|_{x=0} - i\, u_s(0) \quad (4.9d)$$

4.3.3 Definition of Force and Moment Coefficients

The motion-related aerodynamic force and moment coefficients are defined for a single (upper, see fig. 4.1) surface by

$$\tilde{\bar{L}}' = -\int_0^{\bar{c}} \bar{p}(x)\, d\bar{x} = 4\bar{q}_\infty\, \bar{c}k^2 \left[2(\tilde{L}_1 + i\tilde{L}_2)\, \frac{\bar{h}'_y}{c} + (\tilde{L}'_3 + i\tilde{L}'_4)\, \theta + 2\,(\tilde{L}_7 + i\tilde{L}_8)\, \frac{\bar{h}'_x}{\bar{c}} \right] e^{i\bar{\omega}\bar{t}} \qquad (4.10a)$$

$$\bar{M}' = \int_0^{\bar{c}} \bar{x}\, \bar{p}\, (\bar{x})\, d\bar{x} = -\,2\bar{q}_\infty\, \bar{c}^2\, k^2 \left[2\,(M'_1 + iM'_2)\, \frac{\bar{h}'_y}{\bar{c}} + (M'_3 + iM'_4)\, \theta + 2\,(M'_7 + iM'_8)\, \frac{h'_x}{\bar{c}} \right] e^{i\bar{\omega}\bar{t}} \qquad (4.10b)$$

These definitions are similar to those often used in two-dimensional supersonic flutter analysis (e.g., Garrick and Rubinow, 1946). Here, however, the force $\tilde{L}$ is normal to the surface, rather than in the lift direction (indicated by $\sim$ over the L), and subscripts 7 and 8 pertain to fore-and-aft translation parallel to the mean surface position. (The symbol N and the subscripts 5 and 6 are often used for unsteady flap hinge moments and for pertaining to a flap, respectively, see Garrick and Rubinow, 1946.) It might also be noted that no forces along the surface are generated, since the effects of viscous skin friction have been neglected and the base pressure has been assumed to remain constant. The aerodynamic coefficients for a wedge are given in terms of the above definitions in Section 8.3.

4.3.4 Low-k Solution Based on Initial Conditions

The surface pressure for small values of x (i.e., $\bar{\omega}/\bar{u}_0$) can be approximated as

$$p_s(x) = p_s(0) + \left.\frac{dp_s}{dx}\right|_{x=0} x \tag{4.11}$$

Using the boundary conditions (4.3) in equations (4.8) and (4.9) and integrating for the forces and moment coefficients as defined by equation (4.6) gives for small values of k

$$\tilde{L}_1 = \frac{3}{4} M'_1 = -\frac{\rho_0}{2} \left.\frac{dp_{s,h_y}}{dx}\right|_{x=0}$$

$$k\,\tilde{L}_2 = k\,M'_2 = -\frac{\rho_0 u_0}{2}\, p_{s,h_y}(0)$$

$$k^2\,\tilde{L}'_3 = k^2\,M'_3 = -\frac{\rho_0 u_0^2}{2}\, p_{s,\theta}(0)$$

$$k\,\tilde{L}'_4 = \frac{3}{4}\,k\,M'_4 = -\frac{\rho_0 u_0}{2} \left.\frac{dp_{s,\theta}}{dx}\right|_{x=0}$$

$$\tilde{L}_7 = \frac{3}{4} M'_7 = -\frac{\rho_0}{2} \left.\frac{dp_{s,h_x}}{dx}\right|_{x=0}$$

$$k\,\tilde{L}_8 = k\,M'_8 = -\frac{\rho_0 u_0}{2}\, p_{s,h_x}(0) \tag{4.12}$$

where the above coefficients are given for a single exposed surface. Evaluating equations (4.12) using equations (4.3, 4.4, 4.8 and 4.9) leads to the following algebraic expressions for the coefficients involving only the properties of the steady flow p_0, u_0, and so forth, and the shock-wave derivatives P_β, V_v, and so forth.

$$k\,\tilde{L}_2 = \frac{\rho_0 u_0}{2\,V_\beta}\,(P_\beta - A_1 \cos\lambda_0)$$

$$k^2\,\tilde{L}_3' = \frac{\rho_0 u_0^2}{2\,V_\beta}\,P_\beta$$

$$k\,\tilde{L}_8 = \frac{\rho_0 u_0}{2\,V_\beta}\,A_1 \sin\lambda_0$$

$$\tilde{L}_7 = \frac{\rho_0 \tan\lambda_0}{2\,V_\beta\,\Delta}\left[(V_v + M_0^2\,P_\beta \sin\lambda_0)\,A_1 - P_\beta\,A_2 \sin\lambda_0\right]$$

$$\tilde{L}_1 = -\cot\lambda_0\,\tilde{L}_7 - \rho_0\,A_3/2$$

$$k\,\tilde{L}_4' = \frac{\rho_0 u_0}{2}\left[\tan\lambda_0 + P_\beta\,(1 - B_0^2 \tan^2\lambda_0)/\Delta + A_3\right] \qquad (4.13)$$

where

$$A_1 = P_\beta\,V_v - P_v\,V_\beta$$

$$A_2 = U_\beta\,V_v - U_v\,V_\beta$$

$$A_3 = \tan\lambda_0\left\{1 - \frac{1}{V_\beta\,\Delta}\left[\frac{A_1}{\sin\lambda_0} - P_\beta\,(U_\beta - M_0^2\,P_\beta - V_\beta\,B_0^2 \tan\lambda_0)\right]\right\}$$

and Δ is given by equation (4.9b).

4.3.5 Numerical Solution of One-Strip Equations

To determine the variation of the force and moment coefficients with k, equations (4.7) are numerically integrated using a computer subroutine for first-order, real, ordinary differential equations. The complex equations (4.7) are converted to a system of eight coupled, first-order equations relating the real and imaginary parts of

δ, β, u_s, and p_s. Initial values and derivatives at a small value of x are calculated from (4.11), for example, which requires using (4.8) and (4.9) for starting the numerical integration of the differential equations. As $k = \frac{\bar{\omega}}{2} \frac{\bar{c}}{V_\infty} = u_0 x/2$, running integrals over x of the real and imaginary parts of the pressure give the variation of the aerodynamic coefficients with k. Using the definitions (4.10) the coefficients are related to the integral of the pressure for a single exposed surface for the

$$\tilde{L}_{1 \text{ or } 7} = - \frac{\rho_0}{x^2} \int_0^x \text{Re} \left[p_{h_y \text{ or } h_x} (\xi) \right] d\xi$$

$$k\, L_{2 \text{ or } 8} = - \frac{\rho_0 u_0}{2x} \int_0^x \text{Im} \left[p_{h_y \text{ or } h_x} (\xi) \right] d\xi$$

$$M'_{1 \text{ or } 7} = \frac{2\, \rho_0}{x^3} \int_0^x \text{Re} \left[p_{h_y \text{ or } h_x} (\xi) \right] \xi \, d\xi$$

$$k\, M'_{2 \text{ or } 8} = - \frac{\rho_0 u_0}{x^2} \int_0^x \text{Im} \left[p_{h_y \text{ or } h_x} (\xi) \right] \xi \, d\xi \qquad (4.14)$$

where ξ is the variable of integration in the x-direction. Similarly, for pitch,

$$k^2 \tilde{L}'_3 = - \frac{\rho_0 u_0^2}{2x} \int_0^x \text{Re} \left[p_\theta (\xi) \right] d\xi$$

$$k\, \tilde{L}'_4 = - \frac{\rho_0 u_0}{x^2} \int_0^x \text{Im} \left[p_\theta (\xi) \right] d\xi$$

$$k^2 M_3' = -\frac{\rho_0 u_0^2}{x^2}\int_0^x \mathrm{Re}\left[p_\theta(\xi)\right]\xi\, d\xi$$

$$k M_4' = -\frac{2\rho_0 u_0}{x^3}\int_0^x \mathrm{Im}\left[p_\theta(\xi)\right]\xi\, d\xi \qquad (4.15)$$

A computing program is given in Section 8.4 which calculates twice the above integrals. The trapezoidal rule is used for numerical integration of the surface pressures in the integrals to determine to coefficients.

4.4 Results and Discussion

4.4.1 Comments on the Method

One result of applying the method of integral relations is a change in the region of influence of the governing differential equations. Disturbances propagate along the normal coordinate rather than along characteristics and the description of wave-type phenomena is thus altered. The application to steady supersonic flow over pointed bodies has been discussed by South and Newman, 1965. It was found that although the results of the method differed in detail, the exact wave behavior was approximated as a result of compensating effects. The integral method has also been applied to the perturbation of plane entropy layers which involves extensive wave effects with favorable results (George, 1967). As discussed in McIntosh (1965a), and Hui (1969b), the acoustic waves generated by the surface and shock wave are important factors in determining the unsteady forces on the wedge. The description of this wave phenomena by the one-strip integral method

(eqs. 4.7) is investigated by applying it to a steady angular perturbation of a wedge surface. The results are compared in figure 4.2 with the exact solution from hypersonic small disturbance theory of McIntosh (1965a). The results of the one-strip method do not follow the exact wave pattern, but approximate it in a smoothed oscillatory fashion. This is, thus, an important limitation of the method if local details are important. However, it might also be noted that the example cited contains a slope-discontinuity. For cases with continuous slopes, this smoothing should be less severe.

4.4.2 Low Reduced-Frequency Aerodynamic Forces

4.4.2.1 Comparisons with other analytical results and experiment

The exact solutions for low-frequency or stability-derivative-type of aerodynamics of Van Dyke (1953) and Hui (1969a) are available for a symmetrical wedge pitching about an axis located on the chordline at any chordwise location. Direct algebraic comparisons with these results would be rather lengthy. The equations of Van Dyke (1953) were programmed and calculations made for an extensive range of M, γ, and θ_w. The results obtained were identical to the results from using equations (4.13) and the transformation equations of Section 8.3. Furthermore, the results presented in the figures of Hui (1969a) were also reproduced using the one-strip equations. However, no results for $\tilde{L}_1$ are available for comparison. Although not rigorously demonstrated, the results of the one-strip approximation (eqs. 4.13) are thought to be exact for the low-frequency aerodynamics. Further comparisons with the linear theory of Garrick and Rubinow (1946) and the second-order theory

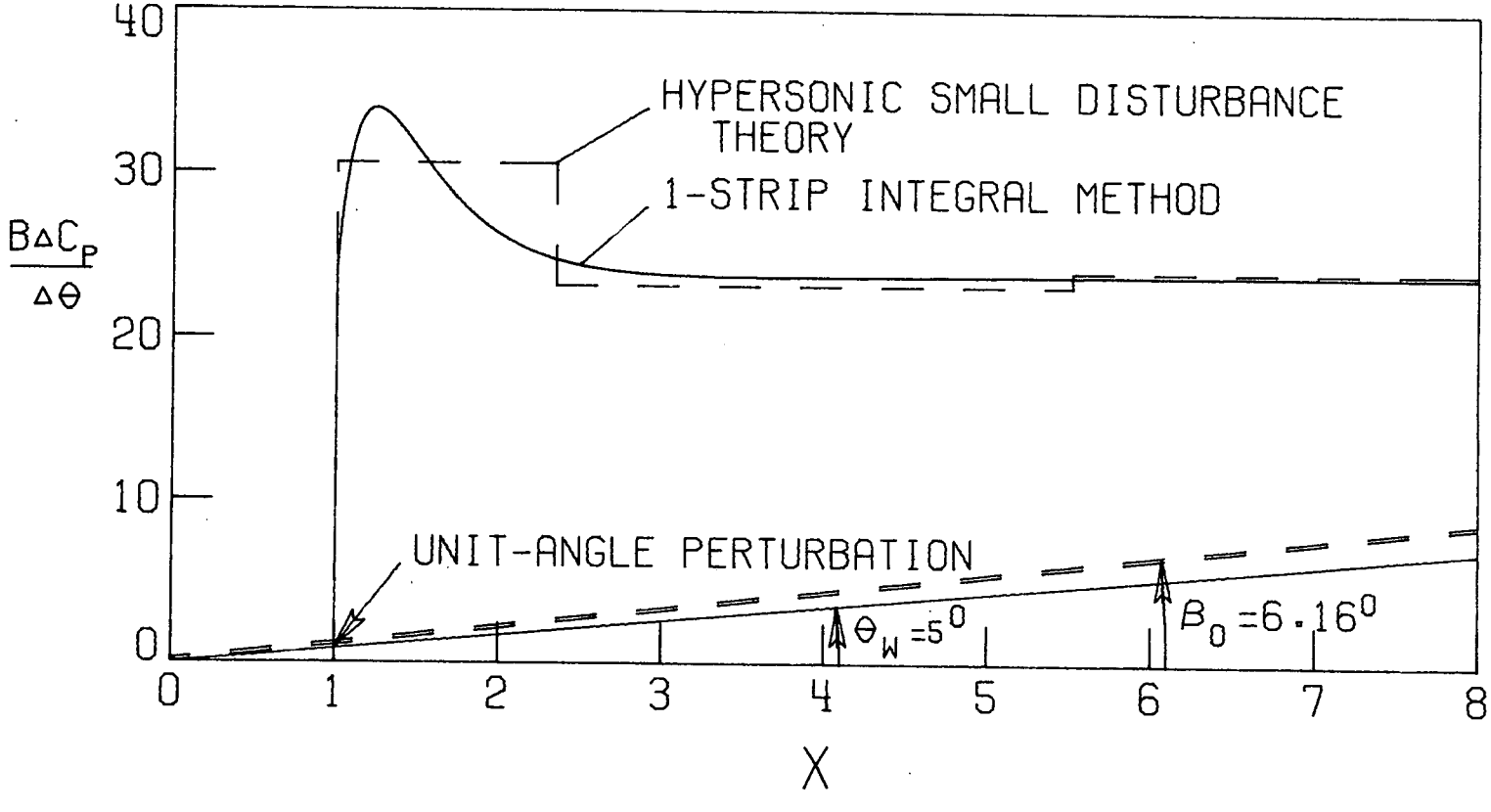

Figure 4.2.- Pressure perturbation downstream of a unit angle change, M = 57.3

of Van Dyke (1954a) were also made by expanding the one-strip results in powers of θ_w and obtaining identical results. Similar expansions for hypersonic small disturbance conditions agreed with the results of McIntosh (1965a,b).

With the previously noted smoothing of the wave behavior by the method of integral relations, the degree of validity of these results may seem surprising. It was found by Hui (1969a), however, that linear functions in x and y satisfied the perturbation equations for the pitching wedge and the caret wing. The linear y-function is the form of solution assumed by the one-strip method of integral relations (i.e., eq. 4.6) and the linear x-function assumed for the low frequency approximation (eq. 4.11).

Calculated results using (4.13) are compared with the experimental data of Pugh and Woodgate (1963) for a symmetrical pitching wedge in figures 4.3 and 4.4. Generally good agreement is obtained with the best agreement for the thinner wedge and higher Mach number.

4.4.2.2 Selected Analytical Results

The six normal-force coefficients (eqs. 4.12-4.13) for a single, inclined surface are presented in figures 4.5 and 4.6 for $M = 2$ and ∞, and for several values of the ratio of specific heats γ. All coefficients vary considerably with inclination angle, particularly for $M = \infty$, and approach infinity as detachment is approached. The coefficients $\tilde{L}_1$ and $k\tilde{L}'_4$ also change sign as detachment is approached. As the damping-in-pitch (about the leading edge) is related to $k\tilde{L}'_4$ (i.e., see eq. 4.12), the damping-in-pitch thus changes to an unstable

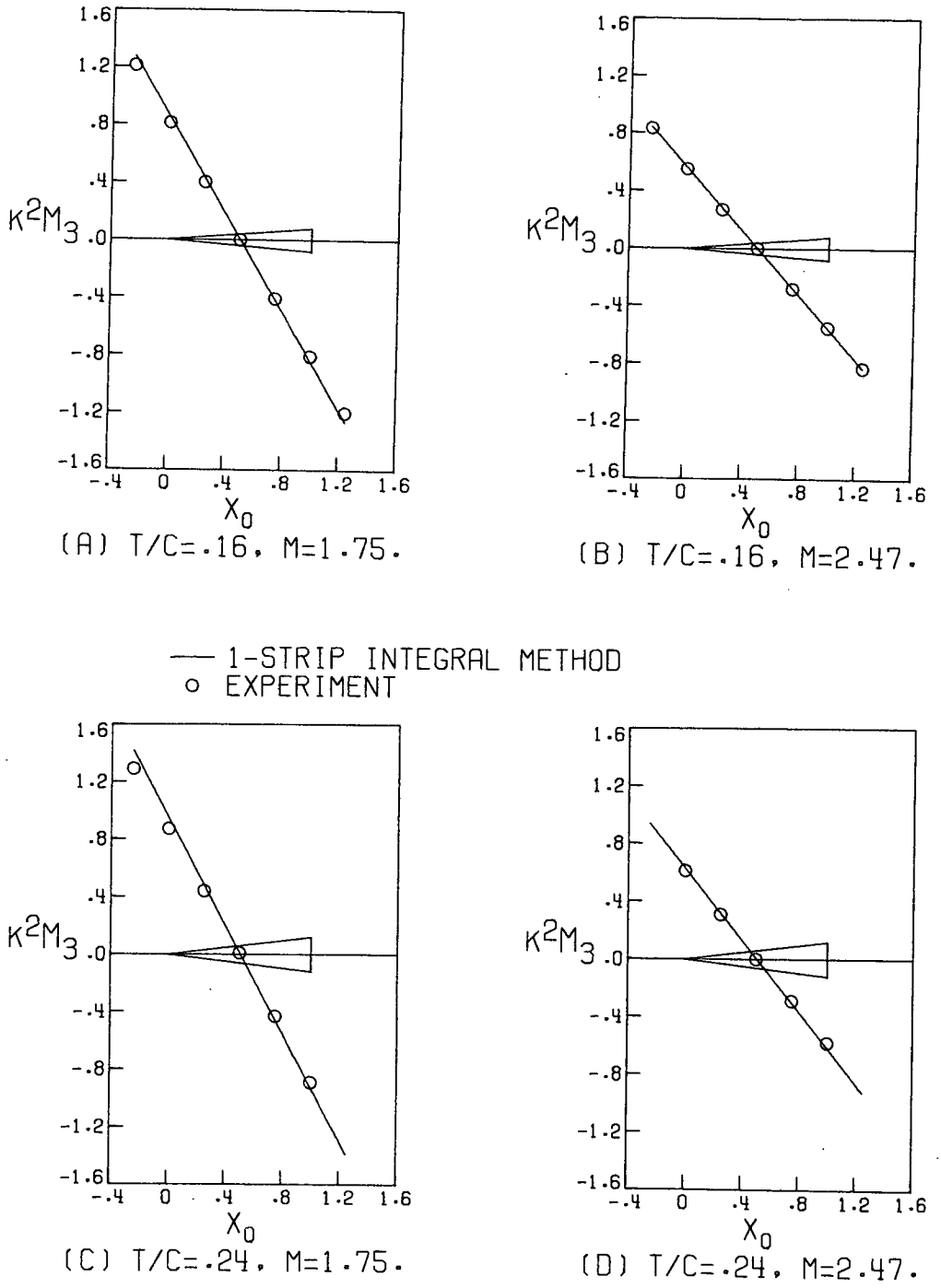

Figure 4.3.- Variation of static moment derivative with pitch axis location

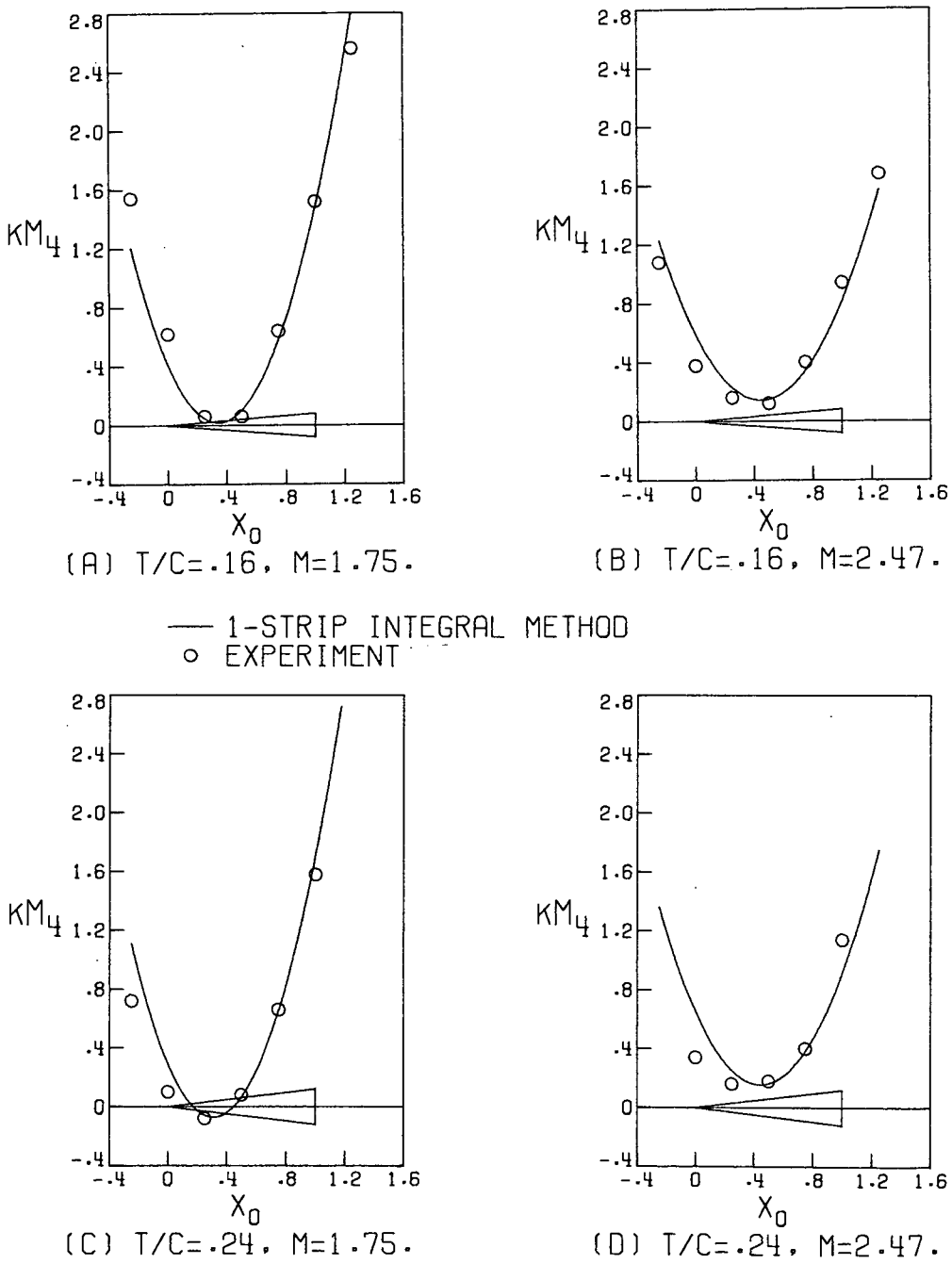

Figure 4.4.- Variation of pitch-rate-damping moment derivative with pitch axis location.

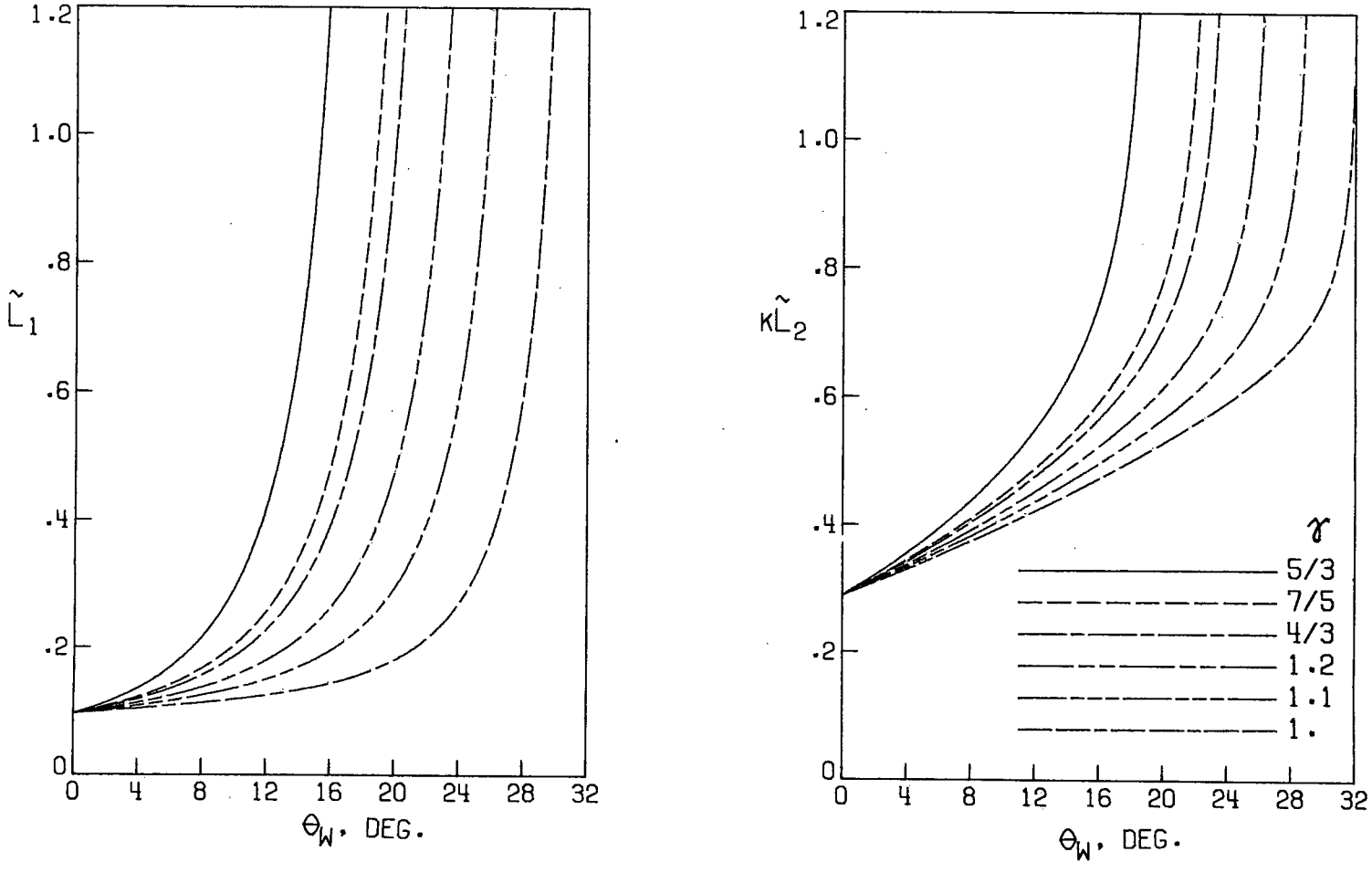

Figure 4.5.- Coefficients for single surface, k = 0, M = 2

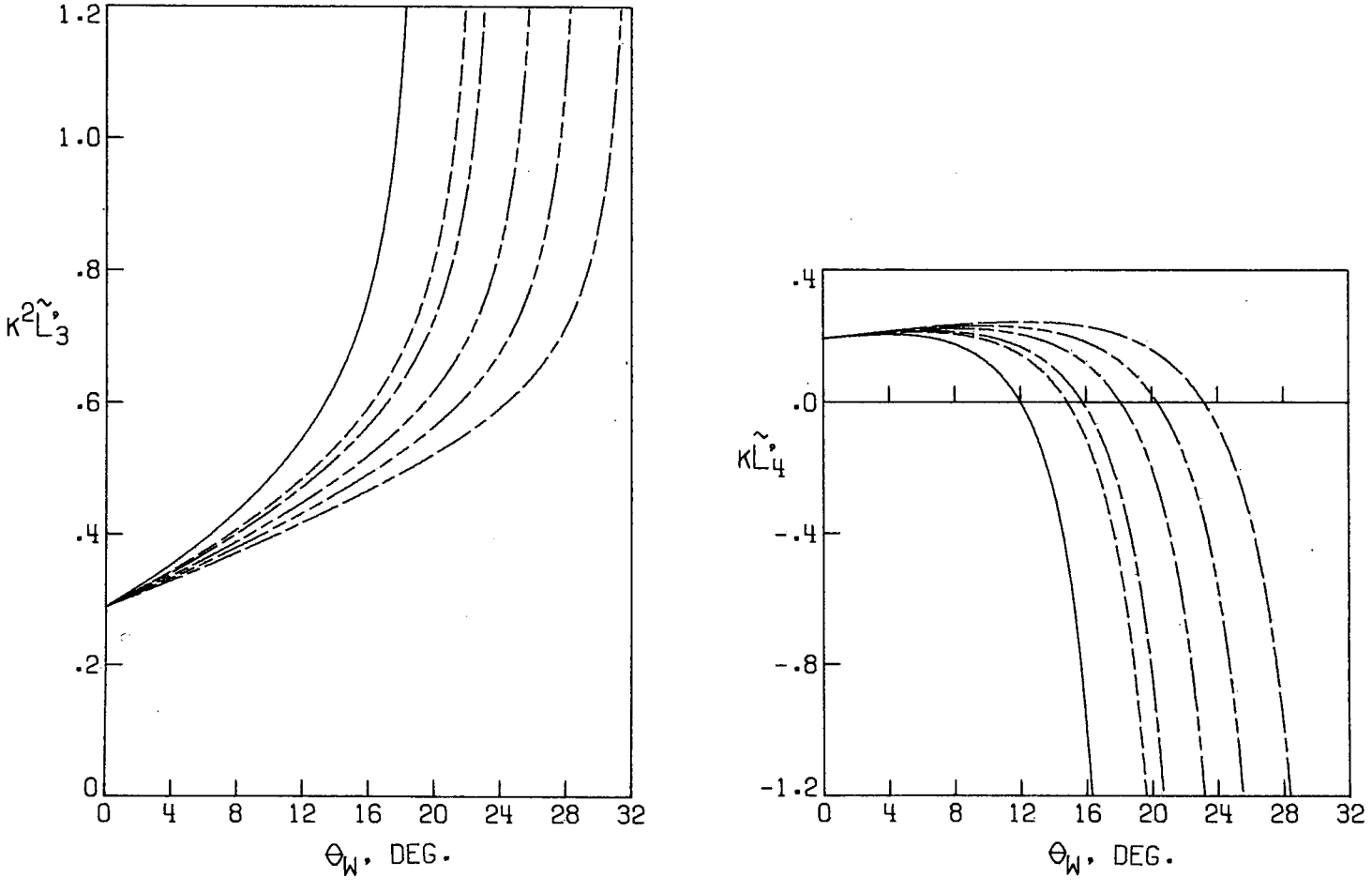

Figure 4.5.- Continued

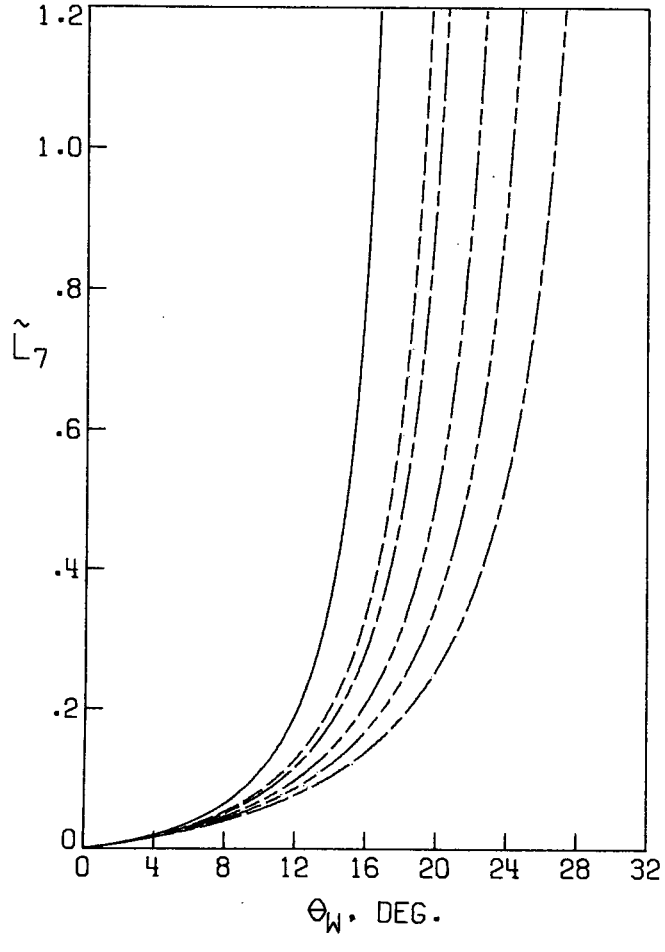

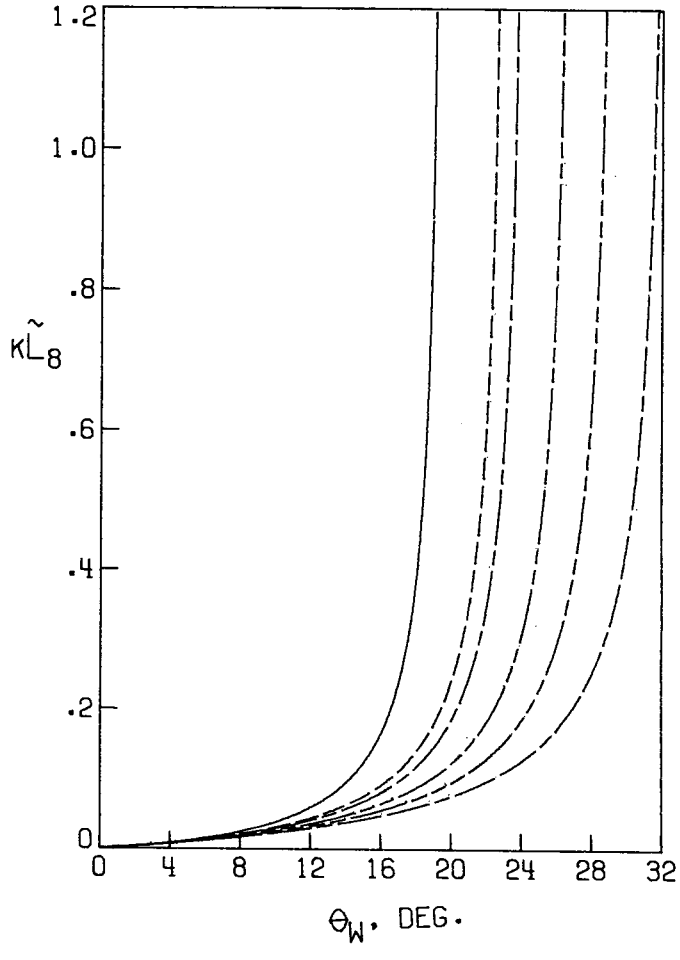

Figure 4.5.- Concluded

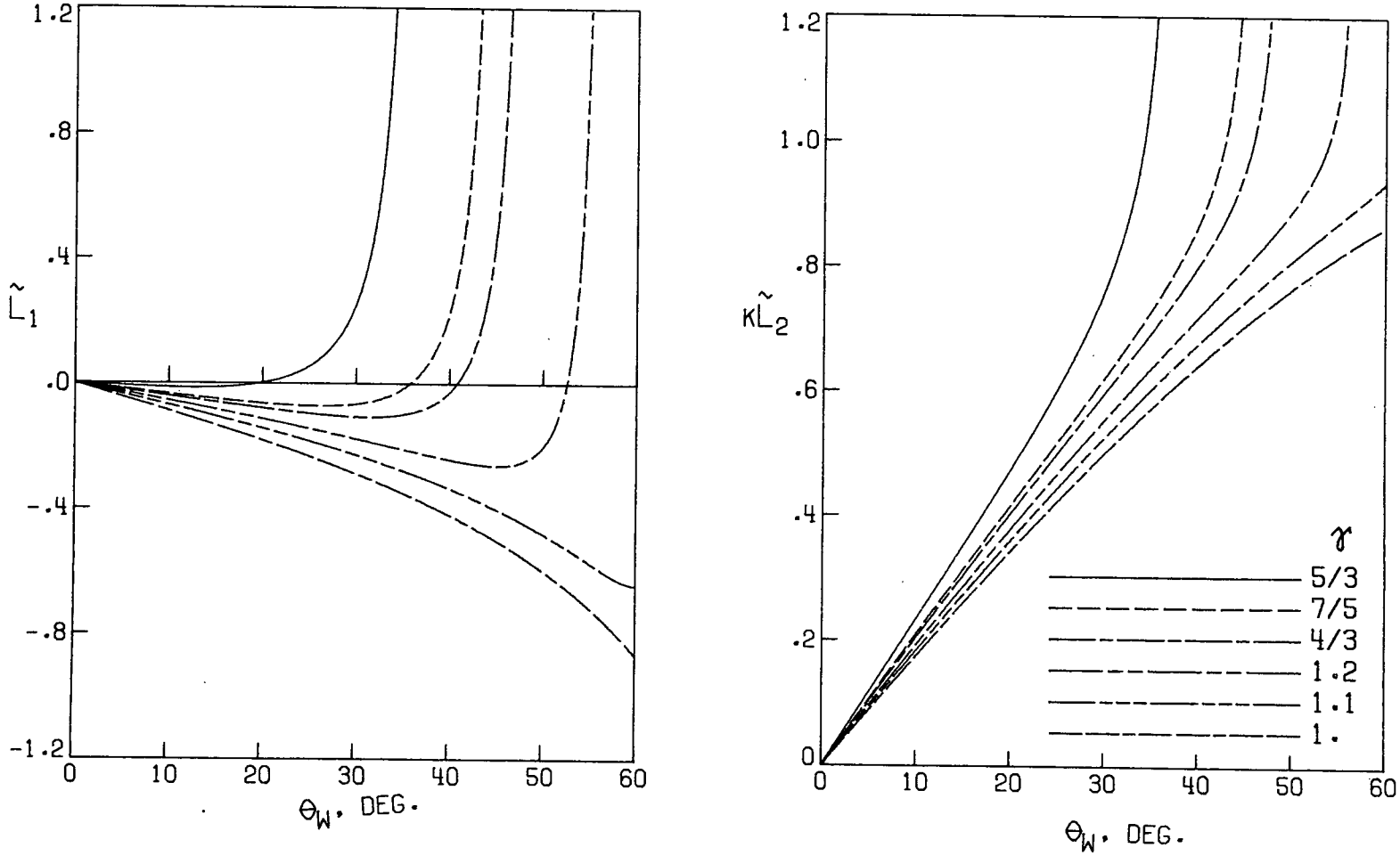

Figure 4.6.- Coefficients for single surface, k = 0, M = ∞

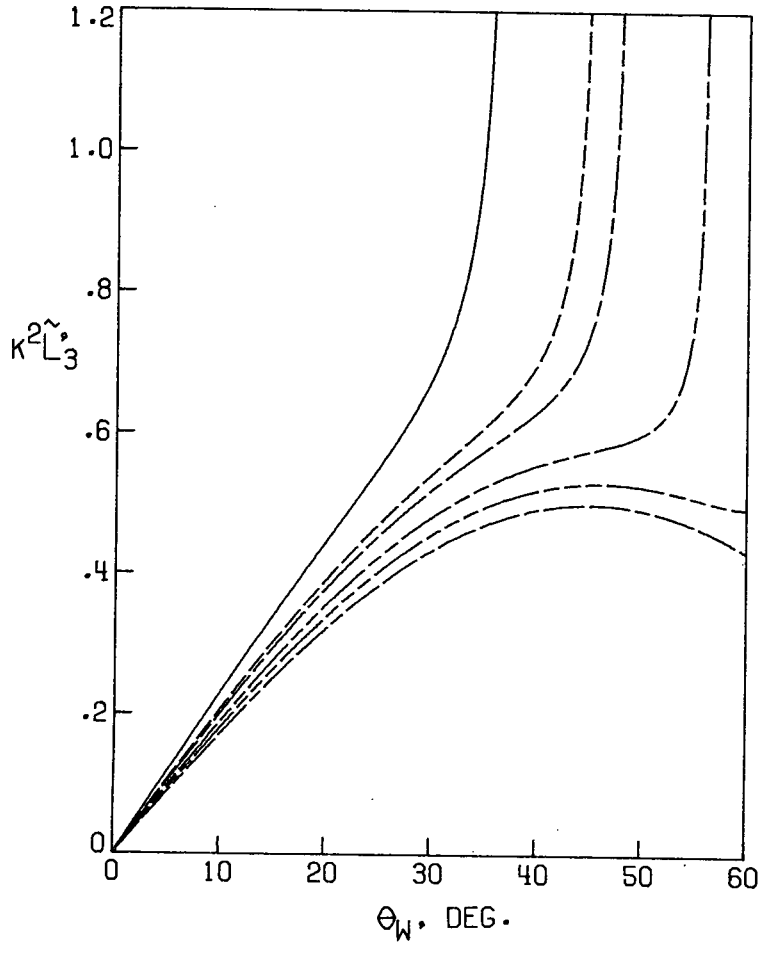

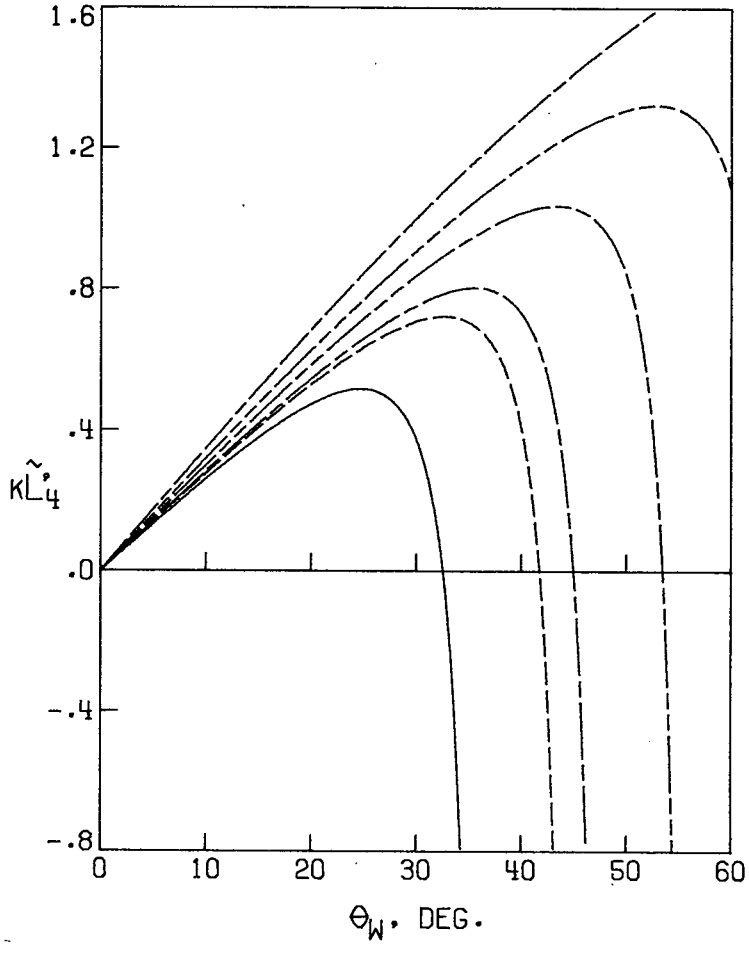

Figure 4.6.- Continued

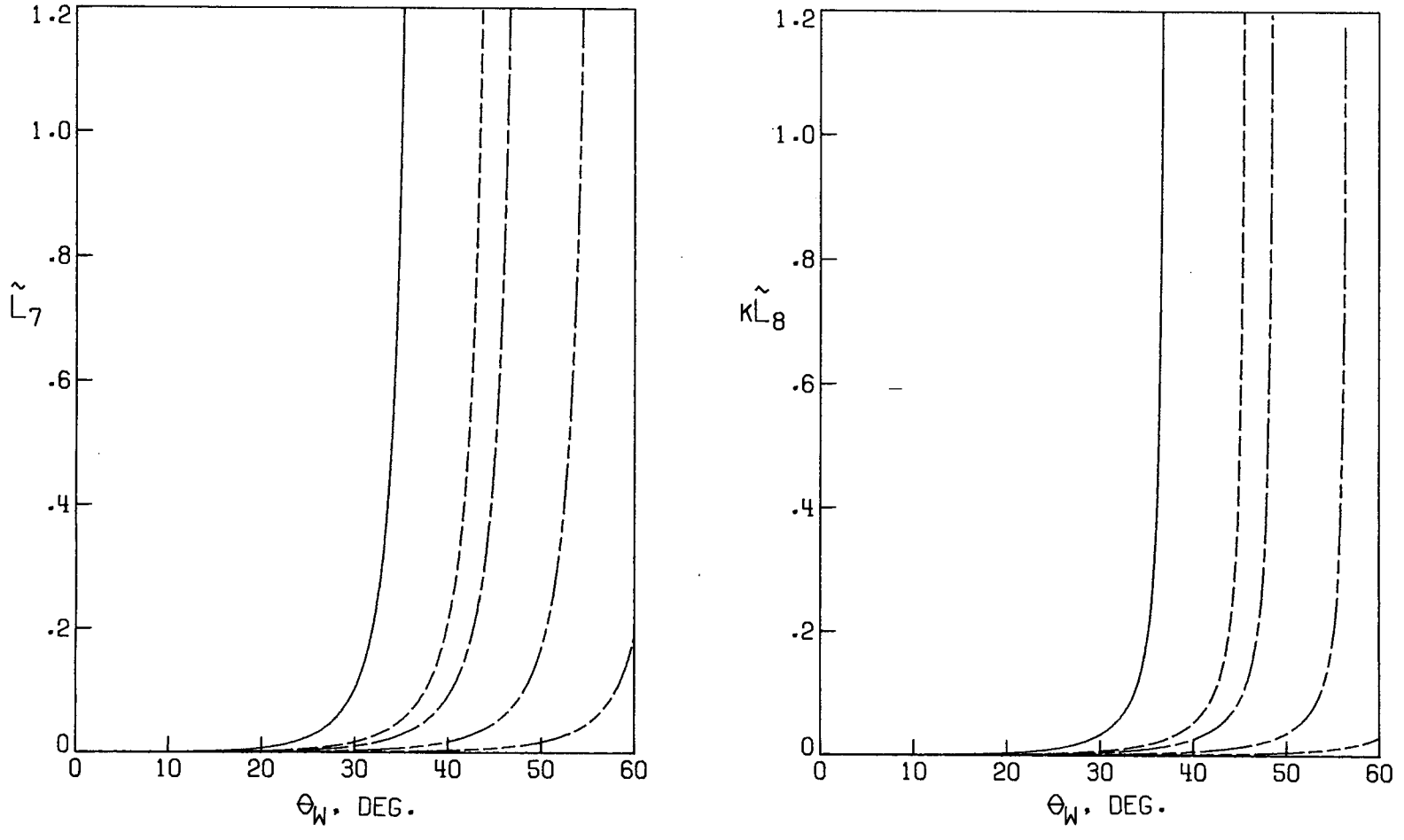

Figure 4.6.- Concluded

value near detachment. This unstable pitch-damping has also been discussed by Hui (1969a).

The effect of γ (figs. 4.5-4.6) is primarily to shift the detachment angle and thus has large effects near detachment even for small changes in the value of γ.

The fore- and aft-coefficients $\tilde{L}_7$ and $k\tilde{L}_8$ are, of course, zero for $\theta_w = 0$ and are somewhat small until the detachment angle is approached.

It appears that the detachment condition leads to singular behavior in each stability derivative. That such is the case for the static forces is apparent from the charts of Ames Research Staff (1953) which show that $dp_s/d\theta_w$ is infinite at detachment. For sonic local embedded flow the static derivatives are not infinite, but are extremely large. For the small range of θ_w for subsonic but attached flow, theories for an infinite wedge are no longer valid as the subsonic flow field between the shock and the surface is not uniform for a finite wedge (e.g., Johnston, 1953). Some implications of the approach to detachment on the flutter characteristics of diamond airfoils have been discussed by Yates and Bennett (1971).

Generally, in linear aerodynamics, the presence of a singularity such as that shown here indicates a need for a more complete treatment of the nonlinear governing flow equations in order to describe a more realistic behavior. Here, however, at least up to conditions of sonic local flow, the exact infinitesimal amplitude results are obtained. Furthermore, the usual transonic refinement to linear theory retains a local x-derivative of the steady flow field as a variable coefficient in

the unsteady equations (e.g., Landahl, 1961); here the term is zero. The results presented here suggest that infinitesimal motion has limited practical significance near detachment since even small finite amplitudes result in rapidly varying aerodynamic forces. Near detachment the condition for infinitesimal motion is that the amplitude of motion must be small compared to $\theta_d - \theta_w$, where θ_d is the detachment angle.

4.4.3 Variation of Aerodynamic Forces With Reduced Frequency

4.4.3.1 Comparisons with other results

There are no results known to the author for the variation of the aerodynamic forces with reduced frequency as computed from the supersonic flow solution for the wedge of Carrier (1949b) or the extension of Van Dyke (1953). Furthermore, such computations would be a rather lengthy task. Consequently, typical results of the integration of equation (4.7) are compared for $\theta_w = 0$ with supersonic linear theory for the flat plate (Garrick and Rubinow, 1946) are compared for small θ_w with second order theory of Van Dyke (1954a), and are compared with supersonic small disturbance theory (McIntosh, 1965a) in figures 4.7-4.9. In general, the one-strip integral method predicts the correct trands, but is accurate only when the frequency effects are small, such as in hypersonic small disturbance theory (fig. 4.9). Such a result might be anticipated in view of the previously discussed treatment of wave behavior by the integral method.

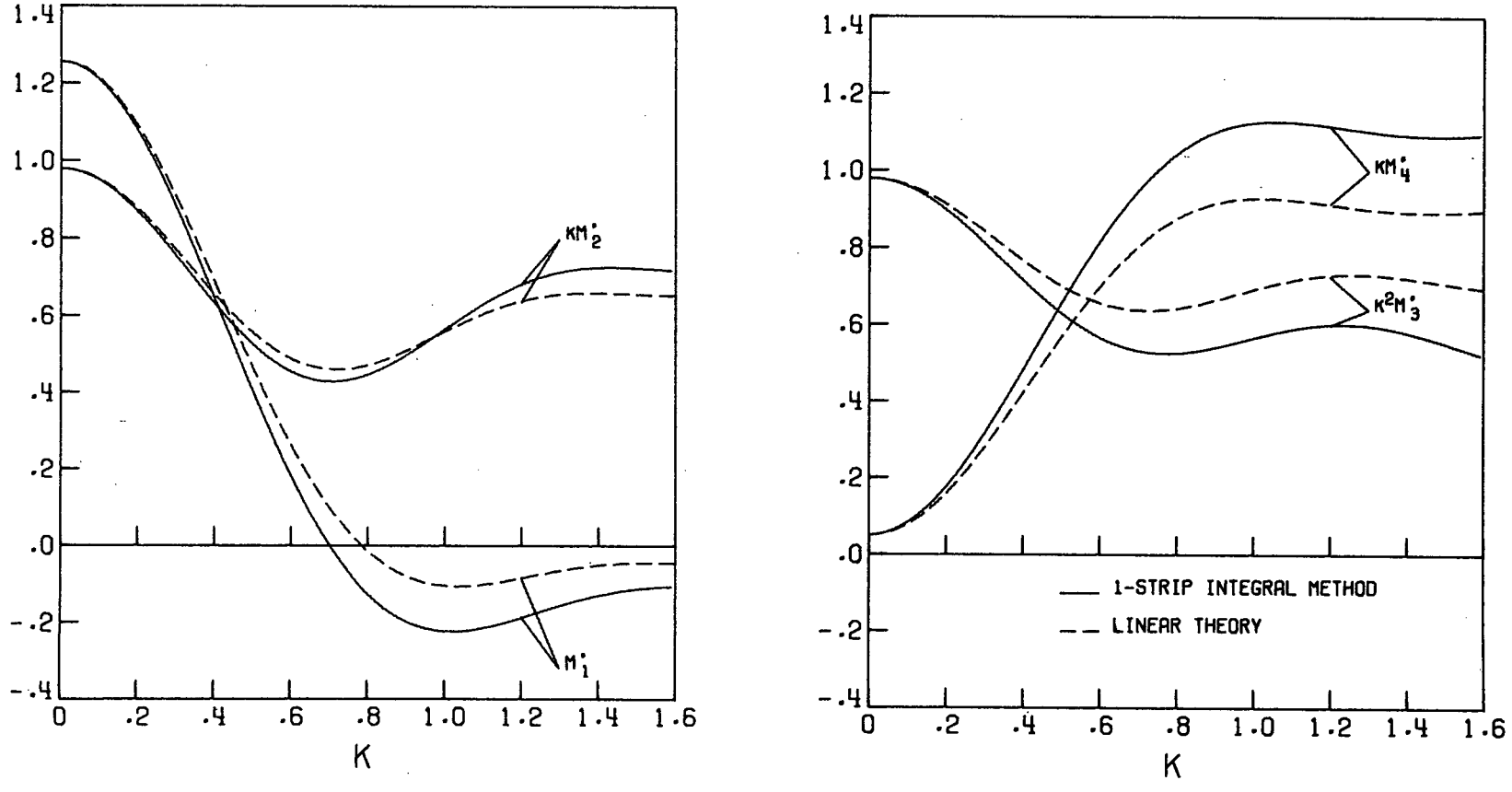

Figure 4.7.- Comparison of frequency effects for t/c = 0, M = 10/7

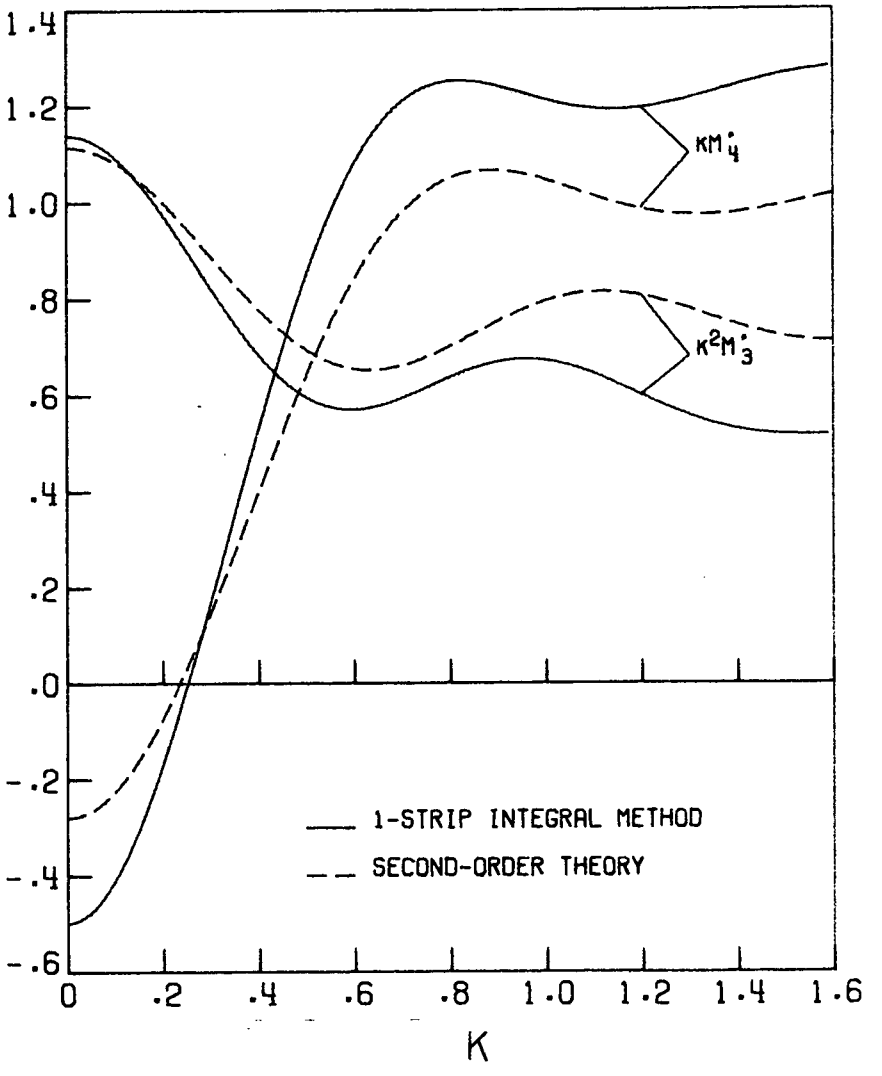

Figure 4.8.- Comparison of frequency effects for t/c = .1, M = 10/7

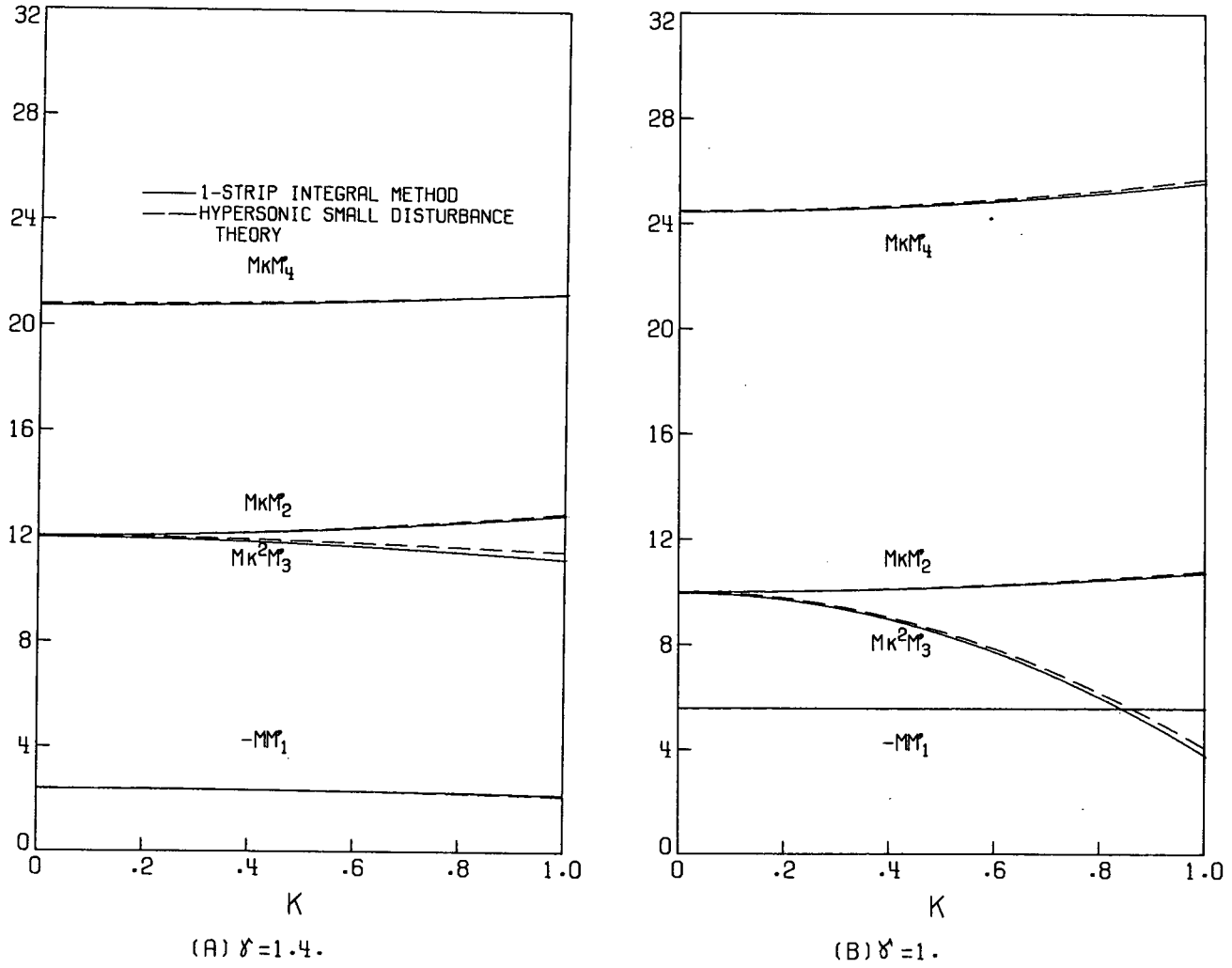

Figure 4.9.- Comparison of frequency effects at M = 57.3, 5° wedge

4.4.3.2 Selected Results

The results of integrating equations (4.7) for $M = \infty$, $\gamma = 7/5$, and $\theta_w = 25^\circ$ are given in figure 4.10. The frequency effects are small for $k \ll 1$ which is the usual range of interest for hypersonic speeds.

As previously discussed, the low frequency aerodynamic coefficients vary rapidly with inclination angle as detachment is approached. Corresponding frequency effects are presented in figure 4.11. A very strong frequency dependence even at low reduced frequencies is evident as detachment is approached. In view of the previous comparisons with other theories (figs. 4.7-4.9), these results may be considered only qualitative in nature. The trends indicated are important ones, however. For example, the coefficient $k \tilde{L}'_4$ for $\theta_w = 22^\circ$ (fig. 4.11) varies so rapidly as to suggest that the linear results may be physically unrealistic. If a nonlinear analysis were required for this region, then the phenomena of subharmonics or higher harmonics may occur which are rejected by the linear theory. In fact the quasi-static results of Kuiken (1969) and Kacprzynski (1968) indicate that for some conditions, the unsteady pressure waveform is not a single harmonic of the frequency of oscillation, and shifts in the mean pressure level can occur even for moderate amplitudes of motion. Taking such nonlinear phenomena into account in a full dynamic analysis would require considerably more effort than would be required for a conventional linear analysis. A further discussion of these effects is given subsequently in Chapter 5.

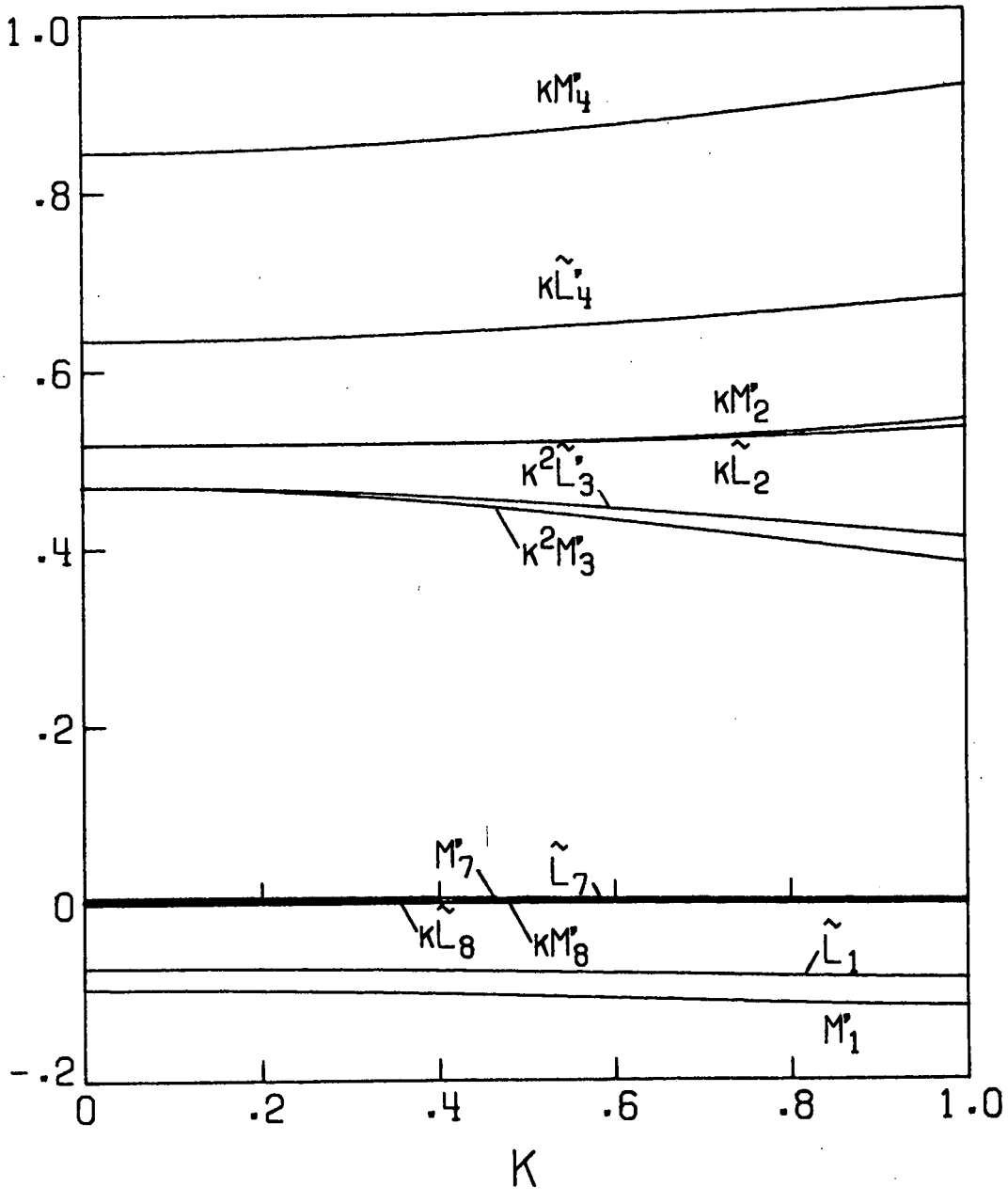

Figure 4.10.- Coefficients for single surface inclined at 25°, M = ∞ and $\gamma = 1.4$

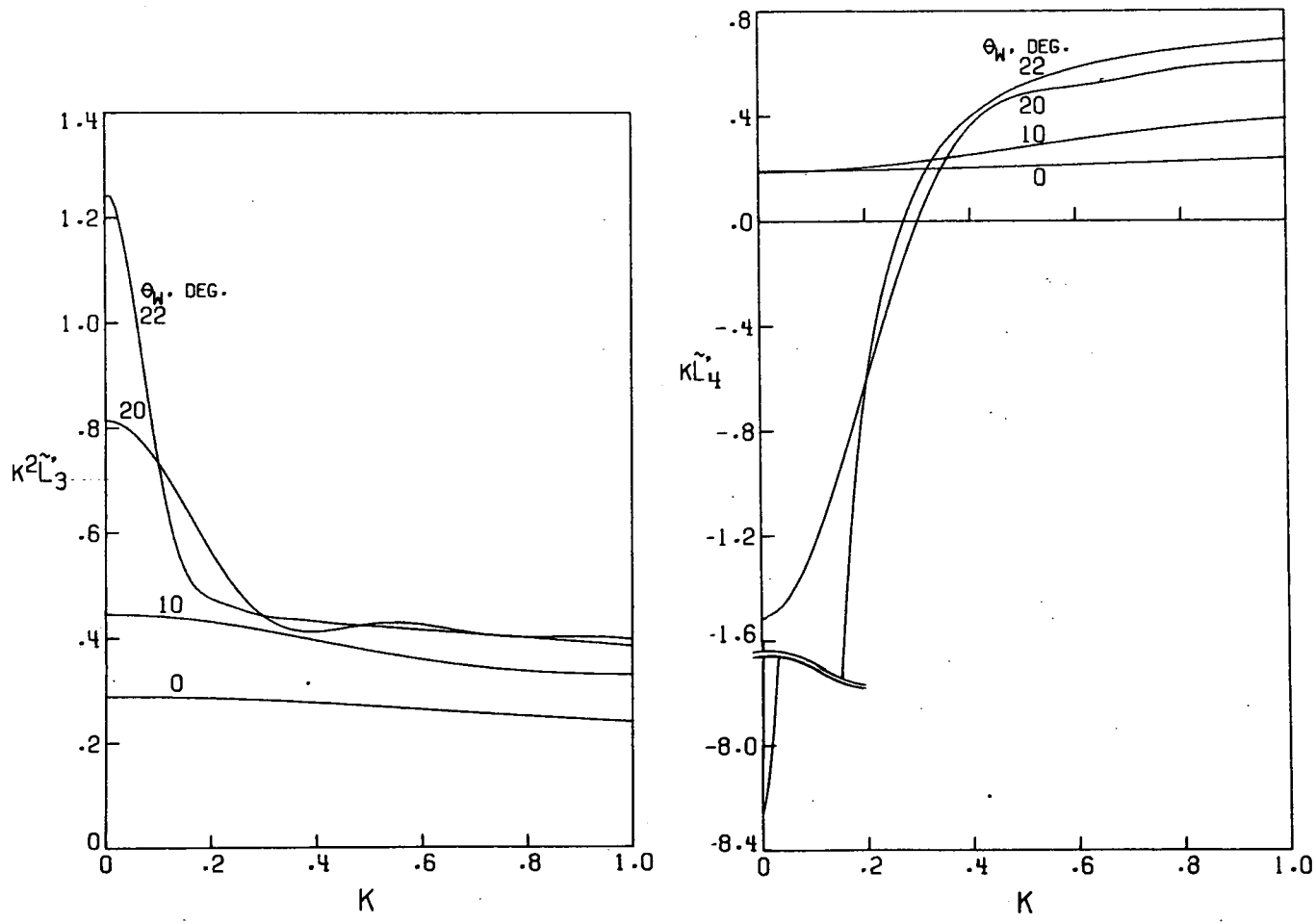

Figure 4.11.- Effects of k for several inclination angles, single surface for M = 2, γ = 1.4

Rapidly varying coefficients may also lead to rapidly varying flutter speed-indices with parameters that affect the resulting k at flutter such as the mass ratio (e.g., see Lambourne, 1967).

5. CALCULATION OF THE UNSTEADY FLOW FIELD BY A NUMERICAL FINITE DIFFERENCE TECHNIQUE

5.1 General Considerations

A numerical finite-difference calculation of the complete unsteady flow field of the wedge is presented in this chapter. The basic motivation is to provide a means of calculating nonlinear aerodynamic forces to assess the range of validity of perturbation analyses and gain insight into the types of phenomena that may be encountered when the full nonlinear governing flow equations are treated. Of particular interest would be a method that could be applied to blunt bodies in order to evaluate the effects of oscillations in the subsonic embedded flow around the nose on the after body. The data of Muhlstein (1971) indicate that even low-amplitude, static perturbations may generate significant nonlinear effects in a transonic flow. Large frequency effects have also been demonstrated in Chapter 4 for wedge flows as the embedded flow field becomes transonic near detachment.

As previously indicated in Section 2.2, several investigators (e.g., Barnwell, 1971 or Moretti and Abbett, 1966) have evaluated steady flow fields from time evolution of an assumed initial flow field. One might anticipate that suitable modifications for motion boundary conditions, unsteady flows could be treated. Moving boundaries, however, become quite difficult to treat numerically if the boundaries move with respect to the grid network. A key factor of the analysis used herein is a formulation of the problem in a body-fixed axis system. The grid network thus moves with the body and the body boundary condition

is considerably simplified. For the wedge in supersonic or hypersonic flow, only the near triangular region bounded by the vertex, by the moving shock wave, and by the wedge surface needs to be treated. Thus the flow field of interest is considerably more confined than a transonic or subsonic flow field. A body-axis formulation of the unsteady flow over a cone has previously been used in a perturbation analysis by Brong (1965).

The use of a body-fixed axis system leads to the inclusion of body-force-type terms in the flow momentum equations that are proportional to $\dot{\theta}$, $\dot{h}_y$, $\ddot{\theta}$, and so forth. Various types of motion can be treated by performing calculations similar to the time asymtotic steady flow calculation. For example, pure pitch rate effects can be obtained by considering $\dot{\theta}$ = constant without applying the real world constraint of $\theta = \int_0^t \theta \, dt$. Similarly, if θ, $\dot{\theta}$, and $\ddot{\theta}$ are constrained appropriately at each time step an oscillation can be executed. Oscillations, however, would require a converged initial flow field for $\dot{\theta}$ and $\ddot{\theta}$, and so forth, at $t = 0$. One of the chief merits of this procedure is the potential for determining steady flows aerodynamics, stability-derivative type aerodynamics, and oscillatory aerodynamics, all out of a single computer program, and thus potentially effecting considerable savings in the writing and debugging of programs.

5.2 Governing Flow Equations

The governing flow equations are written in divergence form in an $(x' - y')$ axis system that is fixed in the surface with its origin at the vertex. That is, the x'-y' axis system is the x-y axis system of

figure 4.1 except that it rotates and translates with the wedge. Here, primed quantities refer to the body-fixed axis system whereas unprimed quantities refer to the x-y system (fig. 4.1). Pitch θ and both translational motions h_x and h_y are treated, and are considered for combined motions. However, it is considered more natural for an aeroelastic problem to measure h_x and h_y relative to the undisturbed position as shown in figure 4.1, rather than in the body-axis system.

The basic transformation equations for the momentum equations are discussed by Pai (1956), and a somewhat similar development stated by Brong (1965). In this chapter quantities are nondimensionalized as $x' = \bar{x}'/\bar{c}$, $y' = \bar{y}'/\bar{c}$, $t = \bar{t}/(\bar{V}_\infty/\bar{c})$ and $u' = \frac{\bar{u}'}{\bar{V}_\infty}$, $v = \frac{\bar{v}'}{\bar{V}_\infty}$, $\rho = \bar{\rho}/\bar{\rho}_\infty$, and $p = \bar{p}/(\bar{\rho}_\infty \bar{V}_\infty^2)$.

The velocities in the axis system are related by

$$u = U_0 + u' + y' \dot{\theta}$$

$$v = V_0 + v' - x' \dot{\theta} \tag{5.1}$$

where U_0, V_0 are the velocities of the origin in the x-y system and are

$$U_0 = -(\dot{h}_x + \cos\theta_w)\cos\theta + (\dot{h}_y - \sin\theta_w)\sin\theta$$

$$V_0 = -(\dot{h}_x + \cos\theta_w)\sin\theta - (\dot{h}_y - \sin\theta_w)\cos\theta \tag{5.2}$$

The substantial derivatives in the x' and y' directions are (Pai, 1956)

$$\frac{du'}{dt} = \frac{\partial u}{\partial t} + v\dot{\theta} + u'\frac{\partial u}{\partial x'} + v'\frac{\partial u}{\partial y'}$$

$$\frac{dv'}{dt} = \frac{\partial v}{\partial t} - u\dot{\theta} + u'\frac{\partial v}{\partial x'} + u'\frac{\partial v}{\partial y'} \tag{5.3}$$

Substituting (5.2) into (5.1) to obtain u and v and differentiating with respect to time and thence substituting into (5.3) gives the resulting momentum equations. The continuity equation in divergence form (Pai, 1956) is

continuity

$$\frac{\partial \rho}{\partial t} + \frac{\partial \rho u'}{\partial x'} + \frac{\partial \rho v'}{\partial y'} = 0 \qquad (5.4a)$$

Using (5.4a) the momentum equations can be written in divergence form as:

x-momentum

$$\frac{\partial \rho u'}{\partial t} + \frac{\partial}{\partial x'}(p + \rho u'^2) + \frac{\partial (\rho u'v')}{\partial y'} - \rho \left[\ddot{h}_x \cos\theta - \ddot{h}_y \sin\theta - y' \ddot{\theta} + x' \dot{\theta}^2 - 2v' \dot{\theta} \right] = 0 \qquad (5.4b)$$

y-momentum:

$$\frac{\partial \rho v'}{\partial t} + \frac{\partial}{\partial x'}(\rho u'v') + \frac{\partial}{\partial y'}(p + \rho v'^2) - \rho \left[\ddot{h}_x \sin\theta + \ddot{h}_y \cos\theta + x' \ddot{\theta} + y' \dot{\theta}^2 + 2u' \dot{\theta} \right] = 0 \qquad (5.4c)$$

The transformation of the flow equations to arbitrary coordinate systems has been considered by Walkden (1966) who shows that the energy equation is essentially invariant under the transformation. For a perfect gas the energy equation written in divergence form is thus

energy:

$$\frac{\partial}{\partial t}\left\{ \frac{p}{\gamma} + \frac{(\gamma - 1)}{2\gamma} \rho (u'^2 + v'^2) \right\} + \frac{\partial}{\partial x'}\left\{ u' \left[p + \frac{(\gamma - 1)}{2\gamma} \rho (u'^2 + v'^2) \right] \right\} + \frac{\partial}{\partial y'}\left\{ v' \left[p + \frac{(\gamma - 1)}{2\gamma} \rho (u'^2 + v'^2) \right] \right\} = 0 \qquad (5.4d)$$

which readily reduces to the more familar form of (e.g., Sauerwine, 1965):

$$\frac{Dh}{Dt} - \frac{1}{\rho}\frac{Dp}{Dt} = 0 \qquad (5.4e)$$

5.3 Finite Difference Equations

Motions of the wedge are treated by a numerical finite-difference calculation using the complete nonlinear flow equations in a body-fixed coordinate system. The explicit finite-difference scheme used is one of first order accuracy given by Lax (1954) for hyperbolic equations. It has been further discussed and applied to aerodynamic problems, for example, by deJarnett (1966), by Bohachevsky and Rubin (1966), and by Bohachevsky and Mates (1966). The method is formulated by writing the governing flow equations in divergence form and replacing them with finite difference equations that contain implicit artificial viscosity terms. Although the region of physical interest is the nearly triangular shock layer beginning at the wedge tip and extending downstream, the hyperbolic stability criterion for the numerical solution requires that the flow field must be known at an initial line downstream of the tip. Furthermore, the technique does not consider a shock wave as a discontinuity but smears the discontinuity over a few mesh points both into the shock layer and into the freestream. This considerably simplifies the treatment of the moving shock boundary, but at the expense of flow field resolution.

Subsequent to Lax (1954), many investigators have presented refined hyperbolic difference schemes, for example, Lax and Wendroff (1964), Burstein (1964, 1967a,b), Moretti and Abbett (1966), Sauerwein (1966), Lapidus (1967), and Gourlay and Morris (1968). Burstein (1964)

and Emery (1968) have presented comparisons of results from several methods, and the book by Richtmeyer and Morton (1967) and the proceedings of a recent symposium (NASA publ., 1970) discuss several methods at length. Variations of the Lax-Wendroff (1964) scheme such as that of MacCormack (1969) are often recommended for both temporal and spatial resolution over the method used herein. The use of Lax's method is considered warranted, however, as it is conceptually one of the simplest and is also used for an intermediate step in at least one of the higher-order methods (Burstein, 1967b).

The flow field is divided into a rectangular grid system for each time step as shown in figure 5.1 with constant values of $\Delta t/\Delta x'$ and $\Delta t/\Delta y'$ as determined from the stability criterion as discussed later.

The system of equations (5.1) to (5.4) can be written as:

$$\frac{\partial A_i}{\partial t} + \frac{\partial B_1}{\partial x'} + \frac{\partial C_i}{\partial y'} + D_i = 0 \qquad (5.5)$$

where

$$A_1 = \rho$$

$$A_2 = \rho u'$$

$$A_3 = \rho v'$$

$$A_4 = \left[\frac{p}{\gamma} + \frac{(\gamma - 1)}{2\gamma}\,\rho U^2\right]$$

$$B_1 = \rho u'$$

$$B_2 = p + \rho u'^2$$

$$B_3 = \rho u' v'$$

$$B_4 = \left[p + \frac{(\gamma - 1)}{2\gamma} \rho U^2 \right] u'$$

$$C_1 = p v'$$

$$C_2 = \rho u' v'$$

$$C_3 = p + \rho v'^2$$

$$C_4 = \left[p + \frac{(\gamma - 1)}{2\gamma} \rho U^2 \right] v'$$

$$D_1 = 0$$

$$D_2 = - \rho \left[\ddot{h}_x \cos\theta - \ddot{h}_y \sin\theta - y' \ddot{\theta} + x' \dot{\theta}^2 - 2 v' \dot{\theta} \right]$$

$$D_3 = - \rho \left[2 u' \dot{\theta} + x' \ddot{\theta} + y' \dot{\theta}^2 + \ddot{h}_x \sin\theta + \ddot{h}_y \cos\theta \right]$$

$$D_4 = 0 \qquad (5.6)$$

and

$$U^2 = u'^2 + v'^2$$

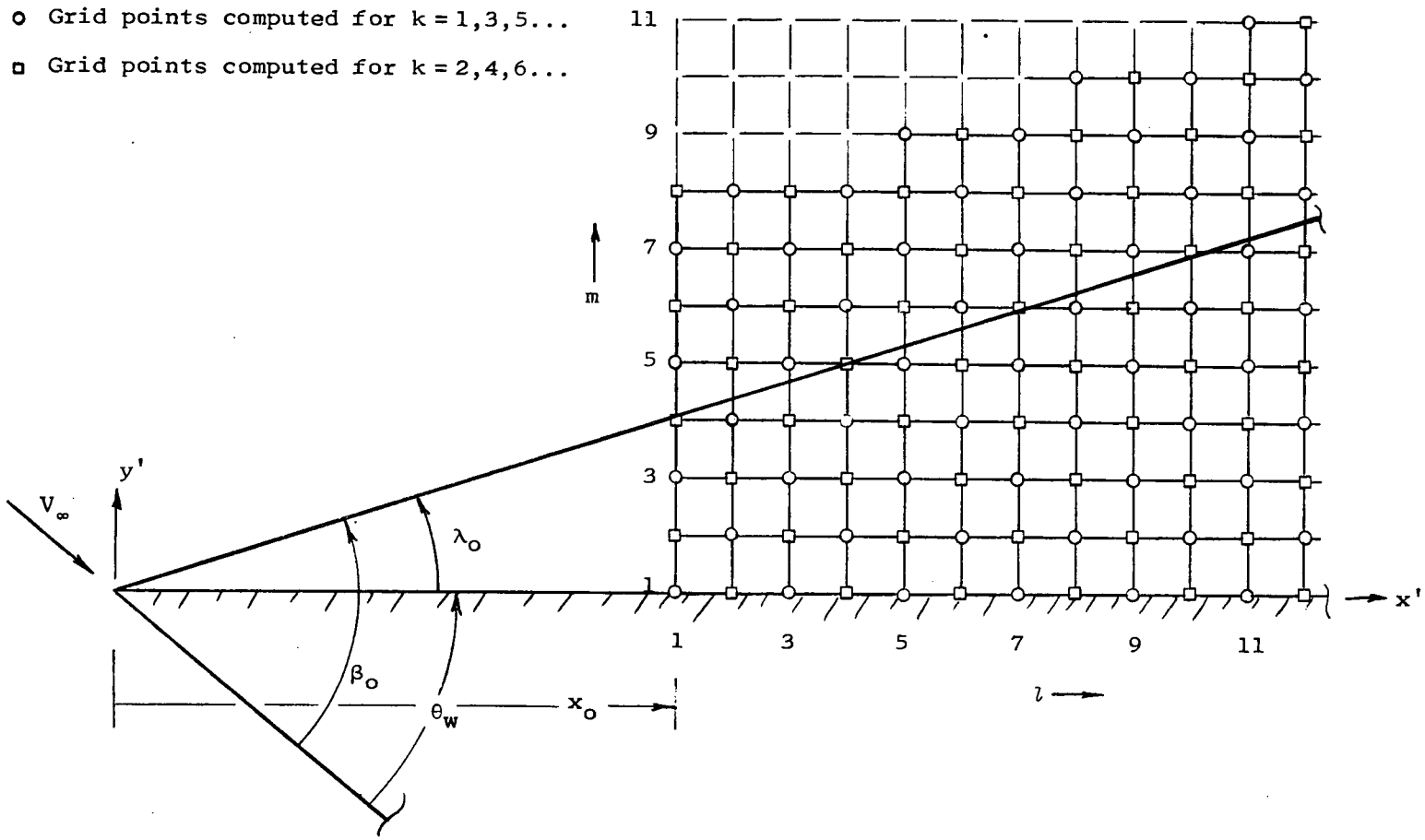

Figure 5.1.- Portion of grid network for finite difference calculation

The procedure of Lax (1954) is to replace time derivatives of time step k with the averaged forward difference,

$$\frac{(A_i)^{k+1}_{l,m} - \frac{1}{4}\left[(A_i)^k_{l+1,m} + (A_i)^k_{l-1,m} + (A_i)^k_{l,m+1} + (A_i)^k_{l,m-1}\right]}{\Delta t}$$

where k, l, and m are indices for t, x', and y', respectively, and to replace $(\partial B_i/\partial x')^k$ and $(\partial C_i/\partial y')^k$ with the symmetric difference expressions

$$\frac{(B_i)^k_{l+1,m} - (B_i)^k_{l-1,m}}{2\,\Delta x'}$$

and

$$\frac{(C_i)^k_{l,m+1} - (C_i)^k_{l,m-1}}{2\,\Delta y'}$$

and to replace $(D_i)^k$ with the averaged value

$$\frac{1}{4}\left[(D_i)^k_{l+1,m} + (D_i)^k_{l-1,m} + (D_i)^k_{l,m+1} + (D_i)^k_{l,m-1}\right]$$

Substitution of these expressions into (5.5) gives the finite difference algorithm,

$$\begin{aligned}(A_i)^{k+1}_{l,m} = {} & \frac{1}{4}\left[(A_i)^k_{l+1,m} + (A_i)^k_{l-1,m} + (A_i)^k_{l,m+1} + (A_i)^k_{l,m-1}\right] \\ & - \frac{\Delta t}{2\,\Delta x'}\left[(B_i)^k_{l+1,m} - (B_i)^k_{l-1,m}\right] - \frac{\Delta t}{2\,\Delta y'}\left[(C_i)^k_{l,m+1} - (C_i)^k_{l,m-1}\right] \\ & - \frac{\Delta t}{4}\left[(D_i)^k_{l+1,m} + (D_i)^k_{l-1,m} + (D_i)^k_{l,m+1}\,(D_i)^k_{l,m-1}\right] \\ & \qquad (i = 1,2,3,4) \qquad (5.7)\end{aligned}$$

Thus, A_i at the $k + 1$ time step can be determined in terms of the known variables at the mesh points $(k,\ell+1,m)$, $(k,\ell-1,m)$, $(k,\ell,m+1)$, and $(k,\ell,m-1)$ at the previous time step, k. This is a one step, explicit, alternating, difference scheme as the point (k,ℓ,m) does not appear, and only values from the previous time step are used to compute the new point. With the A_i determined, the fluid properties at a grid point can be readily determined as can be seen by inspecting the expressions for the A_i, equations (5.6).

Expansion of equation (5.7) by Taylor's series about the point (k,ℓ,m) gives:

$$\left(\frac{\partial A_i}{\partial t}\right)^k_{\ell,m} + \left(\frac{\partial B_i}{\partial x'}\right)^k_{\ell,m} + \left(\frac{\partial C_i}{\partial y'}\right)^k_{\ell,m} + (D_i)^k_{\ell,m} = -\frac{\Delta t}{2}\left(\frac{\partial^2 A_i}{\partial t^2}\right)^k_{\ell,m} + \frac{\Delta x'^2}{4\Delta t}\left(\frac{\partial^2 A_i}{\partial x'^2}\right)^k_{\ell,m} + \frac{\Delta y'^2}{4\Delta t}\left(\frac{\partial^2 A_i}{\partial y'^2}\right)^k_{\ell,m} + O(\Delta^2) \quad (i = 1,2,3,4) \tag{5.8}$$

The last two terms are somewhat analogous to terms that appear in the viscous momentum equations and are called "artificial viscosity" terms. These terms result in a smearing of rapidly varying quantities, such as fluid properties across a shock wave, over several mesh spaces, and in some instances excessive smearing or smoothing of transient phenomena can occur. Barnwell (1967) has applied a modification of this scheme by using the conventional Lax scheme (eq. 5.7) at odd time steps and using an alternate scheme containing no "artificial viscosity" terms for even time steps. The effective smearing of transient phenomena is thus reduced. In some of the higher order difference schemes,

artificial viscosity terms are often added for numerical stability (see, for example, Emery, 1968).

5.3.1 Initial and Boundary Conditions

The oscillating wedge in a supersonic flow with an attached shock is an initial and boundary value problem. The entire flow field over the grid network must be specified for $t = 0$. This is accomplished by initializing the flow field with one for a steady wedge at the equivalent angle of attack for the motion at $t = 0$. The difference technique is then applied until the flow variables converge holding the body forces constant (D_i in eq. (5.7)).

Each of the boundaries of the grid network requires special consideration at each time step, both during the initialization procedure and during computation of the unsteady flow field. As previously noted, the numerical technique does not consider a shock wave as a discontinuity but smears the shock over a few mesh spaces to satisfy the jump conditions. Sufficient freestream points must be retained such that the moving shock remains well within the grid network and such that the flow variables have approached freestream values. About eight additional grid points beyond the nominal location of the moving shock are required. The outermost points are held constant at freestream values of the flow variables.

At the wedge surface the tangential flow condition in the body axis system is $v' = 0$. To calculate the body point at $(k+1, \ell, 1)$, an approximation is used that has been used in the past (i.e., Burstein, 1964), referred to as the reflection approximation. An image point at

a distance $\Delta y'$ inside the body is considered to have associated with it - $(v'_{l,2})^k$, $(p_{l,2})^k$, $(u'_{l,2})^k$ and $(\rho_{l,2})^k$. A slight modification of this approximation is used here to allow for unsteady effects. At $y' = 0$, the y-momentum equation (5.4c) reduces to

$$\frac{\partial p}{\partial y'} = \rho \left[\ddot{h}_x \sin\theta + \ddot{h}_y \cos\theta + x' \ddot{\theta} + 2 u' \dot{\theta} \right], \quad y' = 0 \qquad (5.9)$$

Thus a pressure gradient at the surface exists that is proportional to the motion (for the surface considered which has zero curvature). The pressure for the virtual point is thus modified by setting

$$p^k_{l,-1} = p^k_{l,2} - 2 \Delta y' \frac{\partial p'}{\partial y'} \qquad (5.10)$$

It is also noted that one consequence of the use of this approximation (e.g., deJarnette, 1966) is

$$\frac{\partial v'}{\partial y'} = 0, \quad y' = 0$$

The values for the initial line are calculated from the steady flow oblique shock theory based on the instantaneous angle of attack and Mach number. This is a low reduced frequency approximation which requires that the reduced frequency based on the distance to the starting line be small, usually of order 0.1 unless frequency of amplitude effects are large.

Insufficient data are available to calculate the last line of the grid network at each time step. Either an extremely large region at $t = 0$, or an extrapolation of the data is required. Here the last line is generated by an extrapolation of the at time step k to provide the data to calculate A_i at $k+1$ from,

$$(A_i)^k_{l+1,m} = (A_i)^k_{l,m-1} + (A_i)^k_{l,m+1} - (A_i)^k_{l-2,m} \qquad (5.11)$$

Moretti (1968) has discussed the importance of accurately treating the boundaries in fluid flow problems and incorporates characteristic-type routines for treating the boundary conditions for calculating steady flow fields in a time-asymptotic fashion (see, for example, Moretti and Abbett, 1966). The methods presented herein for treating the boundaries are approximate ones. This is considered an area for possible later development.

5.3.2 Stability Criterion

There is no general stability criterion for nonlinear hyperbolic equations in three independent variables. In numerical solutions such as the one being considered, a criterion based upon local linearization is used as a guide and if instabilities are observed the mesh is suitably adjusted to eliminate the instability. For linearized equations, Hahn (1958) has shown that the Courant-Friedrichs-Lewy (or CFL) condition to be a sufficient condition for stability for simplicial gird networks, that is, a grid network that would use only three base points in the previous time surface to determine the properties at mesh point for two-dimensional unsteady flow. The CFL condition states that the domain of dependence of the difference equations must include the domain of dependence of the differential equations, which is the forward Mach cone. Sauerwein and Sussman (1964) have discussed implementation of the CFL cirterion for various simplicial grid networks.

The grid network for equation (5.7) is nonsimplicial. A necessary condition for the stability of linear, constant-coefficient equations is the vonNeumann condition which requires that the absolute values of the eigenvalues of the amplification matrix of the difference scheme must be less than or equal to one. Heie and Leigh (1965) have applied this criterion to several nonsimplicial networks and demonstrated that some nonsimplicial networks that satisfy the CFL condition do not satisfy the vonNeumann condition and would lead to instabilities in numerical calculations. Furthermore, Burnstein (1967a) has given an example of the calculation of a transient flow problem containing stagnation points and sonic lines, in which the vonNeumann condition was satisfied in a locally linear approximation, but instabilities were encountered in the calculation which used the complete nonlinear equations. In this case the nonlinear effects were considered to be essential to the instability, thus indicating possible limitations on a stability criterion based on linearization of the nonlinear equations being considered. Moretti (1968) has suggested that improper treatment of boundary conditions can lead to instability. Hence, the heuristic stability criterion used herein is the simpler CFL criterion with adjustments made in the grid network as the results dictate.

The application of the CFL condition is illustrated in figure 5.2. To satisfy the CFL condition the diamond connecting the outer base points at time k must enclose base of the forward Mach cone about the particle path from point $(k+1,\ell,m)$. The circle of radius $a\,\Delta t$ must be enclosed by the diamond formed by the outer base points. The ratio of step sizes is then for a square grid,

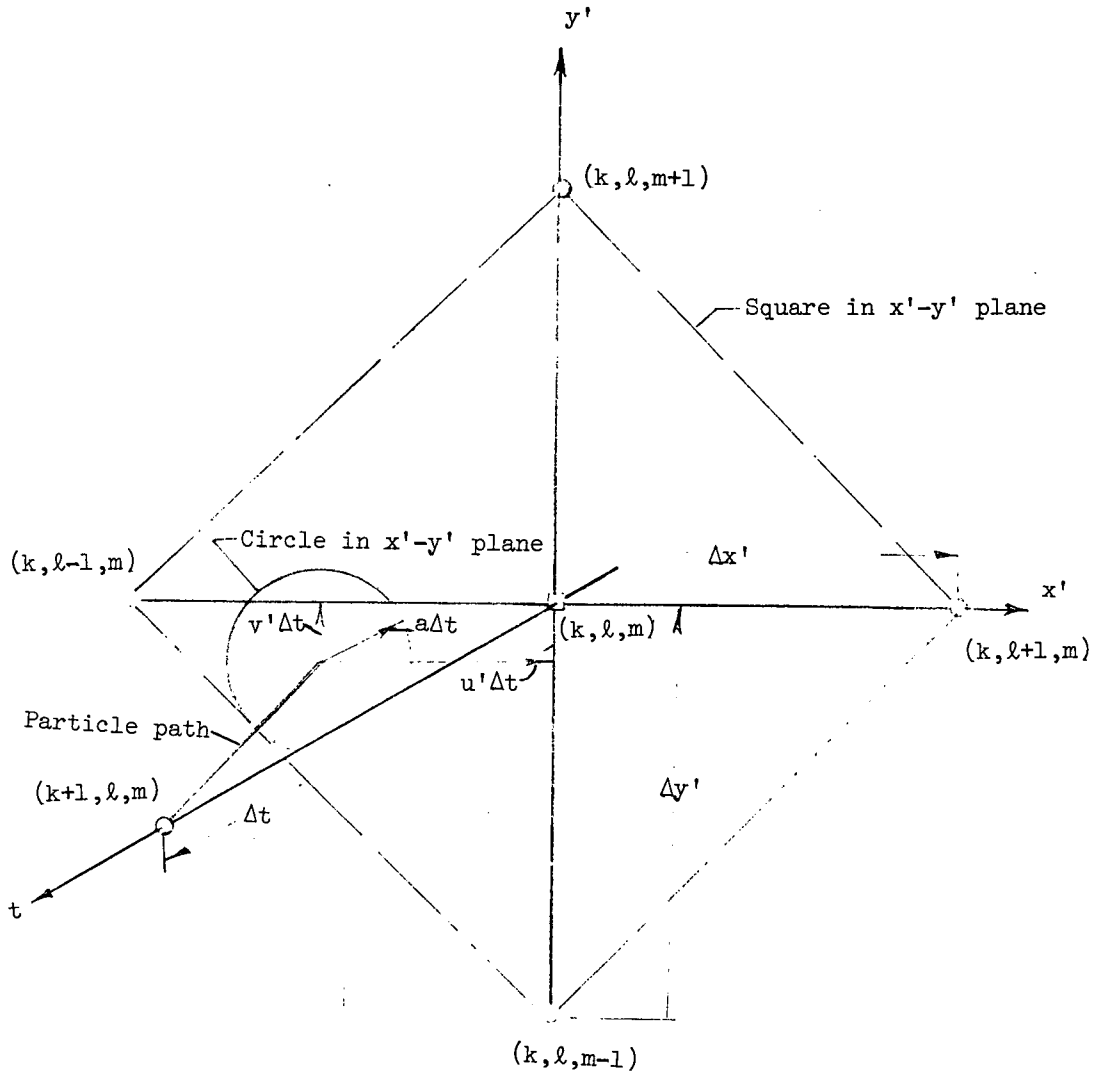

Figure 5.2.- Stability diagram for finite difference technique

$$\frac{\Delta t}{\Delta x'} \leq \frac{1}{|u'| + |v'| + \sqrt{2}\, a} \tag{5.12}$$

where u' and v' include the local translation of the body-fixed grid network relative to the freestream. The ratio of $\Delta x'$ to $\Delta y'$ is somewhat arbitrary. Here the mesh is chosen to be square for simplicity and also for a slight reduction in the number of multiply operations.

As a result of the stability criterion, selection of the position of the initial line and the grid spacing on it sizes the time step and grid spacing downstream. Consider the initial line to be located at x_0' and m_i grid points on the initial line within the shock layer. For a specified frequency of oscillation, the resulting value of k at x_0' is represented by k_{x_0}. The grid spacing is for the square grid,

$$\Delta x' = \Delta y' = \frac{x_0' \tan \lambda_0}{m_i - 1} \tag{5.13}$$

and the corresponding value of k at the body point l is,

$$k_l = k_{x_0} + \frac{l - 1}{m_i - 1} \tan \lambda_0 \tag{5.14}$$

The total number of time steps for a full time step, N_k, is determined from the period of oscillation, P, and the time step,

$$P = 2\, kt = N_k\, \Delta t = 2\pi \tag{5.15}$$

Substituting into (5.15) from (5.14) and (5.13) gives,

$$N_k = \frac{2\pi\,(m_i - 1}{x_0' \tan \lambda_0} \left[\sqrt{2}\, a + |u'| + |v'|\right] \tag{5.16}$$

For initialization or stability derivative-type aerodynamics, the number of time steps need only be sufficient for convergence of the flow field. The values of m_1 and x_0' determine the value of $(\dot{\theta}\bar{c}/2\bar{v})$, for example, at the body points downstream.

5.4 Results and Discussion

5.4.1 Discussion of the Numerical Finite Difference Results

The effect of increasing time step size as fraction of the CFL criterion, on converged steady flow results is shown in figure 5.3 for $\theta_w = 20^\circ$, $M = \infty$ ($M = 1000$ used here) and $\gamma = 1.4$. Stability was maintained up to slightly less the 0.8 of the CFL criterion, with the more accurate results obtained as the step size approaches the maximum. The results of figure 5.3 required approximately 250 time steps for convergence with somewhat fewer time steps required for the larger time step. Convergence proceeds essentially downstream from the initial line with points near the initial line coverging quite rapidly. The finite difference scheme used here is of first order and thus requires a fine grid network to maintain accuracy. In these calculations 16 (unstaggered) grid points were used on the initial line inside the shock layer in order to maintain the limited accuracy of about ten percent.

The results for several inclination angles are shown in figure 5.4. The relative accuracy is about the same for each inclination angle. Thus the difference in pressure level with angle, which would be required for the static aerodynamic force derivatives, would have about the same relative accuracy.

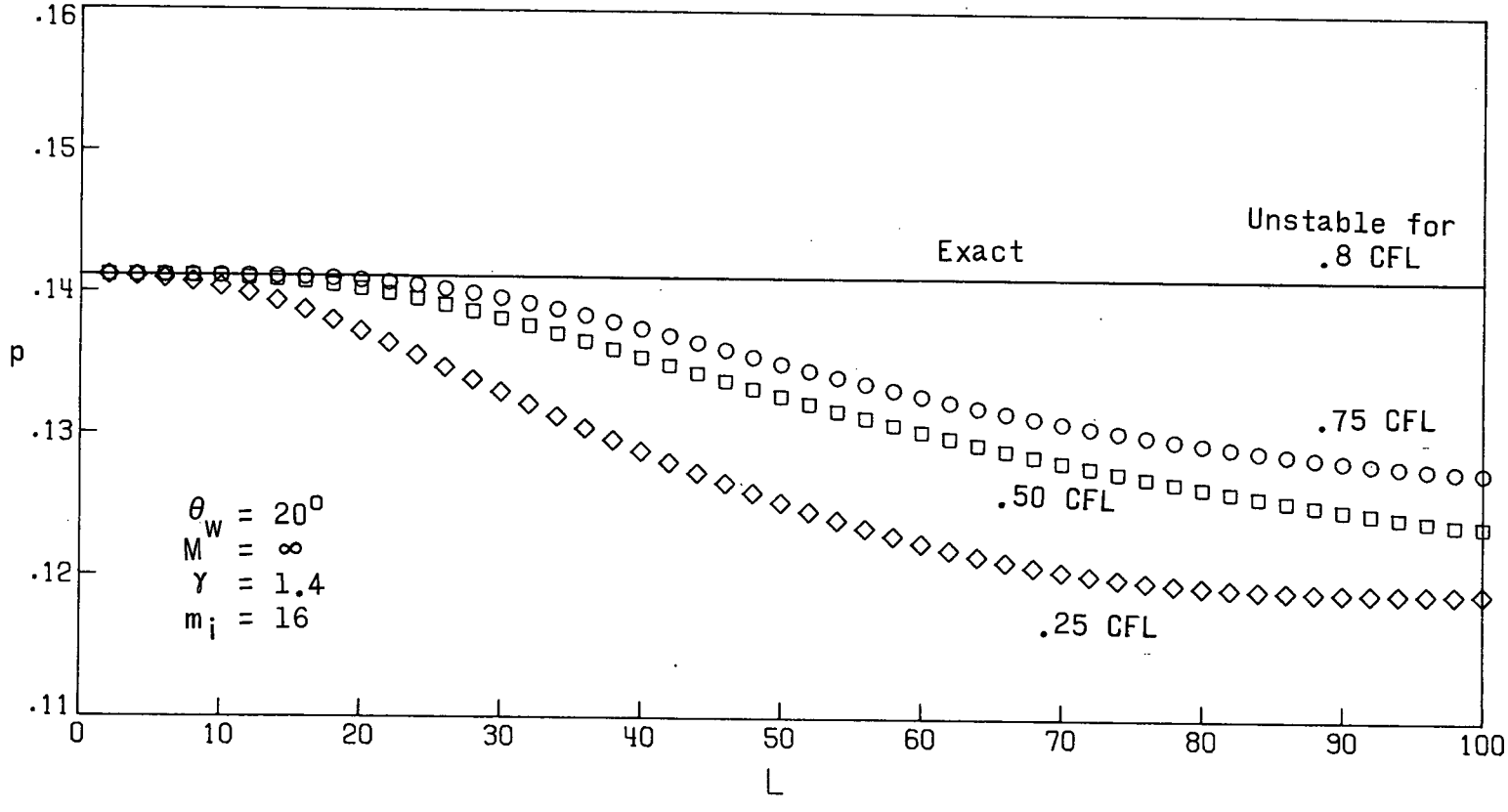

Figure 5.3.- Effect of time step size on converged results

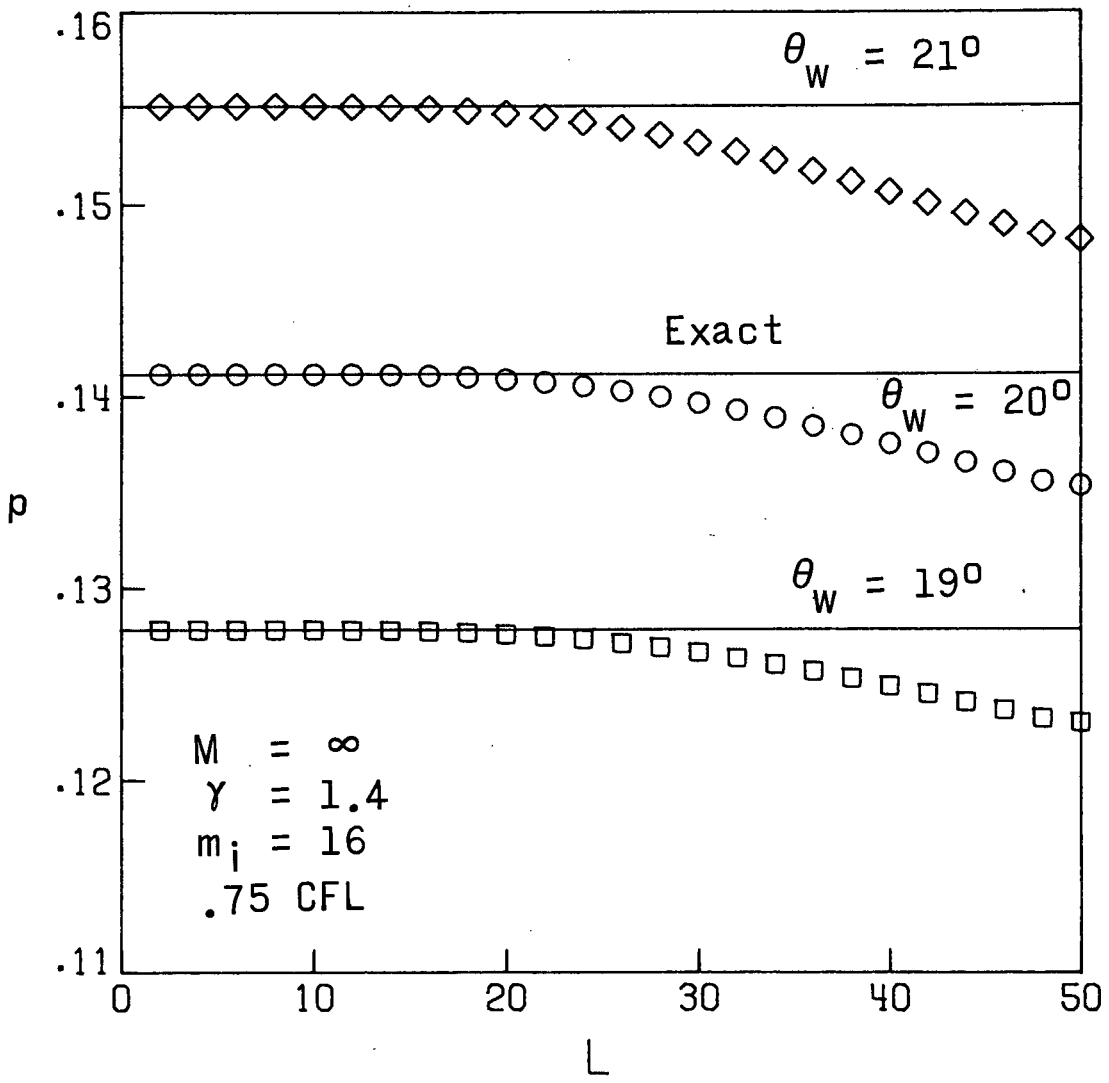

Figure 5.4.- Results of finite difference calculation for several inclination angles

The results for including $\dot{h}_y$ motion are presented in figure 5.5. The results are comparable to the previous results. Inclusion of $\dot{h}_y$ is essentially a change in wedge angle and Mach number and is thus essentially a steady flow calculation as $\dot{h}_y$ does not appear in the momentum equations (5.4).

The results of the finite difference calculation including $\dot{\theta}$ motion is shown in figure 5.6 for $M = 2$ and ∞, $\gamma = 1.4$, and $\theta_w = 20^\circ$. For $M = 2$ an unstable damping in pitch was calculated by the perturbation method (figs. 4.5 and 5.11). The corresponding slopes of the pressure (fig. 5.6) is in the stable sense. However the pressure should extrapolate back to the static value for $(\dot{\theta}\, \bar{c}/2\, \bar{V}_\infty)$ of zero which it does not in this case. This effect results possibly from a large value of $x\dot{\theta}$ at the initial line in conjunction with the surface pressure being constrained to static values at the starting line. It appears that a preferable procedure would be to use the results of the perturbation method of chapter 4 for the starting line in this type of calculation.

The results of the finite difference calculation presented herein are shown to be of limited accuracy both from the use of a first order difference scheme and from relatively simplified treatments of the boundary conditions. The basic formulation of the problem appears to be a useable one, however, but the basic difference grid network is required to be so fine that a significant range of amplitudes, and so forth, cannot be treated in practical terms. For example, the number of steps required from equation (5.16) to execute a cycle of oscillation would be prohibitive for significant results. Second order difference

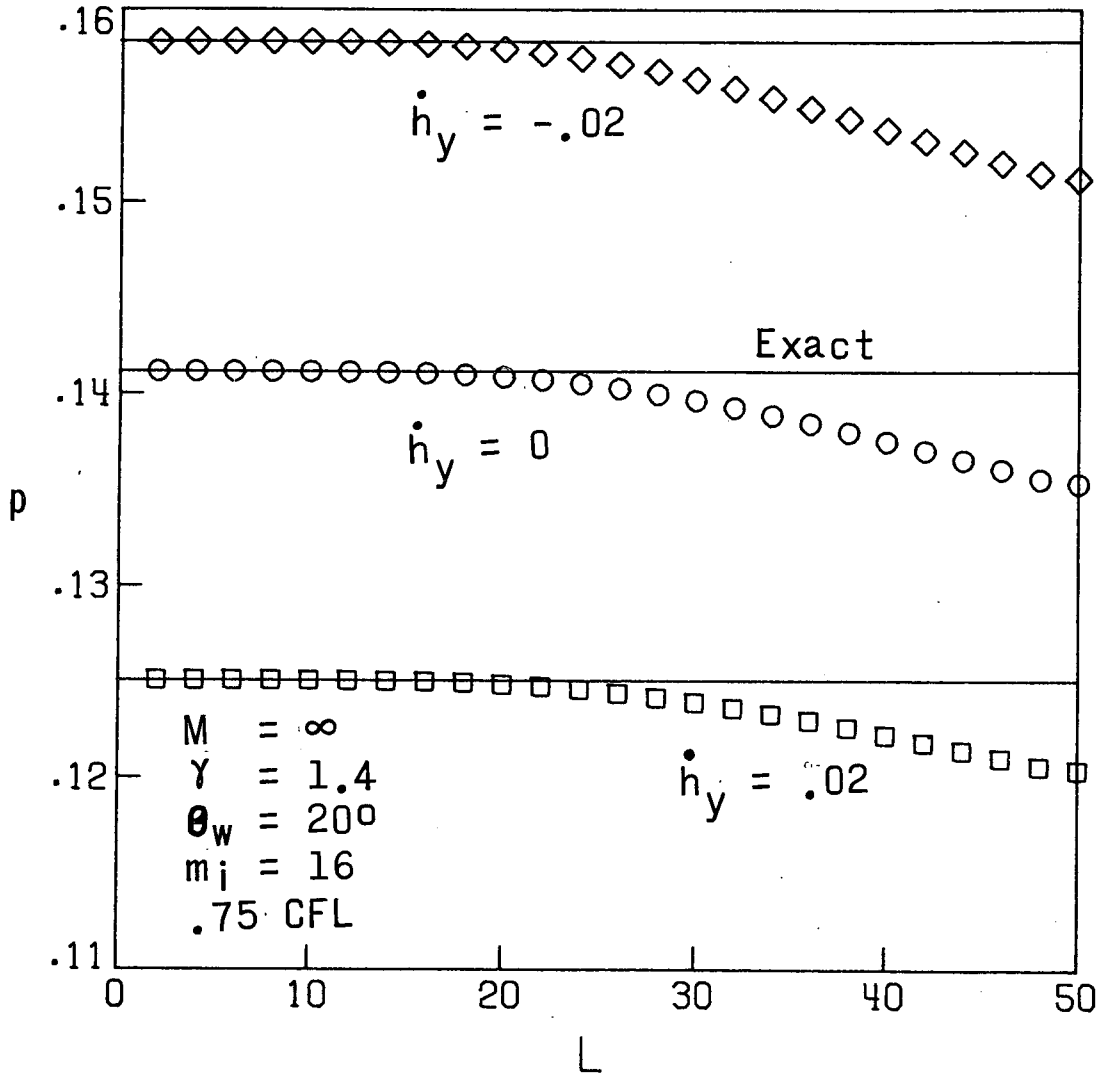

Figure 5.5.- Results of finite difference calculation including $\dot{h}_y$ motion

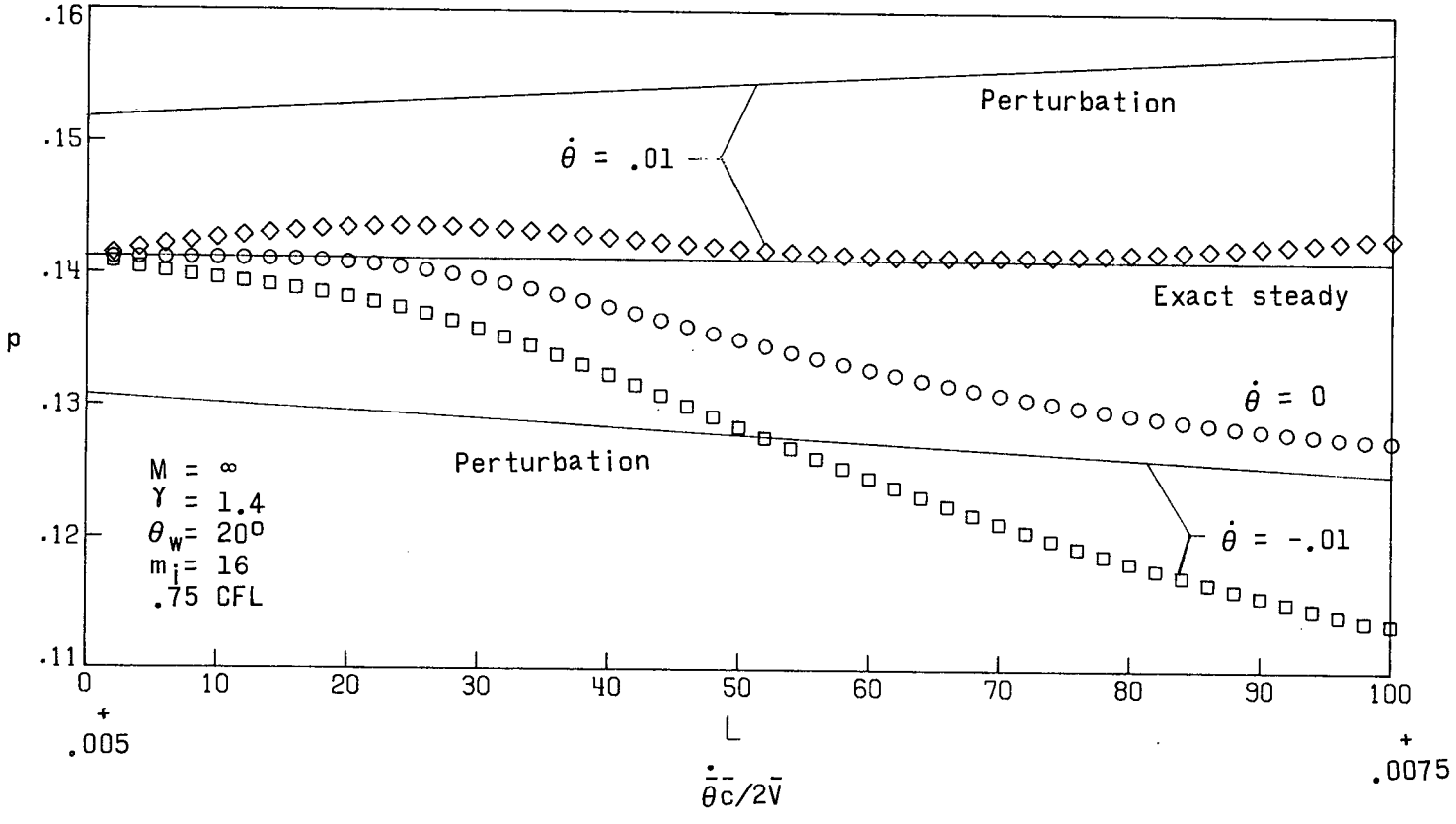

Figure 5.6.- Results of finite difference calculation including $\dot{\theta}$ motion

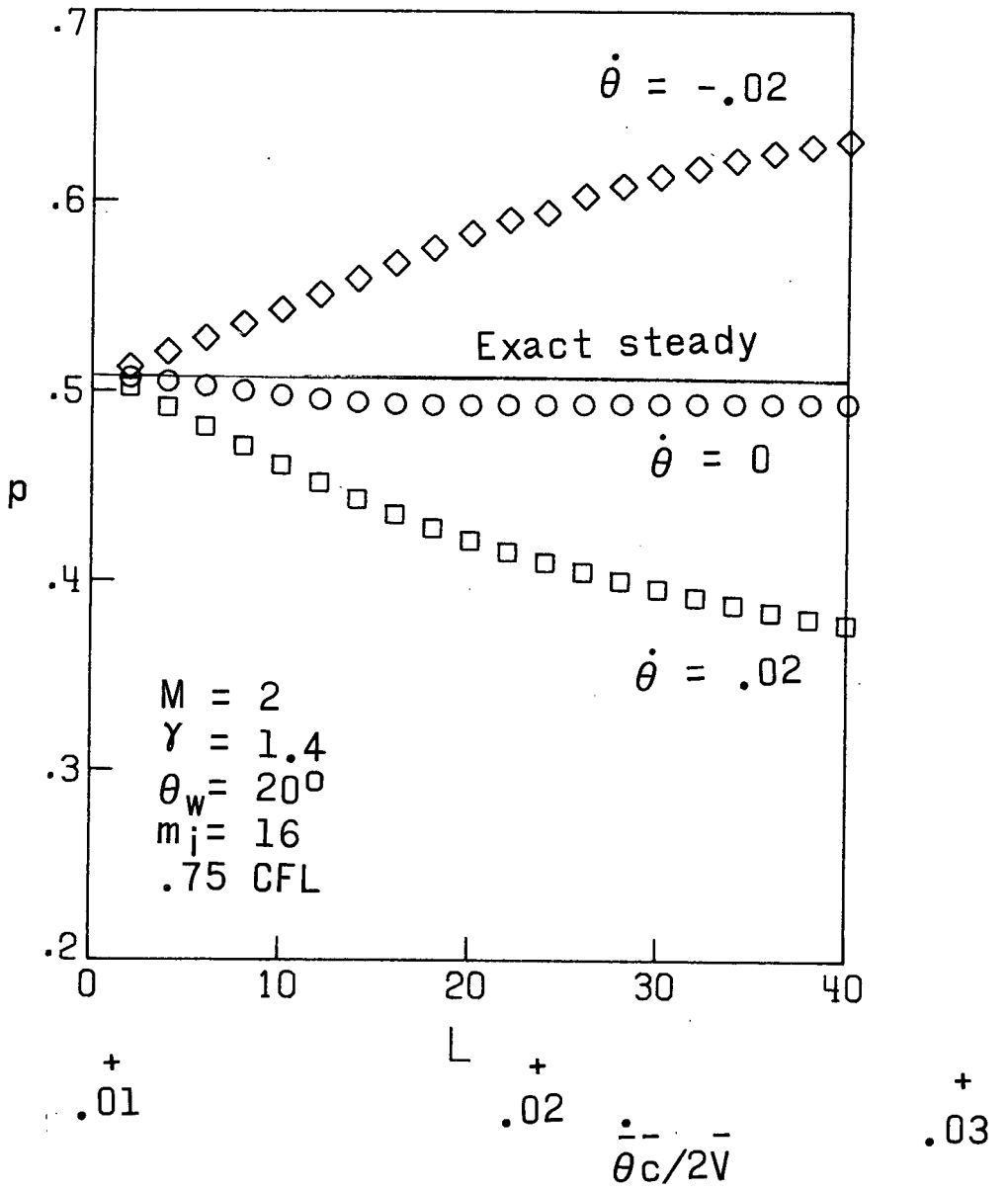

Figure 5.6.- Concluded

schemes such as that used by Barnwell (1971) can give good results with a relatively coarse grid network.

For further development it is recommended that a second-order difference scheme be used. Explicit treatment of the shock boundary condition may also be necessary to reduce the number of grid prints and increase the accuracy of the calculation. The region between the shock and body must thence be mapped such that the shock does not cut across the grid network and reduce the time step severely from the CFL criterion. Furthermore, the treatment of the body boundary condition should be improved by using a characteristic-type method such as that used by Barnwell (1971) or Moretti and Abbett (1966). This would necessitate the derivation of the appropriate compatibility relations. The recent solution of Hui (1970) for the perturbation about the quasi-static flow condition could be used for the initial line to further improve the capability.

5.4.2 Discussion of Quasi-Static Wedge Flows

At high supersonic or hypersonic speeds, the value of k at flutter is generally very small, 0.01 or less. The resulting phase lags from motion are quite small. Although even the small phase lags may be important in the dynamics of an aeroelastic system, the general character of the flow may be assessed by considering instantaneous response of the flow field or a quasi-static flow. Consider a Taylor's series expansion of the steady wedge flow pressure coefficient

$$C_p = C_{p_0} + \frac{\partial C_p}{\partial \theta_w}\theta + \frac{\partial^2 C_p}{\partial \theta_w^2}\frac{\theta^2}{3} + \frac{\partial^3 C_p}{\partial \theta_w^3}\frac{\theta^3}{6} + \frac{\partial^4 C_p}{\partial \theta_w^4}\frac{\theta^4}{24} + \ldots \quad (5.17)$$

where the partial derivatives with respect to t, x, and y are assumed to be zero in accordance with the previous comments. Let θ be described by simple harmonic motion at infinitesmal frequency,

$$\theta = \theta_0 \sin \omega t \tag{5.18}$$

Substituting (5.18) into (5.17) and using trigometric formulas for reducing $\sin^2 \omega t$, and so forth, gives for the difference in pressure from the steady flow value,

$$\begin{aligned}
\Delta C_p = &\left[\left(\frac{\partial^2 C_p}{\partial \theta_w^2} + \frac{\partial^4 C_p}{\partial \theta_w} \frac{\theta_0^2}{16} + \ldots\right) \frac{\theta_0^2}{4}\right] \\
&+ \left[\left(\frac{\partial C_p}{\partial \theta_w} + \frac{\partial^3 C_p}{\partial \theta_w^3} \frac{\theta_0^2}{8} + \ldots\right) \theta_0\right] \sin \omega t \\
&- \left[\left(\frac{\partial^2 C_p}{\partial \theta_w^2} + \frac{\partial^4 C_p}{\partial \theta_w^4} \frac{\theta_0^2}{12} + \ldots\right) \frac{\theta_0^2}{4}\right] \cos 2\omega t \\
&- \left[\left(\frac{\partial^3 C_p}{\partial \theta_w^3} + \ldots\right) \frac{\theta_0^3}{24}\right] \sin 3\omega t \\
&+ \left[\left(\frac{\partial^4 C_p}{\partial \theta_w^4} + \ldots\right) \frac{\theta_0^4}{192}\right] \cos 4\omega t + \ldots
\end{aligned} \tag{5.19}$$

Now from Ames Research Staff (1953)

$$C_p = \frac{4}{\gamma + 1} \left[\sin^2 \beta - 1/M_\infty^2\right] \tag{5.20}$$

where the relation between β and θ_w is a cubic equation in $\sin^2 \beta$ with coefficients as functions of M_∞, γ and θ_w. The derivatives of (5.19) can be evaluated by repeated differentiation of (5.20) and the cubic equation relating β and θ_w.

Inspection of equation (5.19) indicates, first a zero shift if second or higher even-derivatives are large; and higher harmonic terms (i.e., other than involving $\partial C_p/\partial \theta_w$) occur if second or higher derivatives are significantly large. By evaluating these derivatives, the regions of M_∞, γ, and θ_w where significant nonlinear effects of zero shifts and higher harmonics occur can be observed.

In figure 5.7, C_p vs θ_w is given for $M = 2$ and ∞ and for several values of γ. The derivatives through the fourth are presented in figure 5.8. (It might be noted that indeterminant froms of $0/0$ are encountered as $\theta_w \to 0$ and of increasing order for the higher derivatives. These were circumvented by letting $\theta_w \to \epsilon$, a small value, for $M = 2$ and using $C_p = (\gamma + 1) \sin^2 \theta_w$ at $\theta_w = 0$ for $M = \infty$). The character of the derivatives (figure 5.8) is quite different for varying γ and M_∞. All derivatives become infinite as detachment is approached suggesting that nearing detachment leads to large nonlinear effects. The results of hypersonic small disturbance theory were given by Kuiken (1969) for $M\theta_w = 2$ and 5 which indicated large nonlinear effects. For small angles and high Mach numbers the nonlinear effects are also shown here to be large as the higher derivatives are larger in comparison to the lower derivatives.

One implication of (5.19) is that the coefficient of the first harmonic contains contributions from the 3,5,... derivatives. Comparisons of filtered experimental data with a linear theory would be inappropriate if nonlinear effects are large.

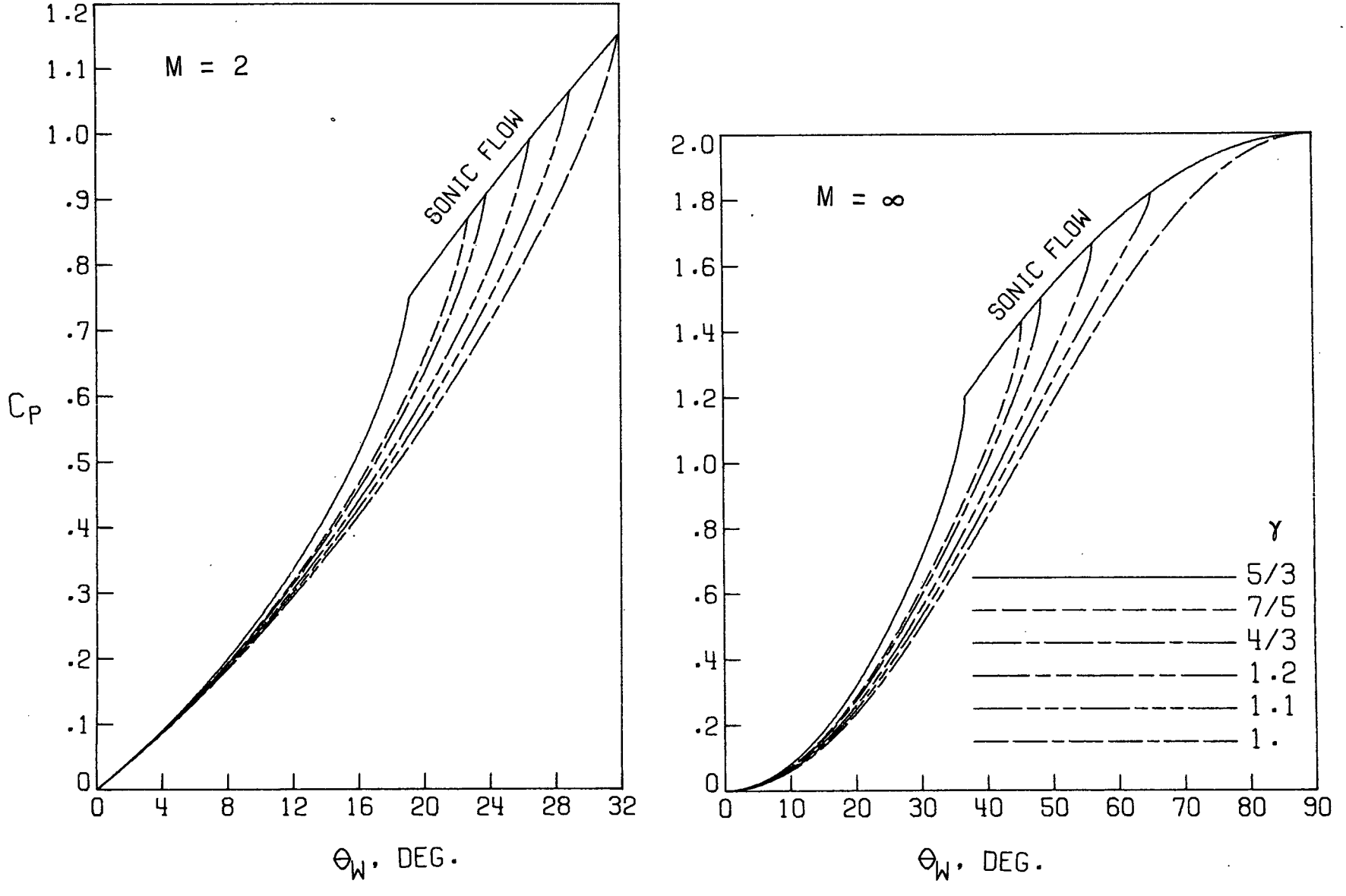

Figure 5.7.- Variation of pressure coefficient with wedge angle

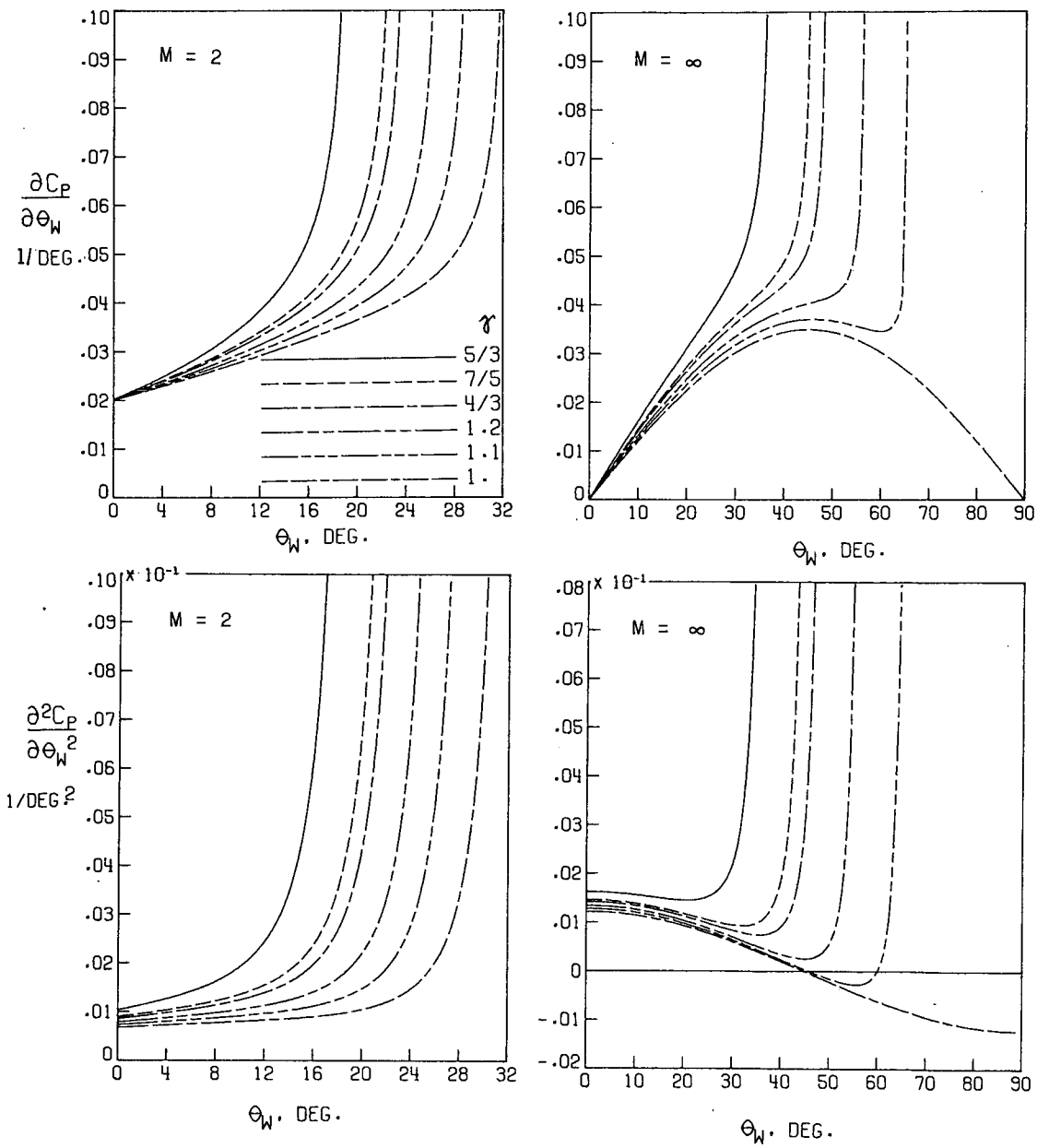

Figure 5.8.- Variation of pressure coefficient derivatives with wedge angle

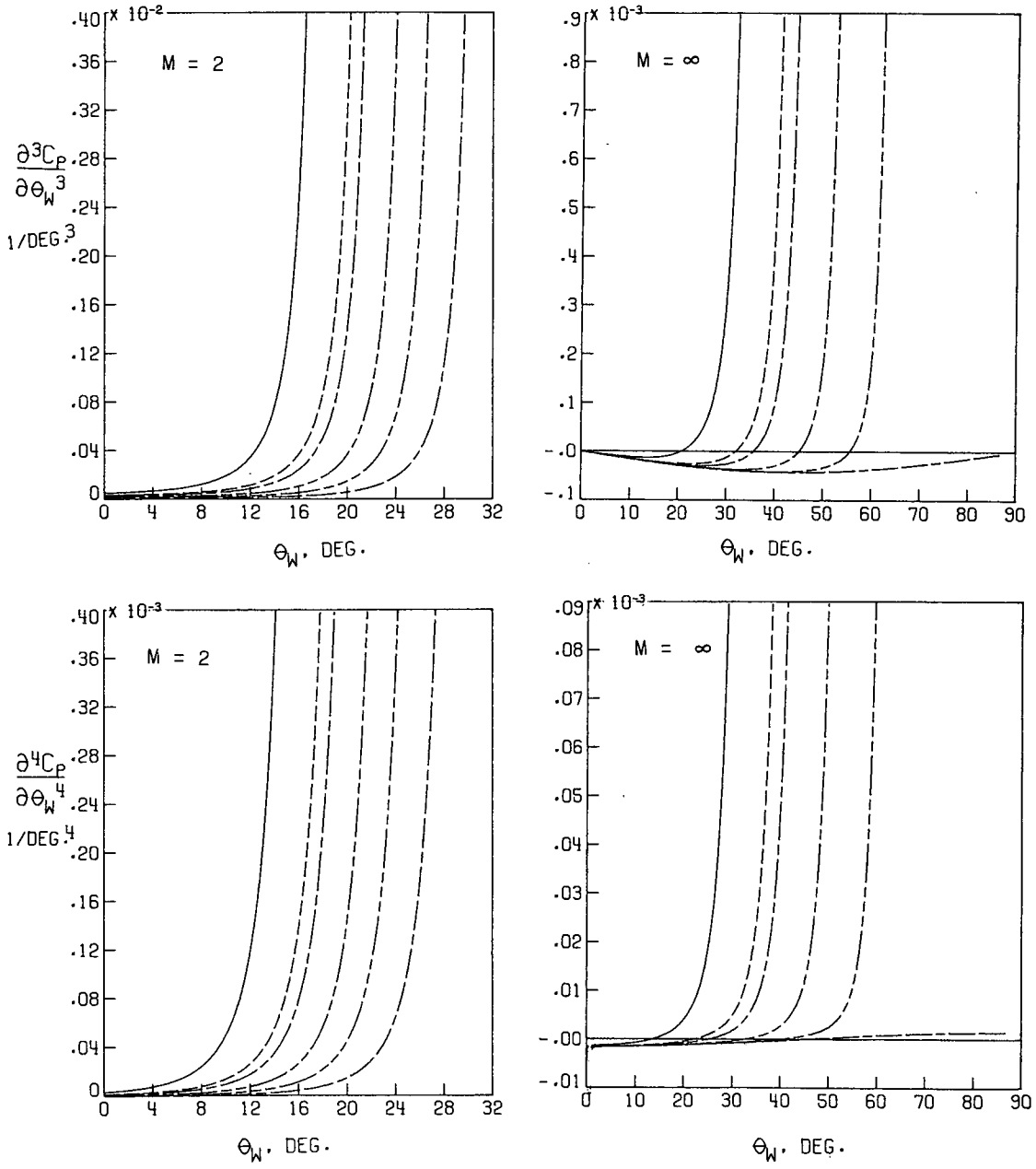

Figure 5.8.- Concluded

It appears from these brief results that significant nonlinear effects are to be encountered near detachment at all Mach numbers and for large amplitude motions of wedges of small angle at hypersonic speeds.

6. CONCLUDING REMARKS

To evaluate both the methods of treating unsteady flows for supersonic flows and the resulting trends, several aspects of the oscillating wedge have been considered. The two perturbation methods-hypersonic small disturbance theory and the more general method-involve only a moderate level of effort for analysis and computation for the oscillating wedge. Further extensions to treat more general configurations would involve considerably more effort as the entire region of interest of the steady flow field must be known in detail. A nonuniform steady flow would lead to variable coefficients in the differential equations governing the perturbation quantities such that interpolation of the steady flow would be required for numerical integration. Methods are of course, available that describe the steady flow field in detail. It would appear that direct numerical solution of the unsteady flows may be practical for complex configurations along the lines of the formulation presented in chapter 5. However, further development is required to assess this possibility in practical terms.

The trends presented for the wedge indicate that for inclination angles near detachment, large nonlinear effects may be anticipated at least for motions occurring at low reduced frequencies. The practical implications of detachment requires further investigation. In particular, the implications for three-dimensional wings and bodies from the two-dimensional wedge may be limited to large aspect ratio surfaces.

7. LIST OF REFERENCES

Ames Research Staff. 1953. Equations, Tables, and Charts for Compressible Flow. NACA Rept. 1135.

Appleton, J. P. 1964. Aerodynamic Pitching Derivatives of a Wedge in Hypersonic Flow. AIAA J. 2(11):2034-2036.

Aroesty, J., A. G. Charwat, S. Y. Chen, and J. D. Cole. 1966. Newtonian Snowplow Theory of Oscillating Airfoils. Rand Corp. Memo RM 4415-ARPA.

Ashley, H. 1970. Aeroelasticity. Appl. Mech. Rev., 23(20) 23(2):119-129.

Ashley, H., and G. Zartarian. 1956. Piston Theory - A New Aerodynamic Tool for the Aeroelastician. J. Aero. Sci. 23(1):1109-1118.

Ashley, H., and G. Zartarian. 1961. Theoretical Hypervelocity Unsteady Aerodynamics. In Proc. of Symposium on Aerothermoelasticity, Oct. 1961. U.S. Air Force ASD TR-61-645, pp. 161-218.

Bailie, J. A., and J. E. McFeely. 1966. Binary Flutter of Wedges in Hypersonic Flow. J. Spacecraft and Rockets 3(7):1130-1132.

Bailie, J. A., and J. E. McFeely. 1968. Panel Flutter in Hypersonic Flow. AIAA J. 6(2):332-337.

Barnwell, R. W. 1967. Numerical Results for the Diffraction of a Shock Wave by a Sphere and for the Subsequent Transient Flow. NASA TR-R-268.

Barnwell, R. W. 1971. A Time-Dependent Method for Calculating Supersonic Angle-of-Attack Flow About Axisymmetric Blunt Bodies With Sharp Shoulders and Smooth Nonaxisymmetric Blunt Bodies. NASA TN D-6283.

Berlotserkovskiy, O. M., and P. I. Chushkin. 1962. The Numerical Method of Integral Relations. U.S.S.R. Comput. Math. Math. Physics, 2(5):731-759. (Also available in English translation as NASA TT F-8356, 1963.)

Bisplinghoff, R. L., and H. Ashley. 1962. The Principles of Aeroelasticity. John Wiley and Sons, Inc., New York, N.Y.

Bohachevsky, I. O., and E. L. Rubin. 1966. A Direct Method for Calculation of Nonequilibrium Flows with Detached Shock Waves. AIAA J. 4(4):600-607.

Bohachevsky, I. O., and R. E. Mates. 1966. A Direct Method for Calculation of the Flow About an Axisymmetric Blunt Body at Angle of Attack. AIAA J. 4(5):776-782.

Brong, E. A. 1965. The Flow Field About a Right Circular Cone in Unsteady Flight. AIAA Paper No. 65-398.

Burstein, S. Z. 1964. Numerical Methods in Multidimensional Shocked Flows. AIAA J. 2(12):2111-2117.

Burstein, S. Z. 1967a. Finite-Difference Calculations for Hydrodynamic Flows Containing Discontinuities. J. of Computation Physics 2:198-222.

Burstein, S. Z. 1967b. High Order Difference Methods in Hydrodynamics in, W. F. Ames, ed. Nonlinear Partial Differential Equations, pp. 279-290, Academic Press, New York, N.Y.

Carrier, G. F. 1949a. On the Stability of the Supersonic Flows Past a Wedge. Quart. Appl. Math. 6(4):367-378.

Carrier, G. F. 1949b. The Oscillating Wedge in a Supersonic Stream. J. Aero. Sci. 16(3):150-152.

Chawla, J. P. 1958. Aeroelastic Instability at High Mach Number. J. Aero. Sci. 25(4):246-258.

Chernyi, G. G. 1961. Introduction to Hypersonic Flow. Academic Press, New York, N.Y.

Chu, B. T. 1952. On Weak Interaction of Strong Shock and Mach Waves Generated Downstream of the Shock. J. Aero. Sci. 19:433-446.

Chu, C. K. 1968. Computational Fluid Dynamics. AIAA Selected Reprint Series, 4.

DeJarnette, F. R. 1966. Application of Lax's Finite Difference Method to Nonequilibrium Hypersonic Flow Problems. NASA TR-R-234.

Dowell, E. H. 1969. Nonlinear Flutter of Curved Plates. AIAA J. 7(3):424-431.

East, R. A. 1962. A Theoretical and Experimental Study of Oscillating Wedge Shaped Aerofoils in Hypersonic Flow. Rept. AASU 228, Dept. of Aero. and Astro., Southampton Univ.

Emery, A. F. 1968. An Evaluation of Several Differencing Methods for Inviscid Fluid Flow Problems. J. of Computational Physics, 2:306-331.

Ericsson, L. E. 1968. Unsteady Aerodynamics of an Ablating Flared Body of Revolution Including Effect of Entropy Gradient. AIAA J. 6(12):2395-2401

Garrick, I. E., and S. I. Rubinow. 1946. Flutter and Oscillating Air-Force Calculations for an Airfoil in Two-Dimensional Supersonic Flow. NACA Report 846.

Garrick, I. E., ed. 1969. Aerodynamic Flutter. AIAA Selected Reprint Series, 5.

George, A. R. 1967. Perturbations of Plane and Axisymmetric Entropy Layers. AIAA J. 5(12):2155-2160.

Gourlay, A. R., and J. D. Morris. 1968. A Multistep Formulation of the Optimized Lax-Wendroff Method for Nonlinear Hyperbolic Systems in Two Space Variables. Math. of Comp. 22(104):715-419.

Hahn, S. G. 1958. Stability Criteria for Difference Schemes. Commun. Pure and Appl. Math. 11:243-255.

Hanson, P. W. 1961. Aerodynamic Effects of Some Configuration Variables on the Aeroelastic Characteristics of Lifting Surfaces at Mach Numbers from 0.7 to 6.86. NASA TN D-984.

Harlow, F. H. 1969. Numerical Methods for Fluid Dynamics, an Annotated Bibliography. Los Alamos Scientific Lab. of Univ. of Calif. Report LA-4281.

Hayes, W. D. 1947. On Hypersonic Similitude. Quart. Appl. Math. 5(1):105-106.

Hayes, W. D., and R. F. Probstein. 1966. Hypersonic Flow Theory. Vol. I. Inviscid Flows, 2nd ed. Academic Press, New York, N.Y.

Heie, H., and D. C. Leigh. 1965. Numerical Stability of Hyperbolic Equations in Three Independent Variables, AIAA J. 3(6):1099-1103.

Hui, W. H. 1969a. Stability of Oscillating Wedges and Caret Wings in Hypersonic and Supersonic Flows. AIAA J. 7(8):1524-1530.

Hui, W. H. 1969b. Interaction of a Strong Shock with Mach Waves in Unsteady Flow. AIAA J. 7(8):1605-1607.

Hui, W. H. 1970. Large-Amplitude Slow Oscillation of Wedges in Inviscid Hypersonic and Supersonic Flows. AIAA J. 8(8):1530-1532.

Hui, W. H., and R. A. East. 1971. Stability Derivatives of Sharp Wedges in Viscous Hypersonic Flow. Aero. Quart. 22:127-145.

Johnston, G. W. 1953. An Investigation of the Flow About Cones and Wedges at and Beyond the Critical Angle. J. Aero. Sci. 20(6):378-382.

Kacprzynski, J. J. 1968. A Low Frequency Solution of Unsteady Inviscid Hypersonic Flow Past an Oscillating Wedge with Attached Shock Wave. Canadian NAE Rep. LTR-UA-5.

King, W. S. 1966. Low-Frequency, Large-Amplitude Fluctuations of the Laminar Boundary Layer. AIAA J. 4(6):994-1001.

Klunker, E. B., J. C. South, Jr., and R. M. Davis. 1971. Calculation of Nonlinear Conical Flows by the Method of Lines. NASA TR R-374.

Kuiken, H. K. 1969. Large Amplitude Low-Frequency Oscillation of a Slender Wedge in Inviscid Hypersonic Flow. AIAA J. 7(9):1767-1774.

Lambourne, N. C. 1967. Calculations Showing the Influence of Aerodynamic Damping on Binary Wing Flutter. British Aero. Res. Council R. and M. 3579.

Landa, P. S., and P. S. Gtrelkow. 1963. Wing Flutter at Nonlinear Aerodynamic Forces. U.S. Air Force FTD-TT-63-201/1+2.

Landahl, M. T. 1961. Unsteady Transonic Flow. Pergamon Press, New York, N.Y.

Lapidus, A. 1967. A Detached Shock Calculation by Second-Order Finite Differences. J. Comp. Phys. 2:154-177.

Lax, P. D. 1954. Weak Solutions of Nonlinear Hyperbolic Equations and Their Numerical Computation. Commun. Pure Appl. Math. 7(1):159-193.

Lax, P. D., and B. Wendroff. 1964. Difference Schemes for Hyperbolic Equations with High Order of Accuracy. Commun. Pure Appl. Math. 17:381-398.

Liepmann, H. W., and A. Roshko. 1957. Elements of Gasdynamics. John Wiley and Sons, Inc., New York, N.Y.

Lighthill, M. J. 1953. Oscillating Airfoils at High Mach Number. J. Aero. Sci. 20(6):402-406.

MacCormack, R. W. 1969. The Effect of Viscosity in Hypervelocity Impact Cratering. AIAA paper 69-354.

Martuccelli, J. R. 1958. Measurement of Pressure Distributions on an Oscillating Wedge in Supersonic Flow. MIT Aeroelastic and Structures Res. Lab. Tech. Rep. 71-2.

McIntosh, S. C. 1965a. Hypersonic Flow Over an Oscillating Wedge. AIAA J. 3(3):433-440.

McIntosh, S. C. 1965b. Studies in Unsteady Hypersonic Flow Theory. Ph. D. Dissertation, Stanford Univ.

Miles, J. W. 1960. Unsteady Flow at Hypersonic Speeds. in, Hypersonic Flow, 185-197, Butterworths Scientific Publications, London.

Moretti, G., and M. A. Abbett. 1966. A Time-Dependent Computational Method for Blunt Body Flows. AIAA J. 4(12):2136-2141.

Moretti, G. 1968. The Importance of Boundary Conditions in the Numerical Treatment of Hyperbolic Equations. Polytechnic Institute of Brooklyn, PIBAL Report No. 68-34.

Morino, L. 1969. A Perturbation Method for Treating Nonlinear Panel Flutter Problems. AIAA J. 7(3):405-411.

Morgan, H. G., H. L. Runyan, and V. Huckel. 1958. Theoretical Considerations of Flutter at High Mach Numbers. J. Aero. Sci. 25(6):371-381.

Muhlstein, L., Jr. 1971. Experimental Investigation of the Influence of the Turbulent Boundary Layer on the Pressure Distribution Over a Rigid Two-Dimensional Wavy Wall. NASA TN D-6477.

NASA SP-228. 1970. Analytic Methods in Aircraft Aerodynamics. In Proc. of Symposium Held at Ames Research Center, Moffett Field, Calif., Oct. 28-30, 1969.

Orlik-Rückemann, K. J. 1966a. Stability Derivatives of Sharp Wedges in Viscous Hypersonic Flow. AIAA J. 4(6):1001-1008.

Orlik-Rückemann, K. J. 1966b. Effect of Wave Reflections on the Unsteady Hypersonic Flow Over a Wedge. AIAA J. 4(10):1884-1886.

Orlik-Rückemann, K. J. 1969. Simple Formulas for Unsteady Pressure on Slender Wedges and Cones in Hypersonic Flow. AIAA J. 6(10):1209-1211.

Orlik-Rückemann, K. J. 1970. Dynamic Viscous Pressure Interaction in Hypersonic Flow. Canadian NAE Rep. LR-535.

Pai, S. H. 1956. Viscous Flow Theory, I-Laminar Flow. D. Van Nostrand Co., Princeton, N.J.

Pugh, P. G. and L. Woodgate. 1963. Measurements of Pitching-Moment Derivatives for Blunt-Nosed Aerofoils Oscillating in Two-Dimensional Supersonic Flow. British Aero. Res. Council R. and M. 3315.

Rakich, J. V. 1969. A Method of Characteristics for Steady Three-Dimensional Supersonic Flow with Application to Inclined Bodies of Revolution. NASA TN D-5341.

Richtmyer, R. D., and K. W. Morton. 1967. Difference Methods for Initial-Value Problems. 2nd ed. J. W. Wiley and Sons, New York, N.Y.

Runyan, H. L., and H. G. Morgan. 1962. Flutter at Very High Speeds. NASA TN D-942.

Sauerwein, H. 1964. The Calculation of Two- and Three-Dimensional Inviscid Unsteady Flows by the Method of Characteristics. Sc. D. Thesis, MIT Fluid Dynamics Lab Report 64-4, USAF OSR 64-1055.

Sauerwein, H. 1965. A general Numerical Method of Characteristics. AIAA Paper 65-25.

Sauerwein, H. 1966. Numerical Calculations of Arbitrary Multi-dimensional and Unsteady Flows by the Method of Characteristics. AIAA Paper 66-412.

Sauerwein, H., and M. Sussman. 1964. Numerical Stability of the Three-Dimensional Method of Characteristics. AIAA J. 2(2):387-389.

South, J. C. 1968. Calculation of Axisymmetric Supersonic Flow Past Blunt Bodies with Sonic Corners Including a Program Description and Listing. NASA TN D-4563.

South, J. C., and P. W. Newman. 1965. Supersonic Flow Past Pointed Bodies. AIAA J. 3(3):1019-1021.

Truitt, R. W. 1959. Hypersonic Aerodynamics. Ronald Press Co., New York, N.Y.

Van Dyke, M. D. 1953. On Supersonic Flow Past an Oscillating Wedge. Quart. Appl. Math. 11(3):360-363.

Van Dyke, M. D. 1954a. Supersonic Flow Past Oscillating Airfoils Including Nonlinear Thickness Effects. NACA Rept. 1183.

Van Dyke, M. D. 1954b. A Study of Hypersonic Small-Disturbance Theory. NACA Rept. 1194.

Walkden, F. 1966. The Equations of Motion of a Viscous Compressible Gas Referred to an Arbitrarily Moving Co-Ordinate System. British RAE Tech. Rep. No. 66140.

Wood, B. M. 1966. A Survey of Unsteady Hypersonic Flow Problems. British Aero. Res. Council C. P. 901.

Woolston, D. S., H. L. Runyan, and T. A. Byrdsong. 1955. Some Effects of System Nonlinearities in the Problem of Aircraft Flutter. NACA TN 3539.

Yates, E. C., Jr., and R. M. Bennett. 1971. Analysis of Supersonic-Hypersonic Flutter of Lifting Surfaces at Angle of Attack. AIAA Paper No. 71-327.

Zartarian, G., and H. Sauerwein. 1962. Further Studies on High-Speed Flow. USAF ASD-TDR-62-463.

8. APPENDIX

8.1 List of Symbols

A partial list of the principal symbols used with their principal definitions is given here. Some of the symbols are defined locally where used. It should be noted that different nondimensional factors are used in Chapter 5 than in Chapter 4. Some symbols also have different meanings in different contexts.

A_i, B_i, C_i, D_i	see equation 5.6
a	local speed of sound
B_0	$\sqrt{M_0^2 - 1}$
b	airfoil semichord
C_p	pressure coefficient, $(\bar{p}_0 - \bar{p}_\infty)/q_\infty$
$\bar{c}$	reference length
F	see equation 3.4
h_x	displacement parallel to surface (fig. 4.1)
h_y	plunging displacement normal to surface (fig. 4.1)
i	$\sqrt{-1}$
K	$M\theta_w$
K_τ	$M\tau$, where τ(also β) is shock wave angle
k	reduced frequency, $\bar{c}\,\bar{\omega}/2\bar{V}_\infty$
k,l,m	finite difference grid indices for t,x,y respectively (fig. 5.1)
$\tilde{L}_j$	coefficient in normal force expression (see eq. 4.10a) $j = 1,2,3,4,7,8$
M	Mach number, V/a
M_j	coefficient in moment expression (see eq. 4.10b) $j = 1,2,3,4,7,8$

m	airfoil mass per unit span
m_i	number of grid points on initial line within shock layer
P_v, P_β	$\partial p_\delta/\partial V_n$, $\partial p_\delta/\partial \beta$
p	pressure
q	dynamic pressure
R_v, R_β	$\partial \rho_\delta/\partial V_n$, $\partial \rho_\delta/\partial \beta$
r_α	section radius of gyration about x_0, units of b
t	time
t/c	thickness/chord ratio
U_v, U_β	$\partial U_\delta/\partial V_n$, $\partial U_\delta/\partial \beta$
u	velocity component in x-direction
V	total speed
V_v, V_β	$\partial V_\delta/\partial V_n$, $\partial V_\delta/\partial \beta$
v	velocity component in y-direction
x	coordinate distance (fig. 4.1)
x_0	pitching axis, fraction of $\bar{c}$ measured from leading edge
y	coordinate distance (fig. 4.1)
β	shock angle (fig. 4.1)
β_n	$2k(\Gamma^n - 1)$ where k is reduced frequency, n = 1,2...
Δ	quantity defined by equation 4.9b
δ	shock displacement perturbation measured normal to steady shock
δ_0	shock layer thickness in y-direction (fig. 4.1)
δ_w	wedge angle ($\delta_w = 1/2 \tan^{-1}$ (t/c) for symmetrical wedge airfoil)
ϵ	perturbation parameter
Γ	see equation 3.4

γ	ratio of specific heats
λ	see equation 3.4
λ_0	included angle between shock and surface (fig. 4.1)
ω	circular frequency of oscillation
ω_h	natural frequency in plunge
ω_α	natural frequency in pitch
ρ	density
θ	pitch angle
θ_w	surface inclination angle
μ	mass ratio, $\bar{m}/\bar{\rho}\ \bar{c}^2$

Subscripts:

f	pertaining to flutter
n	normal to shock wave
s	evaluated at surface
u,l	pertaining to upper or lower surface respectively, for a symmetrical wedge
v	pertaining to normal velocity of shock wave
w	pertaining to symmetrical wedge
β	pertaining to change in shock wave slope
δ	evaluated at shock wave
0	steady flow value in shock layer
1	perturbation quantity
∞	freestream value

Superscripts:

'	pertaining to pitch (or pitching moment) about leading edge or pertaining to body-fixed axis system
~	pertaining to forces normal to surface

Bar over variable indicates dimensional quantity

Dot over variable indicates d/dt

8.2 Perturbations of Flow Variables at a Moving Oblique Shock Wave

The incremental values of p, ρ, u, and v resulting from perturbations of slope and normal velocity of the moving oblique shock wave are required as the boundary conditions for a perturbation analysis. The shock wave perturbation is measured normal to the steady shock wave position as shown in figure 4.1. The appropriate perturbations of the Rankine-Hugoniot conditions in a coordinate system aligned with the steady shock wave have been developed by Carrier (1949a). They have also been given in the surface coordinate system used here (fig. 4.1) specialized to $\gamma = 7/5$ (Carrier, 1949a and Van Dyke, 1953), and for general values of γ but in somewhat different nondimensional units by Carrier (1949a) and Hui (1969a).

With the normal velocity of the shock wave given by:

$$v_n = i\delta(x) \tag{8.1}$$

the perturbations are written in the following form (omitting $e^{i\omega t}$):

$$\begin{aligned} p_\delta &= P_\beta \beta + iP_v \delta \\ \rho_\delta &= R_\beta \beta + iR_v \delta \\ u_\delta &= U_\beta \beta + iU_v \delta \\ v_\delta &= V_\beta \beta + iV_v \delta \end{aligned} \tag{8.2}$$

where

$$P_\beta = \partial p_\delta / \partial \beta, \quad P_v = \partial p_\delta / \partial v_n, \text{ etc.}$$

evaluated at the steady shock wave position and subscript δ denotes conditions just aft of the shock wave. Letting

$$M_n = M_\infty \sin \beta_0$$
$$U_n = \frac{2(M_n^2 + 1)}{(\gamma + 1)M_n^2} \tag{8.3}$$

then the shock derivatives can be written as

$$P_v = \frac{4}{(\gamma + 1)\rho_0 u_0} \sin \beta_0$$
$$R_v = \frac{4}{(\gamma + 1)} \frac{\rho_0}{M_n^2 \sin \beta_0} \tag{8.4}$$
$$U_v = - U_n \sin \lambda_0$$
$$V_v = U_n \cos \lambda_0$$

and

$$P_\beta = \frac{P_v}{u_0} \cos \beta_0$$
$$R_\beta = R_v \cos \beta_0$$
$$U_\beta = \frac{U_n}{u_0} \sin \theta_w - \rho_0 P_v \cos \lambda_0 \tag{8.5}$$
$$V_\beta = \frac{U_n}{u_0} \cos \theta_w - \rho_0 P_v \sin \lambda_0$$

The above relations reduce to those given by McIntosh (1965a) in the hypersonic small disturbance limit. It can also be shown with a similar development, that perturbations of the shock wave tangential to the steady shock position results in second order perturbations in the flow variables.

The steady flow values of pressure, density, and velocities within the shock layer are given in Ames Research Staff (1953) as functions of γ, M_∞, and β_0. The corresponding relation between β_0 and θ_w is also given as a cubic in $\sin^2 \beta_0$ with coefficients as functions of γ and θ_w. These relations are solved numerically for the steady flow field parameters.

8.3 Calculation of Aerodynamic Coefficients for a Wedge from Surface Coefficients

The unsteady aerodynamic coefficients for a single isolated surface have been derived in the body of this report (Chapter 4) for rigid body pitch and translation perpendicular and parallel to the surface. The coefficients and k were based on $\bar{c}$, the length of the surface and the pitch axis was located at the leading edge. The coefficients for a symmetrical wedge at an angle of attack are given here in terms of the surface coefficients. The pitch axis is assumed to be on the wedge midplane or chordline. The derivation of these relations are briefly outlined and the results summarized.

8.3.1 Force and Motion Transfer

The forces and moments for a symmetrical wedge (subscript w) are related to the previously given coefficients for a single surface by

$$\begin{aligned} \bar{L}_w &= \pm \tilde{\bar{L}} \cos \delta_w \\ \bar{C}_w &= - \tilde{\bar{L}} \sin \delta_w \\ \bar{M}'_w &= \pm \bar{M}' \end{aligned} \tag{8.6}$$

where the upper sign is for an upper surface. The pitch axis is displaced from the surface and the chords related by

$$\begin{aligned} \bar{c} &= \bar{c}_w/\cos\delta_w \\ \bar{x}_0 &= \bar{x}_{0,w}\cos\delta_w \\ \bar{y}_0 &= -\bar{x}_{0,w}\sin\delta_w \end{aligned} \tag{8.7}$$

The perturbation displacements are related by

$$\begin{aligned} \bar{h}_y &= \pm\bar{h}_{y_w}\cos\delta_w - \bar{h}_{x_w}\sin\delta_w - \bar{x}_{0,w}\cos\delta_w\,\theta \\ \bar{h}_x &= \bar{h}_{x_w}\cos\delta_w \pm \bar{h}_{y_w}\sin\delta_w - \bar{x}_{0,w}\sin\delta_w\,\theta \\ \theta_{u,l} &= \pm\theta \end{aligned} \tag{8.8}$$

where again the upper sign pertains to the upper surface.

The force and moment coefficients are defined by equation 4.10 for a single surface. By defining the coefficients in manner similar to (4.10) for the wedge, the coefficients for the surfaces and the wedge can be related through the use of (8.6) for the dimensional forces. Then substituting (8.7) and (8.8) into the expression for the surface coefficients, the wedge coefficients can be equated to the equivalent combination of surface coefficients.

8.3.2 Coefficients for Wedge

The results for the coefficients of lift for the wedge are:

$$\begin{aligned} L_1 &= (\tilde{L}_{1u} + \tilde{L}_{1l}) + (\tilde{L}_{7u} + \tilde{L}_{7l})\tan\delta_w \\ L_2 &= (\tilde{L}_{2u} + \tilde{L}_{2l}) + (\tilde{L}_{8u} + \tilde{L}_{8l})\tan\delta_w \end{aligned}$$

$$L'_3 = (\tilde{L}'_{3u} + \tilde{L}'_{3l})/\cos^2 \delta_w$$

$$L'_4 = (\tilde{L}'_{4u} + \tilde{L}'_{4l})/\cos^2 \delta_w$$

$$L_7 = (\tilde{L}_{7u} - \tilde{L}_{7l}) - (\tilde{L}_{1u} - \tilde{L}_{1l}) \tan \delta_w$$

$$L_8 = (\tilde{L}_{8u} - \tilde{L}_{8l}) - (\tilde{L}_{2u} - \tilde{L}_{2l}) \tan \delta_w \qquad (8.9)$$

and

$$M'_1 = [(M'_{1u} + M'_{1l}) + (M'_{7u} + M'_{7l}) \tan \delta_w]/\cos^2 \delta_w$$

$$M'_2 = [(M'_{2u} + M'_{2l}) + (M'_{8u} + M'_{8l}) \tan \delta_w]/\cos^2 \delta_w$$

$$M'_3 = (M'_{3u} + M'_{3l})/\cos^4 \delta_w$$

$$M'_4 = (M'_{4u} + M'_{4l})/\cos^4 \delta_w$$

$$M'_7 = [(M'_{7u} - M'_{7l}) - (M'_{1u} - M'_{1l}) \tan \delta_w]/\cos^2 \delta_w$$

$$M'_8 = [(M'_{8u} - M'_{8l}) - (M'_{2u} - M_{2l}) \tan \delta_w]/\cos^2 \delta_w \qquad (8.10)$$

where the subscript has been omitted from the left hand side of (8.9) and (8.10). The relationship for reduced frequency for the wedge is

$$k = k_{u \text{ or } l} \cos \delta_w \qquad (8.11)$$

It may also be noted that for zero angle of attack, the coefficients for the upper and lower surfaces are equal and thus the coefficients L_7, kL_8, M_7, and kM_8 are zero. Such would not be the case for nonzero angles of attack, however.

For pitch axis locations other than $x_{0,w} = 0$, the transfer relations are found from the same procedure to be the conventional ones (e.g. Garrick and Rubinow, 1946) and are

$$L_1 = L_1'$$

$$L_2 = L_2'$$

$$L_3 = L_3' - 2x_0 L_1$$

$$L_4 = L_4' - 2x_0 L_2$$

$$L_7 = L_7'$$

$$L_8 = L_8'$$

and

$$M_1 = M_1' - 2x_0 L_1$$

$$M_2 = M_2' - 2x_0 L_2$$

$$M_3 = M_3' - 2x_0 (M_1' + L_3' - 2x_0 L_1)$$

$$M_4 = M_4' - 2x_0 (M_2' + L_4' - 2x_0 L_2)$$

$$M_7 = M_7' - 2x_0 L_7$$

$$M_8 = M_8' - 2x_0 L_8 \qquad (8.12)$$

where $x_0 = x_{0,w}$ in (8.12).

8.4 Description of Computer Programs

The two principal programs used to generate the results presented in chapters 4 and 5. The FORTRAN computer program for numerically integrating the complex system of equations (4.7) to obtain the aerodynamic coefficients as a function of k from the perturbation is presented first. A library routine, INT2A, for integrating a system of real, first-order, differential equations is used to integrate (4.7) after expanding into real form. The pitch and two translational motions are treated separately. The program for finite difference calculation

of the unsteady flow field is then presented which can treat steady, oscillatory, or quasi-static motions. Pitch and the two translational motions may be treated separately or combined.

These programs were written by the author for use on the Control Data 6000 - series machines at Langley Research Center using the RUN compiler and the Langley Research Center version of the SCOPE 3.0 operating system. Approximately 14 significant figures were used in the computations. The compiler used permits the use of multiple arithmetic statement on one card when separated by the character $. It might also be noted that the quantity 1777000000000000000000_8 signifies an indefinite (undefined) quantity.

8.4.1 Program for Perturbation Analysis

8.4.1.1 Input

Each case consists of a single card (80 characters) of identification for labeling the printout only, and list of variables in a NAMELIST called INPDATA. The FORTRAN variables and their definitions are as follows.

FORTRAN VARIABLE	Definition
XM	M_∞
THWD	θ_w, degrees
G	γ
XO	starting value of k for beginning numerical integration
XSTOP	stopping value of k
CI	k - increment for numerically integrating the differential equation
SPEC	k - increment for printing results

8.4.1.2 Output

The program lists each aerodynamic coefficient for each value of k requested (by SPEC) and the real and imaginary parts of the perturbation variables. The coefficients are also written on tape in coded (BCD) form for subsequent use by plotting program.

8.4.1.3 Listing of Perturbation Program.

```
      OVERLAY(PF1STRP,0,0)
      PROGRAM PF1STRP(INPUT=1,OUTPUT,TAPE7,TAPE5=INPUT)
*************************************************************************
*  PROGRAM PF1STRP CALCULATES THE UNSTEADY FORCES ON AN OSCILLATING,     *
*    INCLINED FLAT SURFACE IN A SUPERSONIC PERFECT GAS FLOW.             *
*    THE LINEARIZED PERTURBATIONS ABOUT THE MEAN STEADY FLOW ARE         *
*    CONSIDERED, WITH SOLUTION GIVEN BY A ONE-STRIP INTEGRAL METHOD.     *
*    TWICE THE FORCES AND MOMENTS FOR A SINGLE SURFACE ARE PRINTED.      *
*************************************************************************
      COMMON/BLOCK1/CUVAR(9),DER(9),VAR(9),PDB,RODB,UDB,VDB,XM2S,XBOS,
     + RBOS,CVSR,CPLGI,CPTHI,CTNL2,DVSDXR,DVSDXI,RVDB,PDV,UDV,VDV,RCNL
     +,DRO,DIO
      DIMENSION IDENT(8),DATE(2),ELE1(8),ELE2(8),ERRVAL(8)
      EXTERNAL DERSUB,CHSUB
      NAMELIST/INPDATA/XM,THWD,G,XOK,XSTOPK,CIK,SPECK
C
  110 FORMAT(5E16.8)
  109  FORMAT(1H1//*  RIGID BODY FORE AND AFT TRANSLATION*)
  108 FORMAT(/7X*K*4X*KSQL3P*6X*KL4P*4X*KSQM3P*6X*KM4P*8X*BR*8X*BI*
     + 8X*PR*8X*PI*8X*UR*8X*UI*8X*DR*8X*DI*/)
  107  FORMAT(1H1//*  RIGID BODY PITCH*)
  106 FORMAT(/7X*K*7X*L1*7X*KL2*7X*M1P*6X*KM2P*8X*BR*8X*BI*
     + 8X*PR*8X*PI*8X*UR*8X*UI*8X*DR*8X*DI*/)
  105  FORMAT(1H1//*  RIGID BODY PLUNGE NORMAL TO SURFACE*)
  104 FORMAT(XF6.4,4G11.4,8G10.3)
  103 FORMAT(/7X*K*7X*L7*7X*KL8*7X*M7P*6X*KM8P*8X*BR*8X*BI*
     + 8X*PR*8X*PI*8X*UR*8X*UI*8X*DR*8X*DI*/)
  102 FORMAT(//*  PDB=*G16.8,* RODB=*G16.8,* UDB=*G16.8,* VDB=*G16.8
     +/*  PDV=*G16.8,* RODV=*G16.8,* UDV=*G16.8,* VDV=*G16.8/)
  101 FORMAT(/2X*M2=*G16.8,* P21=*G16.8,* R21=*G16.8,* V21=*G16.8,* BO=*
     +G16.8)
      DATA FMT1,FMT2,FMT3/6H(8A10),10H(1H110A10),10H(* IOB*I4)/
C
C  VAR(1,..,9)=X,BR,BI,PR,PI,UR,UI,DR,DI. RF=.5*V21*X
C
      REWIND 7
    1 READ FMT1,IDENT $ IF(EOF,5)999,2
    2 CALL DAYTIM(DATE) $ PRINT FMT2,IDENT,DATE $ READ INPDATA
      PRINT INPDATA $ THW=THWD/57.2957795130823
      CALL WEDGE(XM,G,THW,XM2,P21,R21,V21,BO,IEOBS)
      IF(IEOBS.EQ.0)GO TO 3 $ PRINT FMT3,IEOBS $ GO TO 1
    3 PRINT 101,XM2,P21,R21,V21,BO
      CALL SHKDERV(XM,G,THW,BO,R21,V21,PDV,RODV,UDV,VDV,PDB,RODB,UDB,
     + VDB) $ XM2S=XM2**2 $ XBOS=XM2S-1.
      PRINT 102,PDB,RODB,UDB,VDB,PDV,RODV,UDV,VDV $ PRINT 105
      RBOS=1./XBOS $ RVDB=1./VDB $ PCON=-R21*V21 $ CONM=PCON/3.
      CONTM=-2.*R21/3. $ XO=2.*XOK/V21 $ XSTOP=2.*XSTOPK/V21
      CI=2.*CIK/V21 $ SPEC=2.*SPECK/V21
```

```
C
C RIGID BODY PLUNGE
C
      CVSR=0. $ CPLGI=-1. $ CPTHI=0. $ II=0 $ DRO=-COS(BO-THW) $ DIO=0.
      CALL INIC(DPDXR,DPDXI,XO,THW,BO,PROO,PIOO,TNL) $ CTNL2=2./TNL
      CL1O=-R21*DPDXR $ CM1PO=4.*CL1O/3. $ CKL2O=PCON*PIOO $ XK=0.
      WRITE(7,110)XK,CL1O,CKL2O,CM1PO,CKL2O
      PRINT 106 $PRINT104,XK,CL1O,CKL2O,CM1PO,CKL2O
      CALL INT2A(II,8,DUM,CI,SPEC,DUM,DUM,VAR,CUVAR,DER,ELE1,ELE2,DUM,
     + ERRVAL,DERSUB,CHSUB,DUM)  $ XOO=VAR(1)
      CL1=-R21*(PROO+VAR(4))/XOO $ CKL2=.5*PCON*(PIOO+VAR(5))
      CM1P=CONTM*(PRCO+2.*VAR(4))/XOO $ CKM2P=CONM*(PIOO+2.*VAR(5))
      XSAV=VAR(1) $ PRSAV=VAR(4) $ PISAV=VAR(5) $ XK=.5*V21*VAR(1)
      WRITE(7,110)XK,CL1,CKL2,CM1P,CKM2P
      PRINT 104,XK,CL1,CKL2,CM1P,CKM2P,(VAR(I),I=2,9)  $ II=1
    7 CALL INT2A(II,8,DUM,CI,SPEC,DUM,DUM,VAR,CUVAR,DER,ELE1,ELE2,DUM,
     + ERRVAL,DERSUB,CHSUB,DUM)
      XS=VAR(1) $ RXSQ=1./XS**2 $ DX=XS-XSAV
      RX=XSAV/XS $ RX2=RX*RX $ RX3=RX2*RX
      CL1  =RX2*CL1-R21*DX*(PRSAV+VAR(4))*RXSQ
      CKL2=RX*CKL2+.5*PCON*DX*(PISAV+VAR(5))/XS
      TX1=VAR(1)+2.*XSAV $ TX2=2.*VAR(1)+XSAV
      CKM2P=RX2*CKM2P+CONM*RXSQ*DX*(TX1*PISAV+TX2*VAR(5))
      CM1P=RX3*CM1P+CONTM*RXSQ*DX*(TX1*PRSAV+TX2*VAR(4))/XS
      XSAV=VAR(1) $ PRSAV=VAR(4) $ PISAV=VAR(5) $ XK=.5*V21*VAR(1)
      WRITE(7,110)XK,CL1,CKL2,CM1P,CKM2P
      PRINT 104,XK,CL1,CKL2,CM1P,CKM2P,(VAR(I),I=2,9)
      IF(XS.LT.XSTOP)GO TO 7 $ ENDFILE 7 $ PRINT 109
C
C RIGID BODY FORE AND AFT TRANSLATION
C
      CVSR=CPLGI=CPTHI=DIO=0. $ II=0 $ DRO=SIN(BO-THW)
      CALL INIC(DPDXR,DPDXI,XO,THW,BO,PROO,PIOO,TNL) $ PRINT 103
      CL7O=-R21*DPDXR $ CM7PO=4.*CL7O/3. $ CKL8O=PCON*PIOO $ XK=0.
      WRITE(7,110)XK,CL7O,CKL8O,CM7PO,CKL8O
      PRINT 104,XK,CL7O,CKL8O,CM7PO,CKL8O
      CALL INT2A(II,8,DUM,CI,SPEC,DUM,DUM,VAR,CUVAR,DER,ELE1,ELE2,DUM,
     + ERRVAL,DERSUB,CHSUB,DUM)  $ XOO=VAR(1)
      CL7=-R21*(PROO+VAR(4))/XOO $ CKL8=.5*PCON*(PIOO+VAR(5))
      CM7P=CONTM*(PRCO+2.*VAR(4))/XOO$ CKM8P=CONM*(PIOO+2.*VAR(5))
      XSAV=VAR(1) $ PRSAV=VAR(4) $ PISAV=VAR(5) $ XK=.5*V21*VAR(1)
      WRITE(7,110)XK,CL7,CKL8,CM7P,CKM8P
      PRINT 104,XK,CL7,CKL8,CM7P,CKM8P,(VAR(I),I=2,9)  $ II=1
    8 CALL INT2A(II,8,DUM,CI,SPEC,DUM,DUM,VAR,CUVAR,DER,ELE1,ELE2,DUM,
     + ERRVAL,DERSUB,CHSUB,DUM)
      XS=VAR(1) $ RXSQ=1./XS**2 $ DX=XS-XSAV
      RX=XSAV/XS $ RX2=RX*RX $ RX3=RX2*RX
      CL7=RX2*CL7-R21*DX*(PRSAV+VAR(4))*RXSQ
      CKL8=RX*CKL8+.5*PCON*DX*(PISAV+VAR(5))/XS
      TX1=VAR(1)+2.*XSAV $ TX2=2.*VAR(1)+XSAV
      CKM8P=RX2*CKM8P+CONM*RXSQ*DX*(TX1*PISAV+TX2*VAR(5))
      CM7P=RX3*CM7P+CONTM*RXSQ*DX*(TX1*PRSAV+TX2*VAR(4))/XS
      XSAV=VAR(1) $ PRSAV=VAR(4) $ PISAV=VAR(5) $ XK=.5*V21*VAR(1)
      WRITE(7,110)XK,CL7,CKL8,CM7P,CKM8P
      PRINT 104,XK,CL7,CKL8,CM7P,CKM8P,(VAR(I),I=2,9)
      IF(XS.LT.XSTOP)GO TO 8 $ ENDFILE 7 $ PRINT 107
```

```
C
C RIGID BODY PITCH
C
      CVSR=-1. $ CPLGI=0. $ CPTHI=-1.  $ II=0 $ DRO=DIO=0.
      CALL INIC(DPDXR,DPDXI,XO,THW,BO,PROO,PIOO,TNL)$ PRINT 108
      CKSL3PO=V21*PCON*PROO $CKL4PO=PCON*DPDXI $CKM4PO=4.*CKL4PO/3.
      XK=0. $ WRITE(7,110)XK,CKSL3PO,CKL4PO,CKSL3PO,CKM4PO
      PRINT 104,XK,CKSL3PO,CKL4PO,CKSL3PO,CKM4PO
      CALL INT2A(II,8,DUM,CI,SPEC,DUM,DUM,VAR,CUVAR,DER,ELE1,ELE2,DUM,
     + ERRVAL,DERSUB,CHSUB,DUM)  $ XOO=VAR(1)
      CKSL3P=.5*PCON*V21*(PROO+VAR(4)) $ CKL4P=PCON*(PIOO+VAR(5))/XOO
      CKSM3P=CONM*V21*(PROO+2.*VAR(4))
      CKM4P=2.*CONM*(PIOO+2.*VAR(5))/XOO
      XSAV=VAR(1) $ PRSAV=VAR(4) $ PISAV=VAR(5) $ XK=.5*V21*VAR(1)
      WRITE(7,110)XK,CKSL3P,CKL4P,CKSM3P,CKM4P
      PRINT 104,XK,CKSL3P,CKL4P,CKSM3P,CKM4P,(VAR(I),I=2,9) $ II=1
    9 CALL INT2A(II,8,DUM,CI,SPEC,DUM,DUM,VAR,CUVAR,DER,ELE1,ELE2,DUM,
     + ERRVAL,DERSUB,CHSUB,DUM)
      XS=VAR(1) $ RXSQ=1./XS**2 $ DX=XS-XSAV
      RX=XSAV/XS $ RX2=RX*RX $ RX3=RX2*RX
      CKSL3P=RX*CKSL3P+.5*DX*V21*PCON*(PRSAV+VAR(4))/XS
      CKL4P=RX2*CKL4P +DX*RXSQ*PCON*(PISAV+VAR(5))
      TX1=VAR(1)+2.*XSAV $ TX2=2.*VAR(1)+XSAV
      CKSM3P=RX2*CKSM3P+CONM*V21*RXSQ*DX*(TX1*PRSAV+TX2*VAR(4))
      CKM4P=RX3*CKM4P +2.*CONM*RXSQ*DX*(TX1*PISAV+TX2*VAR(5))/XS
      XSAV=VAR(1) $ PRSAV=VAR(4) $ PISAV=VAR(5) $ XK=.5*V21*VAR(1)
      PRINT 104,XK,CKSL3P,CKL4P,CKSM3P,CKM4P,(VAR(I),I=2,9)
      WRITE(7,110)XK,CKSL3P,CKL4P,CKSM3P,CKM4P
      IF(XS.LT.XSTOP)GO TO 9 $ ENDFILE 7 $ GO TO 1
  999 REWIND 7
      END            PROGRAM PF1STRP
```

```
      SUBROUTINE INIC(DPDXR,DPDXI,XO,THW,BO,PRO,PIO,TNL)
*************************************************************************
*  SUBROUTINE INIC CALCULATES THE INITIAL VALUES AND DERIVATIVES FOR    *
*    BEGINNING THE NUMERICAL INTEGRATION AT XO.                         *
*************************************************************************
      COMMON/BLOCK1/CUVAR(9),DER(9),VAR(9),PDB,RODB,UDB,VDB,XM2S,XBOS,
     + RBOS,CVSR,CPLGI,CPTHI,CTNL2,DVSDXR,DVSDXI,RVDB,PDV,UDV,VDV,RCNL
     +,DRO,DIO
      VSR=CVSR         $  VSI=CPLGI        $ DVSDXI=CPTHI     $ DVSDXR=0.
      TNL=TAN(BO-THW) $  SNL=SIN(BO-THW) $ CNL=COS(BO-THW) $ RCNL=1./CNL
      BRO=(VSR+VDV*DIO)/VDB $ PRO=PDB*BRO-PDV*DIO
      BIO=(VSI-VDV*DRO)/VDB $ PIO=PDB*BIO+PDV*DRO
      URO=UDB*BRO-UDV*DIO $ UIO=UDB*BIO+UDV*DRO
      PRINT 1,VSR,VSI,BRO,BIO,PRO,PIO,URO,UIO,DRO,DIO
    1 FORMAT(/*  VSR=*G16.8,* VSI=*G16.8,* BRO=*G16.8,* BIO=*G16.8/
     +       *  PRO=*G16.8,* PIO=*G16.8,* URO=*G16.8,* UIO=*G16.8/,
     +       *  DRO=*G16.8,* DIO=*G16.8/)
      BNUM1=1.-XBOS*TNL*TNL $ BNUM2=.5*XBOS*TNL*TNL
      BNUM3=TNL*(XM2S*PDV-UDV+.5*VDV*XBOS*TNL)
      BNUM4=TNL*(XM2S*PDB-UDB+VDV/SNL+.5*XBOS*TNL*(VDB+2.*PDV/SNL))
      DENOM=VDB+XBOS*TNL*PDB
      DBDXR=(BNUM1*DVSDXR+BNUM2*VSI+BNUM3*DRO+BNUM4*BIO)/DENOM
      DBDXI=(BNUM1*DVSDXI-BNUM2*VSR+BNUM3*DIO-BNUM4*BRO)/DENOM
      DPDXR=PDB*DBDXR+TNL*(DVSDXR-.5*(VSI+VDV*DRO+BIO*(VDB+2.*PDV/SNL)))
      DPDXI=PDB*DBDXI+TNL*(DVSDXI+.5*(VSR-VDV*DIO+BRO*(VDB+2.*PDV/SNL)))
      DUDXR=-DPDXR+UIO $ DUDXI=-DPDXI-URO
      PRINT 2,DBDXR,DBDXI,DPDXR,DPDXI,DUDXR,DUDXI
    2 FORMAT(* DBDXR=*G16.8,* DBDXI=*G16.8,* DPDXR=*G16.8,* DPDXI=*G16.8
     +,/     * DUDXR=*G16.8,* DUDXI=*G16.8/)
      VAR(2)=BRO+XO*DBDXR $ VAR(3)=BIO+XO*DBDXI $ VAR(1)=XO
      VAR(4)=PRO+XO*DPDXR $ VAR(5)=PIO+XO*DPDXI
      VAR(6)=URO+XO*DUDXR $ VAR(7)=UIO+XO*DUDXI
      VAR(8)=DRO+XO*BRO*RCNL $ VAR(9)=DIO+XO*BIO*RCNL $ RETURN
      END            SUBROUTINE INIC

      SUBROUTINE CHSUB $ RETURN
*************************************************************************
*  DUMMY SUBROUTINE CALLED BY INT2A.                                    *
*************************************************************************
      END            SUBROUTINE CHSUB
```

```
      SUBROUTINE DERSUB
*************************************************************************
*  SUBROUTINE DERSUB CALCULATES THE FIRST ORDER DERIVATIVES FOR EACH    *
*     STEP OF THE NUMERICAL INTERGRATION.  DERSUB IS CALLED BY INT2A.   *
*************************************************************************
      COMMON/BLOCK1/CUVAR(9),DER(9),VAR(9),PDB,RODB,UDB,VDB,XM2S,XBOS,
     + RBOS,CVSR,CPLGI,CPTHI,CTNL2,DVSDXR,DVSDXI,RVDB,PDV,UDV,VDV,RCNL
     +,DRO,DIO
      X= CUVAR(1) $ BR=CUVAR(2) $ BI=CUVAR(3) $ PR=CUVAR(4)
      PI=CUVAR(5) $ UR=CUVAR(6) $ UI=CUVAR(7) $ DR=CUVAR(8) $DI=CUVAR(9)
      VSR=CVSR     $ VSI=(CPLGI+X*CPTHI)     $ RX=1./X
      DER(2)=((VDB*BR+CTNL2*(PR-PDB*BR)+(CTNL2*PDV-VDV)*DI-VSR)*RX
     1 -DVSDXR+((VDB+VDV*RCNL)*BI+VSI+VDV*DR))*RVDB
      DER(3)=((VDB*BI+CTNL2*(PI-PDB*BI)-(CTNL2*PDV-VDV)*DR-VSI)*RX
     1 -DVSDXI-((VDB+VDV*RCNL)*BR+VSR-VDV*DI))*RVDB
      DER(4)=(RX*(CTNL2*VSR+(CTNL2*VDV-XBOS*PDV)*DI+(PDB*XBOS-VDB*
     1 CTNL2)*BR-XBOS*PR)-XBOS*PDB*DER(2)+((PDV*XM2S-UDV)*DR-UI
     2 +XM2S*PI+(PDB*XM2S-UDB+XBOS*PDV*RCNL)*BI))*RBOS
      DER(5)=(RX*(CTNL2*VSI-(CTNL2*VDV-XBOS*PDV)*DR+(PDB*XBOS-VDB*
     1 CTNL2)*BI-XBOS*PI)-XBOS*PDB*DER(3)+((PDV*XM2S-UDV)*DI+UR
     2 -XM2S*PR-(PDB*XM2S-UDB+XBOS*PDV*RCNL)*BR))*RBOS
      DER(6)=RX*((PDB+UDB)*BR-PR-UR-(PDV+UDV)*DI)-DER(4)
     1 -(PDB+UDB)*DER(2)+(UI+(UDB+(UDV+PDV)*RCNL)*BI+UDV*DR)
      DER(7)=RX*((PDB+UDB)*BI-PI-UI+(PDV+UDV)*DR)-DER(5)
     1 -(PDB+UDB)*DER(3)-(UR+(UDB+(UDV+PDV)*RCNL)*BR-UDV*DI)
      DER(8)=BR*RCNL $ DER(9)=BI*RCNL $ RETURN
      END             SUBROUTINE DERSUB


      SUBROUTINE SHKDERV(XM,G,THW,BO,ROO,UO,PV,ROV,UV,VV,PB,ROB,UB,VB)
*************************************************************************
*  CALCULATES SLOPE AND NORMAL VELOCITY DERIVATIVES OF P,RO,U, AND V FOR*
*     AN OBLIQUE SHOCK WAVE. DERIVATIVES ARE NORMALIZED BY FLOW VARIABLES*
*     BEHIND THE SHOCK WAVE.                                            *
*************************************************************************
      SLO=SIN(BO-THW) $ CLO=COS(BO-THW) $ SB=SIN(BO) $ CB=COS(BO)
      SQMN=(XM*SB)**2 $ FG1=4./(G+1.)    $ RUO=1./UO
      PN= FG1*SB*RUO  $ PV=PN/ROO        $ PB=PV*CB*RUO
      ROV=FG1*ROO/(SQMN*SB)          $ ROB=ROV*CB
      UN=.5*FG1*(SQMN+1.)/SQMN       $ UB=UN*RUO*SIN(THW)-PN*CLO
      UV=-UN*SLO       $ VV=UN*CLO   $ VB=UN*RUO*COS(THW)-PN*SLO
      RETURN
      END             SUBROUTINE SHKDERV
```

```
      SUBROUTINE WEDGE(XM,G,THW,XM2,P2OP1,R2OR1,V2OV1,BETAO,IER)
*************************************************************************
*  CALCULATES SHOCK WAVE ANGLE BETAO (RADIANS) FOR A WEDGE OF ANGLE     *
*    THETA (RADIANS) FOR INPUT VALUES OF MACH NUMBER XM AND GAMMA G -   *
*    FLOW CONDITIONS BEHIND THE SHOCK ARE CALCULATED FROM BETAO,XM,AND G*
*************************************************************************
      RINDF=01777C000000000000017 $ IF(XM.GE.1.)GO TO 1$ IER=1 $ GO TO 9
    1 IF(THW)8,7,2
    2 STSQ=SIN(THW)**2 $ SQM=XM*XM $ RSQM=1./SQM
      B=-RSQM*(SQM+2.)-G*STSQ      $ D=(STSQ-1.)*RSQM**2
      C=(2.*SQM+1.)*RSQM**2+(.25*(G*(G+2.)+1.)+RSQM*(G-1.))*STSQ
      CALL WDETACH(XM,G,TDET) $ IF(THW.LE.TDET)GO TO 3 $ IER=3 $ GO TO 9
    3 X=-.333333333333333*B        $ TCORR=1. $ DO 4 I=1,100
      CORR=-(D+X*(C+X*(B+X)))/(C+X*(2.*B+3.*X)) $ XT=X $ X=X+CORR
      IF(I.NE.1.AND.(TCORR*CORR.LE.0..OR.X.EQ.XT))GO TO 5
    4 TCORR=CORR $ IER=4           $ SMN=X*SQM $ GO TO 6
    5 IER=0       $ SMN=X*SQM
    6 P2OP1=(2.*G*SMN-G+1.)/(G+1.) $ R2OR1=(G+1.)*SMN/(2.+SMN*(G-1.))
      V2OV1=SQRT(1.-4.*(SMN-1.)*(G*SMN+1.)/(SMN*SQM*(G*(G+2.)+1.)))
      XM2=XM*V2OV1*SQRT(R2OR1/P2OP1) $ BETAO=ASIN(SQRT(X))       $ RETURN
    7 P2OP1=R2OR1=V2OV1=1. $ XM2=XM $ BETAO=ASIN(1./XM) $ IER=0 $ RETURN
    8 IER=2
    9 P2OP1=R2OR1=V2OV1=BETAO=XM2=RINDF $ RETURN
      END             SUBROUTINE WEDGE

      SUBROUTINE WDETACH(XM,G,DEL) $ XMS=XM*XM $ GP=G+1.
*************************************************************************
*  CALCULATES WEDGE ANGLE FOR SHOCK DETACHMENT DEL (RADIANS) FOR INPUT  *
*    VALUES OF MACH NUMBER XM AND GAMMA G                               *
*************************************************************************
      XMNS=.25*(GP*XMS-4.+SQRT(GP*(XMS*(GP*XMS+8.*(G-1.))+16.)))/G
      SINDEL=SQRT((XMS-XMNS*(2.*XMS+1.-XMNS*(XMS+2.-XMNS)))/
     +(1.+XMNS*(G-1.+.25*XMS*GP*GP-G*XMNS)))/XM$ DEL=ASIN(SINDEL)$RETURN
       END            SUBROUTINE WDETACH
```

```
      SUBROUTINE INT2A(II,N,NT,CI,SPEC,CIMAX, IERR ,VAR,CUVAR,DER,ELE1,
     1ELE2,ELT,ERRVAL,DERSUB,CHKSUB,ITEXT)
*************************************************************************
*     VERSION OF LRC CDC 6600 LIBRARY ROUTINE D2.4                      *
*     USES FIXED INTERVAL, SINGLE PRECISION, 4TH-ORDER ADAMS-BASHFORTH  *
*     PREDICTOR, 4TH-ORDER ADAMS-MOULTON CORRECTOR, 4TH-ORDER RUNGE-    *
*     KUTTA STARTER.  NT,CIMAX,IERR,ELT, AND ITEXT ARE DUMMY (UNUSED).  *
*************************************************************************
      DIMENSION DER(21),ELE1(20),ELE2(20),ELT(20),ERRVAL(20),TEMP(20),
     1 DER1(20),DER2(20),DER3(20),S1VAR(21),VAR(21),CUVAR(21)
      A=0.0  $  IF(II)1,1,2
C     INITIALIZATION SECTION
    1 IF(CI) 3,4,3
C     SAVE CI
    4 PRINT 1000 $ STOP
 1000 FORMAT(11HOCI=0  STOP)
    3 H=CI
   18 IERR=1 $ TO = VAR(1) $ MODE=1 $ II= 1 $ N1=N+1 $ DO 5 J=1,N1
      CUVAR(J)=VAR(J)
    5 CONTINUE
C     EVALUATION SECTION HERE
    8 CALL DERSUB $ IF(MODE.LE.1)GO TO 7 $ IF(II-3)36,36,7
   36 CALL CHKSUB $ IF(II.EQ.2) GO TO 1
   37 DO 38 J=1,N1
   38 VAR(J)=CUVAR(J) $ IF(II-3)6,7,7
    7 RETURN
    6 IF(SPEC) 9,7,9
    9 DEL=     VAR(1) -TO $ DELP=DEL*(1.+1.0E-11)
      IF(ABS(DELP)-ABS(SPEC)) 2,10,10
   10 TO = VAR(1) $ GO TO 7
    2 II=1 $ IF(MODE-4) 11,12,12
C     RUNGE-KUTTA
   11 DO 20 J=2,N1 $ DER3(J-1)=DER2(J-1) $ DER2(J-1)=DER1(J-1)
      DER1(J-1)=DER(J) $ ELE1(J-1)=DER(J) $ CUVAR(J)=A
      DELT=0.4*ELE1(J-1)*H $ S1VAR(J)=VAR(J) $ CUVAR(J)=S1VAR(J)+DELT
   20 CONTINUE $ S1VAR(1)=VAR(1) $ CUVAR(1)=S1VAR(1)+0.4*H $ CALL DERSUB
```

```
      IF(II-3)23,23,7
   23 CUVAR(1)=S1VAR(1)+0.455737254218 79*H $ DO 24 J=2,N1
      ELE2(J-1)=DER(J)
      DELT=(0.29697760924775*ELE1(J-1)+0.15875964497104*ELE2(J-1))*H
      CUVAR(J)=S1VAR(J)+DELT
   24 CONTINUE $ CALL DERSUB $ IF(II-3)25,25,7
   25 CUVAR(1)=S1VAR(1)+H $ DO 26 J=2,N1 $ TEMP(J-1)=DER(J)
      DELT=(0.21810038822592*ELE1(J-1)-3.05096514869293*ELE2(J-1)
     1+3.83286476046701*TEMP(J-1))*H $ CUVAR(J)=S1VAR(J)+DELT
   26 CONTINUE $ CALL DERSUB $ IF(II-3)27,27,7
   27 DH=H $ CUVAR(1)=VAR(1)+DH $ DO 28 J=2,N1
      DOUB=     (0.17476028226269*ELE1(J-1)-0.55148066287873*ELE2(J-1)
     1+1.20553559939652*TEMP(J-1)+0.17118478121952*DER(J))
      CUVAR(J)=VAR(J)+DH*DOUB
   28 CONTINUE $ MODE=MODE+1 $ GO TO 8
C     ADAMS-MOULTON, ADAMS-BASHFORTH PREDICTOR
   12 CUVAR(1)=VAR(1)+H $ DH=H/24.0 $ DO 13 J=2,N1
      DOUB=     (55.0*DER(J)-59.0*DER1(J-1)+37.0*DER2(J-1)-9.0*DER3(J-1))
      CUVAR(J)=VAR(J)+DH*DOUB
   13 CONTINUE $ DO 14 J=1,N $ DER3(J  )=DER2(J) $ DER2(J  )=DER1(J)
   14 DER1(J  )=DER(J+1) $ CALL DERSUB $ IF(II-3)15,15,7
C     ADAMS-MOULTON CORRECTOR
   15 DO 16 J=2,N1 $ TEMP=CUVAR(J)
      DOUB=     (9.0*DER(J)+19.*DER1(J-1)-5.0*DER2(J-1)+DER3(J-1))
      CUVAR(J)=VAR(J)+DH*DOUB
   16 ERRVAL(J-1)=(TEMP-     CUVAR(J)) /14.21052631579847
   19 GO TO 8
      END            SUBROUTINE INT2A
```

8.4.2 Program for Finite Difference Calculations

The version of the program discribed here calculates either time asymtotic steady flows or flows with constant rates or accelerations. For an oscillation the flow field has to be converged for the initial rates and accelerations and the results used for the flow field for k = 1. Thus subroutine INIFLD would have to be modified slightly to perform an oscillation.

8.4.2.1 Input

Each case consists of 11 cards of input data. Card 1 consists of 80 columns of identification in an 8A10 format. Card 2 contains MSI, the number of (unstaggered) grid points between the shock and body; MFRES, the number of (unstaggered) grid points in the freestream on the initial line; LMAX, the number of grid points in the x-direction; and KMAX, the number of time steps in a 20I4 format. Card 3 contains NFDTX, the number of CFL fractions; NMACH, the number of Mach numbers; and NTHW, the number of wedge angles in a 20I4 format. Card 5 contains FDTX, the CFL fraction array, in a 4E20.12 format. Card 6 contains of THETAD, the wedge angle array in degrees, in a 4E20.12 format. Card 7 contains XO, the x for the initial line, and HXAMP, HYAMP, and THMAMP, the values of h_x, h_y, and θ for oscillations, respectively in a 4E20.12 format. Card 8 contains G, the value of γ, in format 4E20.12. Card 9 contains IOSC, which is 1 for this version, in a 20I4 format. Card 10 contains HXDOT, HXDTDT, HYDOT, and HYDTDT, the values of $\dot{h}_x$, $\ddot{h}_x$, $\dot{h}_y$, and $\ddot{h}_y$ respectively in format 4E20.12. Card 11 contains THMDOT and THMDTDT, the values of $\dot{\theta}$, and $\ddot{\theta}$ respectively in a 4E20.12

format. When only part of the card is used, the leading fields are of course used.

8.4.2.2 Output

All case input parameters, effective wedge flow variables, the loop indexing for each line and k-step, and the flow variables on the initial line are printed. The version of the program listed here prints the flow variables for each body point for every 50th time step and for the last four time steps.

8.4.2.3 Listing of Finite Difference Program.

```
      OVERLAY(LAX2DU,0,0)
      PROGRAM LAX2DU(INPUT=1,OUTPUT=1,TAPE7=1,TAPE5=INPUT)
C*****************************************************************
C*  PROGRAM CALCULATES THE SUPERSONIC FLOW FIELD OVER A TWO-DIMENSIONAL  *
C*    WEDGE AIRFOIL UNDERGOING  SPECIFIED MOTION IN A PERFECT GAS.       *
C*    THE FINITE DIFFERENCE TECHNIQUE OF LAX IS USED.  MAIN PROGRAM      *
C*    PRIMARILY CONTROLS THE INDEXING AND LOOPING.  SUBROUTINE INIFLD    *
C*    READS THE CASE INPUT DATA, CALCULATES THE INDICES, AND CALCULATES  *
C*    THE INITIAL FLOW FIELD.                                            *
C*****************************************************************
      COMMON/NLOOP/NFDTX,NMACH,NTHW
      COMMON/INDEX/NME(100),NMO(100),NMTMOD(100),MDIM,LDIM,LMAX,KMAX,
     + MSI,MFRES
    1 NMACH=NTHW=NFDTX=1
      DO 300 MACH=1,NMACH $  DO 300 NTHD=1,NTHW $  DO 300 NFDT=1,NFDTX
      CALL INIFLD(MACH,NTHD,NFDT)
      DO 200 K=2,KMAX  $ KEVEN=MOD(K,2)
      DO 100 L=2,LMAX  $ LKBDY=MOD(L+K+1,2)
      IFRES=MOD(NMTMOD(L)+LKBDY+1,2)  $ MFL=NMO(L)-IFRES
      IF(KEVEN.EQ.0)MFL=NME(L)-IFRES
      IF(LKBDY.EQ.0)GO TO 50  $ IF(L.EQ.LMAX)GO TO 20
      CALL RFBDYPT(1,L+1,1,L,1,L-1,LKBDY)     $ DO 10 M=2,MFL
   10 CALL LXFLDPT(M,L+1,M,L,M,L-1,M-1,L,K,LKBDY) $ GO TO 90
   20 CALL RFBDYPT(1,L,1,L-1,1,L,LKBDY)       $ DO 30 M=2,MFL
   30 CALL EXENDPT(M,L,M,L-1,M-1,L,K,LKBDY)  $ GO TO 90
   50 IF(L.EQ.LMAX)GO TO 70                   $ DO 60 M=1,MFL
   60 CALL LXFLDPT(M,L+1,M+1,L,M,L-1,M,L,K,LKBDY) $ GO TO 90
   70 DO 80 M=1,MFL
   80 CALL EXENDPT(M+1,L,M,L-1,M,L,K,LKBDY)
   90 CALL MAXMPT(IFRES,MFL,L,K,LKBDY)
  100 CONTINUE
      CALL LSHIFT(KEVEN,K)
      IF(MOD(K,50).EQ.0.AND.K.LT.(KMAX-3))CALL FPRINT(KEVEN,K)
      IF(K.GE.(KMAX-3))CALL FPRINT(KEVEN,K)
  200 CONTINUE
  300 CONTINUE $ GO TO 1
      END            PROGRAM LAX2DU
```

```
      SUBROUTINE INIFLD(MACH,NTHD,NFDT)
*************************************************************************
*  THIS SUBROUTINE INITIALIZES THE ENTIRE FLOW FIELD FOR K=1 AND        *
*    CALCULATES AND STORES THE INDEXING PARAMETERS FOR THE STAGGERED    *
*    GRID NETWORK AND FOR SUBSEQUENT TIME STEPS.                        *
*  INPUT DATA ARE ALSO READ FOR MULTIPLE CASES.                         *
*************************************************************************
      COMMON/NLOOP/NFDTX,NMACH,NTHW
      COMMON/INDEX/NME(100),NMO(100),NMTMOD(100),MDIM,LDIM,LMAX,KMAX,
     + MSI,MFRES
      COMMON/FLOWPAR/P(25,100),RO(25,100),U(25,100),V(25,100),RINDF,
     + G,PF,SINT,COST
      COMMON/MOTION/IOSC,XO,THMAMP,THMDOT,THMDTDT,SINTHM,COSTHM,HXAMP,
     + HXDOT,HXDTDT,HYAMP,HYDOT,HYDTDT
      COMMON/GRIDPAR/DX,DT,DTX,GDTX,G12
      COMMON/FLINE/XM,THW,SINDT,COSDT,PINI(25),ROINI(25),UINI(25),
     + VINI(25),MFFI,MSI2,MSI21
      DIMENSION IDENT(8),DATE(2),AMACH(4),FDTX(4),THETAD(4)
      DATA MDIM,LDIM/25,100/
      DATA FMT1,FMT2,FMT3,A10,I4,E20/5H(1H1),10H(/X10A10/),6H(X9I4),
     + 6H(8A10),6H(20I4),9H(4E20.12)/
      DATA DEGRAD,TWOPI,RINDF/.0174532925199433,6.2831853071796,
     + 0177700000000000000013/
      DO 1 J=1,LDIM $ NME(J)=NMO(J)=NMTMOD(J)=0 $ DO 1 I=1,MDIM
    1 P(I,J)=RO(I,J)=U(I,J)=V(I,J)=RINDF $ CALL DAYTIM(DATE)
      IF((MACH+NTHD+NFDT).GT.3)GO TO 20
      READ A10,IDENT $ IF(EOF,5)999,2
    2 PRINT FMT1
      PRINT FMT2,IDENT,DATE $ READ I4,MSI,MFRES,LMAX,KMAX
      READ I4,NFDTX,NMACH,NTHW $ READ E20,AMACH,FDTX,THETAD
      READ E20,XO,HXAMP,HYAMP,THMAMPD,G
      READ I4,IOSC $ THMAMP=DEGRAD*THMAMPD
      IF(IOSC.EQ.1)READ E20,HXDOT,HXDTDT,HYDOT,HYDTDT,THMDOT,THMDTDT
      SINTHM=0. $ COSTHM=1.
   20 IF(IOSC.NE.0)GO TO 3 $ HXDTDT=HYDTDT=THMDTDT=THM=0.
      HXDOT=HXAMP $ HYDOT=HYAMP
    3 WRITE(7,A10)IDENT,DATE $ XM=AMACH(MACH) $ DTXF=FDTX(NFDT)
      THD=THETAD(NTHD) $ THW=DEGRAD*THD $ COST=COS(THW) $ SINT=SIN(THW)
      VXE=COST+HXDOT $ VYE=-SINT+HYDOT
      EM=XM*SQRT(VXE*VXE+VYE*VYE) $ THE=ATAN(-VYE/VXE)
      CALL WEDGE(EM,G,THE,XMS,P2OP1,RS,US,BETA,IEW) $ IF(IEW.NE.0)STOP 1
      PF=1/(G*XM*XM)$ PS=PF*P2OP1$ TANBT=TAN(BETA-THE)$ THED=THE/DEGRAD
      PRINT 100,XM,G,THD,THE,DTXF,XMS,P2OP1,RS,US,BETA,THED,EM,
     + MDIM,LDIM,LMAX,MSI,MFRES
```

```
      CFL1=1./(SQRT(2.)/XM+COST+SINT) $ CFL2=1./(SQRT(2.)*US/XMS+US)
      CFL=AMIN1(CFL1,CFL2) $ DTXA=CFL*DTXF $ DX=XO*TANBT/(MSI-1.)
      DT=DTXA*DX $ IF(IOSC.NE.0)GO TO 4
      KMAX=2+TWOPI/DT $ DT=TWOPI/(KMAX-1) $ DTXA=DT/DX
    4 PRINT 104,XO,DX,DT,CFL,KMAX
      PRINT 105,IOSC,HXAMP,HXDOT,HXDTDT,HYAMP,HYDOT,HYDTDT,
     + THMAMP,THMDOT,THMDTDT
      DTX=.5*DTXA $ GDTX=G*DTX $ G12=.5*(G-1.) $ PRINT 101
      DO 6 L=1,LMAX $ NMS=MSI+(L-1)*TANBT
      NMT=NMS+MFRES $ NMTMOD(L)=MOD(NMT,2) $ MODL2=MOD(L,2)
      NME(L)=NMT/2+NMTMOD(L)*MOD(L+1,2) $ NMO(L)=NMT/2+NMTMOD(L)*MODL2
      PRINT FMT3,L,NMO(L),NME(L),NMT,NMTMOD(L)
      MSL=NMS/2+MOD(NMS,2)*MODL2
      DO 5 M=1,MSL $ P(M,L)=PS $ RO(M,L)=RS $ U(M,L)=US
    5 V(M,L)=0.     $ MFL=MSL+1 $ MFF=NMO(L) $ DO 6 M=MFL,MFF
      P(M,L)=PF     $ RO(M,L)=1.$ U(M,L)=VXE-(2*M-1-MODL2)*DX*THMDOT
    6 V(M,L)=VYE+(XO+DX*(L-1))*THMDOT
      MFFI=NMO(1) $ PRINT 102  $ DO 8 M=1,MFFI
      PINI(M)=P(M,1) $ ROINI(M)=RO(M,1) $ UINI(M)=U(M,1)$ VINI(M)=V(M,1)
    8 PRINT 103,M,PINI(M),ROINI(M),UINI(M),VINI(M)
      MSI2=MSI/2 $ MSI21=MSI2+1    $   RETURN
  100 FORMAT(/*   XM=*E21.13*   G=*E21.13* THD,DEG.=*E21.13* THE=*E21.13
     1/* DTXF=*E21.13* XMS=*E21.13*     P2PO1=*E21.13/
     2 *   RS=*E21.13*  US=*E21.13*      BETA=*E21.13//
     3 * THED=*E21.13*  EM=*E21.13//
     4 * MDIM=*I4* LDIM=*I4* LMAX=*I4* MSI=*I4* MFRES=*I4//)
  101 FORMAT(//3X*L   NMO   NME   NMT   NMTMOD*)
  102 FORMAT(////3X*MI*9X*PINI*17X*ROINI*17X*UINI*17X*VINI*)
  103 FORMAT(I4,4E21.13)
  104 FORMAT(/* XO=*E21.13* DX=*E21.13* DT=*E21.13* CFL=*E21.13* KMAX=*
     + I10//)
  105 FORMAT(* MOTION PARAMETERS AT K=1,  IOSC=*I4//
     1*  HXAMP=*G21.14*  HXDOT=*G21.14*  HXDTDT=*G21.14/
     2*  HYAMP=*G21.14*  HYDOT=*G21.14*  HYDTDT=*G21.14/
     3* THMAMP=*G21.14* THMDOT=*G21.14* THMDTDT=*G21.14//)
  999 CONTINUE
      END            SUBROUTINE INIFLD
```

```
      SUBROUTINE LXFLDPT(M1,L1,M2,L2,M3,L3,M4,L4,K,LKBDY)
*************************************************************************
*  SUBROUTINE CALCULATES FLOW VARIABLES AT A FIELD POINT GIVEN THE      *
*    INDICES FOR THE FOUR BASE POINTS.  ENTRY POINT BNDRYPT IS USED TO  *
*    PERFORM SAME OPERATIONS ON BOUNDARY POINTS GIVEN FLOW VARIABLES    *
*    AT FOUR EFFECTIVE BASE POINTS.                                     *
*************************************************************************
      COMMON/FLOWPAR/P(25,100),RO(25,100),U(25,100),V(25,100),RINDF,
     + G,PF,SINT,COST
      COMMON/GRIDPAR/DX,DT,CTX,GDTX,G12
      COMMON/MOTION/IOSC,XO,THMAMP,THMDOT,THMDTDT,SINTHM,COSTHM,HXAMP,
     + HXDOT,HXDTDT,HYAMP,HYDOT,HYDTDT
      COMMON/GRIDVAR/P1,P2,P3,P4,RO1,RO2,RO3,RO4,U1,U2,U3,U4,V1,V2,V3,V4
      P1=P(M1,L1) $ RO1=RO(M1,L1) $ U1=U(M1,L1) $ V1=V(M1,L1)
      P2=P(M2,L2) $ RO2=RO(M2,L2) $ U2=U(M2,L2) $ V2=V(M2,L2)
      P3=P(M3,L3) $ RO3=RO(M3,L3) $ U3=U(M3,L3) $ V3=V(M3,L3)
      P4=P(M4,L4) $ RO4=RO(M4,L4) $ U4=U(M4,L4) $ V4=V(M4,L4)
      ENTRY BNDRYPT
      ROU1=RO1*U1    $ ROU2=RO2*U2    $ ROU3=RO3*U3    $ ROU4=RO4*U4
      ROV1=RO1*V1    $ ROV2=RO2*V2    $ ROV3=RO3*V3    $ ROV4=RO4*V4
      ROUS1=ROU1*U1  $ ROUS2=ROU2*U2  $ ROUS3=ROU3*U3  $ ROUS4=ROU4*U4
      ROVS1=ROV1*V1  $ ROVS2=ROV2*V2  $ ROVS3=ROV3*V3  $ ROVS4=ROV4*V4
      UROAV=.25*(ROU1+ROU2+ROU3+ROU4) $ ROAV=.25*(RO1+RO2+RO3+RO4)
      VROAV=.25*(ROV1+ROV2+ROV3+ROV4) $ DY=DX
      XLM=XO+DX*L3   $ YLM=DY*(M2+M4+LKBDY-1)
      TRO=ROAV-DTX*(ROU1-ROU3+ROV2-ROV4)
      IF(TRO.GT.0)GO TO 1 $ IFD=1 $ GO TO 2
    1 RTRO=1./TRO
      TU=RTRO*(UROAV-DTX*(P1-P3+ROUS1-ROUS3+ROU2*V2-ROU4*V4)
     +   -DT*(ROAV*(HYDTDT*SINTHM-HXDTDT*COSTHM)+THMDTDT*(ROAV*YLM
     +   +.25*DY*(RO2-RO4))+THMDOT*(2.*VROAV-THMDOT*(ROAV*XLM
     +   +.25*DX*(RO1-RO3)))))
      TV=RTRO*(VROAV-DTX*(P2-P4+ROVS2-ROVS4+ROU1*V1-ROU3*V3)
     +   +DT*(ROAV*(HXDTDT*SINTHM+HYDTDT*COSTHM)+THMDTDT*(ROAV*XLM
     +   +.25*DX*(RO1-RO3))+THMDOT*(2.*UROAV+THMDOT*(ROAV*YLM
     +   +.25*DY*(RO2-RO4)))))
      TP=.25*(P1+P2+P3+P4)-GDTX*(P1*U1-P3*U3+P2*V2-P4*V4)
     + +G12*((.25-DTX*U1)*(ROUS1+ROVS1)+(.25+DTX*U3)*(ROUS3+ROVS3)
     +       +(.25-DTX*V2)*(ROUS2+ROVS2)+(.25+DTX*V4)*(ROUS4+ROVS4)
     +       -TRO*(TU*TU+TV*TV))
      IF(TP.GT.0)GO TO 4 $ IFD=2
    2 PRINT 3,IFD,K,LKBDY,M1,L1,M2,L2,M3,L3,M4,L4,P1,P2,P3,P4,RO1,RO2,
     + RO3,RO4,U1,U2,U3,U4,V1,V2,V3,V4,TP,TRO,TU,TV $ STOP 6
    3 FORMAT(* IFD,K,LKBDY,ML1234=*11I6/* PRUV1234T=*/(2X4E22.14/))
    4 P(M3,L3)=TP $ RO(M3,L3)=TRO $ U(M3,L3)=TU $ V(M3,L3)=TV $ RETURN
      END             SUBROUTINE LXFLDPT
```

```
      SUBROUTINE RFBDYPT(M1,L1,M2,L2,M3,L3,K,LKBDY)
*****************************************************************************
*  THIS SUBROUTINE TREATS THE BODY POINTS BY CALCULATING AN EFFECTIVE       *
*    POINT INSIDE THE BODY USING THE REFLECTION APPROXIMATION WITH          *
*    ALLOWANCE FOR DP/DY FROM UNSTEADY EFFECTS.                             *
*****************************************************************************
      COMMON/FLOWPAR/P(25,100),RO(25,100),U(25,100),V(25,100),RINDF,
     + G,PF,SINT,COST
      COMMON/GRIDPAR/DX,DT,DTX,GDTX,G12
      COMMON/MOTION/IOSC,XO,THMAMP,THMDOT,THMDTDT,SINTHM,COSTHM,HXAMP,
     + HXDOT,HXDTDT,HYAMP,HYDOT,HYDTDT
      COMMON/GRIDVAR/P1,P2,P3,P4,RO1,RO2,RO3,RO4,U1,U2,U3,U4,V1,V2,V3,V4
      P1=P(M1,L1) $ RO1=RO(M1,L1) $ U1=U(M1,L1) $ V1=V(M1,L1)
      P2=P(M2,L2) $ RO2=RO(M2,L2) $ U2=U(M2,L2) $ V2=V(M2,L2)
      P3=P(M3,L3) $ RO3=RO(M3,L3) $ U3=U(M3,L3) $ V3=V(M3,L3)
      RO4=RO2  $ U4=U2  $  V4=-V2 $ M4=-M2 $ L4=-1  $ DY=DX
      XLM=XO+(L2-1.)*DX
      P4=P2-DY*(RO1+RO3)*(HXDTDT*SINTHM+HYDTDT*COSTHM+XLM*THMDTDT
     + +(U1+U3)*THMDOT)
      CALL BNDRYPT(M1,L1,M2,L2,M3,L3,M4,L4,K,LKBDY) $ RETURN
      END            SUBROUTINE RFBDYPT

      SUBROUTINE MAXMPT(IFRES,MFL,L,K,LKBDY)
*****************************************************************************
*  SUBROUTINE TREATS MAXIMUM Y-POINT FOR A GIVEN L BY SETTING THE FLOW      *
*    VARIABLES TO FREESTREAM VALUES OR TO INDEFINITES AS APPROPRIATE.       *
*****************************************************************************
      COMMON/FLOWPAR/P(25,100),RO(25,100),U(25,100),V(25,100),RINDF,
     + G,PF,SINT,COST
      COMMON/MOTION/IOSC,XO,THMAMP,THMDOT,THMDTDT,SINTHM,COSTHM,HXAMP,
     + HXDOT,HXDTDT,HYAMP,HYDOT,HYDTDT
      COMMON/GRIDPAR/DX,DT,DTX,GDTX,G12
      MF=MFL+1 $ L1=L-1 $ IF(IFRES.EQ.0)GO TO 1 $ XLM=XO+L1*DX
      YLM=(2*MFL-1-LKBDY)*DX $ VX=HXDOT+COST $ VY=HYDOT-SINT
      UBF=VX*COSTHM-VY*SINTHM-YLM*THMDOT
      VBF=VX*SINTHM+VY*COSTHM+XLM*THMDOT
      P(MF,L1)=PF $ RO(MF,L1)=1. $ U(MF,L1)=UBF $ V(MF,L1)=VBF $ RETURN
    1 MIF=MF+IFRES $ P(MIF,L1)=RO(MIF,L1)=U(MIF,L1)=V(MIF,L1)=RINDF
      RETURN
      END            SUBROUTINE MAXMPT
```

```
      SUBROUTINE EXENDPT(M2,L2,M3,L3,M4,L4,K,LKBDY)
*************************************************************************
*  THIS SUBROUTINE EXTRAPOLATES THE AI TO DETERMINE THE FLOW VARIABLES  *
*    FOR CALCULATION OF THE LAST L COLUMN OF THE GRID.                  *
*************************************************************************
      COMMON/FLOWPAR/P(25,100),RO(25,100),U(25,100),V(25,100),RINDF,
     + G,PF,SINT,COST
      COMMON/GRIDPAR/DX,DT,DTX,GDTX,G12
      COMMON/GRIDVAR/P1,P2,P3,P4,RO1,RO2,RO3,RO4,U1,U2,U3,U4,V1,V2,V3,V4
      P2=P(M2,L2) $ RO2=RO(M2,L2) $ U2=U(M2,L2) $ V2=V(M2,L2)
      P3=P(M3,L3) $ RO3=RO(M3,L3) $ U3=U(M3,L3) $ V3=V(M3,L3)  $ M1=-1
      P4=P(M4,L4) $ RO4=RO(M4,L4) $ U4=U(M4,L4) $ V4=V(M4,L4) $ L1=L2+1
      RO1=RO2+RO4-RO3 $ IF(RO1.GT.0.)GO TO 1    $ IEND=1 $ GO TO 2
    1 U1=(RO2*U2+RO4*U4-RO3*U3)/RO1 $ V1=(RO2*V2+RO4*V4-RO3*V3)/RO1
      P1=P2+P4-P3+G12*(RO2*(V2*V2+U2*U2)+RO4*(V4*V4+U4*U4)
     + -RO3*(V3*V3+U3*U3)-RO1*(V1*V1+U1*U1))
      IF(P1.GT.0.)GO TO 4 $ IEND=2
    2 PRINT 3,IEND,K,LKBDY,M2,L2,M3,L3,M4,L4,P1,P2,P3,P4,RO1,RO2,RO3,
     + RO4,U1,U2,U3,U4,V1,V2,V3,V4  $ STOP 10
    3 FORMAT(* IEND,K,LKBDY,ML234=*9I6/* PRUV1234=*/(2X4E22.14/))
    4 CALL BNDRYPT(M1,L1,M2,L2,M3,L3,M4,L4,K,LKBDY) $ RETURN
      END            SUBROUTINE EXENDPT

      SUBROUTINE LSHIFT(KEVEN,K)
*************************************************************************
*  SUBROUTINE SHIFTS FLOW VARIABLES OVER ONE COLUMN IN THE TWO-         *
*    DIMENSIONAL ARRAYS AND CALLS INILINE TO DETERMINE NEW INITIAL LINE *
*    FOR L=1.                                                           *
*************************************************************************
      COMMON/FLOWPAR/P(25,100),RO(25,100),U(25,100),V(25,100),RINDF,
     + G,PF,SINT,COST
      COMMON/INDEX/NME(100),NMO(100),NMTMOD(100),MDIM,LDIM,LMAX,KMAX,
     + MSI,MFRES
      DO 1 M=1,MDIM $ P(M,LMAX)=RO(M,LMAX)=U(M,LMAX)=RINDF
    1 V(M,LMAX)=RINDF  $ DO 2 L=2,LMAX $ LST=LMAX+2-L  $ MFLT=NMO(LST)+1
      IF(KEVEN.EQ.0)MFLT=NME(LST)+1     $ LL=LST-1 $ DO 2 M=1,MFLT
      P(M,LST)=P(M,LL) $ RO(M,LST)=RO(M,LL) $ U(M,LST)=U(M,LL)
    2 V(M,LST)=V(M,LL) $ CALL INILINE(KEVEN,K) $ RETURN
      END            SUBROUTINE LSHIFT
```

```
      SUBROUTINE INILINE(LKBDY,K)
*************************************************************************
*  THIS SUBROUTINE FILLS THE L=1 LINE FOR EACH TIME STEP.  FLOW         *
*    VARIABLES ARE BASED ON THE QUASI-STATIC WEDGE ANGLE AND MACH       *
*    NUMBER INCLUDING MOTION.  CALLED BY LSHIFT ONLY.                   *
*************************************************************************
      COMMON/MOTION/IOSC,XO,THMAMP,THMDOT,THMDTDT,SINTHM,COSTHM,HXAMP,
     + HXDOT,HXDTDT,HYAMP,HYDOT,HYDTDT
      COMMON/FLOWPAR/P(25,100),RO(25,100),U(25,100),V(25,100),RINDF,
     + G,PF,SINT,COST
      COMMON/FLINE/XM,THW,SINDT,COSDT,PINI(25),ROINI(25),UINI(25),
     + VINI(25),MFFI,MSI2,MSI21
      COMMON/GRIDPAR/DX,DT,DTX,GDTX,G12
      IF(IOSC.EQ.0)GO TO 2 $ DO 1 M=1,MFFI $ P(M,1)=PINI(M)
      RO(M,1)=ROINI(M)      $U(M,1)=UINI(M)
    1 V(M,1)=VINI(M)        $ RETURN
    2 COSTIME=COS(DT*(K-1.)) $ SINTIME=SIN(DT*(K-1.))
      THM=THMAMP*SINTIME $ THMDOT=THMAMP*COSTIME $ THMDTDT=-THM
      SINTHM=SIN(THM) $ COSTHM=COS(THM)
      HYDOT=HYAMP*COSTIME $ HYDTDT=-HYAMP*SINTIME
      HXDOT=HXAMP*COSTIME $ HXDTDT=-HXAMP*SINTIME
      VXE=COS(THW-THM)-HYDOT*SINTHM+HXDOT*COSTHM
      VYE=-SIN(THW-THM)+HYDOT*COSTHM+HXDOT*SINTHM
      EM=XM*SQRT(VXE*VXE+VYE*VYE) $ THE=ATAN(-VYE/VXE)
      CALL WEDGE(EM,G,THE,XMS,P2OP1,RS,US,BETA,IEW) $ IF(IEW.NE.0)STOP 3
      VX=HXDOT+COST $ VY=HYDOT-SINT $ UBFM=VX*COSTHM-VY*SINTHM
      VBF=VX*SINTHM+VY*COSTHM+XO*THMDOT
      DO 3 M=1,MSI2 $ P(M,1)=PF*P2OP1 $ RO(M,1)=RS $ U(M,1)=US
    3 V(M,1)=0.     $ DO 4 M=MSI21,MFFI     $ P(M,1)=PF
      RO(M,1)=1. $ U(M,1)=UBFM-DX*(2*M-1-LKBDY)*THMDOT
    4 V(M,1)=VBF $ RETURN
      END            SUBROUTINE INILINE

      SUBROUTINE FPRINT(KEVEN,K)
*************************************************************************
*  SUBROUTINE PRINTS INDEX AND FLOW VARIABLES FOR BODY POINTS AND       *
*    ALSO WRITES THEM ON TAPE7 FOR USE BY PLOTTING PROGRAM.             *
*************************************************************************
      COMMON/FLOWPAR/P(25,100),RO(25,100),U(25,100),V(25,100),RINDF,
     + G,PF,SINT,COST
      COMMON/INDEX/NME(100),NMO(100),NMTMOD(100),MDIM,LDIM,LMAX,KMAX,
     + MSI,MFRES
      PRINT 100,K $ L1=2-KEVEN $ DO 1 L=L1,LMAX,2
      IF(K.EQ.KMAX)WRITE(7,103)L,P(1,L),RO(1,L),U(1,L),V(1,L)
    1 PRINT 101,L,P(1,L),RO(1,L),U(1,L),V(1,L) $ RETURN
  100 FORMAT(//* BODY POINTS FOR FINAL FLOW FIELD, L,P,RO,U,V, - K=*I6/)
  101 FORMAT(2XI4,4E20.12)
  103 FORMAT(I8,4E18.8)
      END            SUBROUTINE FPRINT
```

```
      SUBROUTINE WEDGE(XM,G,THW,XM2,P2OP1,R2OR1,V2OV1,BETAO,IER)
*************************************************************************
*  CALCULATES SHOCK WAVE ANGLE BETAO (RADIANS) FOR A WEDGE OF ANGLE     *
*    THETA (RADIANS) FOR INPUT VALUES OF MACH NUMBER XM AND GAMMA G -   *
*    FLOW CONDITIONS BEHIND THE SHOCK ARE CALCULATED FROM BETAO,XM,AND G*
*************************************************************************
      RINDF=.01777000000000000017 $ IF(XM.GE.1.)GO TO 1$ IER=1 $ GO TO 9
    1 IF(THW)8,7,2
    2 STSQ=SIN(THW)**2 $ SQM=XM*XM $ RSQM=1./SQM
      B=-RSQM*(SQM+2.)-G*STSQ      $ D=(STSQ-1.)*RSQM**2
      C=(2.*SQM+1.)*RSQM**2+(.25*(G*(G+2.)+1.)+RSQM*(G-1.))*STSQ
      CALL WDETACH(XM,G,TDET) $ IF(THW.LE.TDET)GO TO 3 $ IER=3 $ GO TO 9
    3 X=-.333333333333333*B        $ TCORR=1. $ DO 4 I=1,100
      CORR=-(D+X*(C+X*(B+X)))/(C+X*(2.*B+3.*X)) $ XT=X $ X=X+CORR
      IF(I.NE.1.AND.(TCORR*CORR.LE.0..OR.X.EQ.XT))GO TO 5
    4 TCORR=CORR $ IER=4           $ SMN=X*SQM $ GO TO 6
    5 IER=0       $ SMN=X*SQM
    6 P2OP1=(2.*G*SMN-G+1.)/(G+1.) $ R2OR1=(G+1.)*SMN/(2.+SMN*(G-1.))
      V2OV1=SQRT(1.-4.*(SMN-1.)*(G*SMN+1.)/(SMN*SQM*(G*(G+2.)+1.)))
      XM2=XM*V2OV1*SQRT(R2OR1/P2OP1) $ BETAO=ASIN(SQRT(X))      $ RETURN
    7 P2OP1=R2OR1=V2OV1=1. $ XM2=XM $ BETAO=ASIN(1./XM) $ IER=0 $ RETURN
    8 IER=2
    9 P2OP1=R2OR1=V2OV1=BETAO=XM2=RINDF $ RETURN
      END            SUBROUTINE WEDGE

      SUBROUTINE WDETACH(XM,G,DEL) $ XMS=XM*XM $ GP=G+1.
*************************************************************************
*  CALCULATES WEDGE ANGLE FOR SHOCK DETACHMENT DEL (RADIANS) FOR INPUT  *
*    VALUES OF MACH NUMBER XM AND GAMMA G                               *
*************************************************************************
      XMNS=.25*(GP*XMS-4.+SQRT(GP*(XMS*(GP*XMS+8.*(G-1.))+16.)))/G
      SINDEL=SQRT((XMS-XMNS*(2.*XMS+1.-XMNS*(XMS+2.-XMNS)))/
     +(1.+XMNS*(G-1.+.25*XMS*GP*GP-G*XMNS)))/XM$ DEL=ASIN(SINDEL)$RETURN
       END           SUBROUTINE WDETACH
```